Supporting information

Design and characterisation of bodipy sensitizers for dye-sensitized NiO solar cells.

Gareth H. Summers[1,2†], Jean-François Lefebvre[1†], Fiona A. Black[2], E. Stephen Davies[1], Elizabeth A. Gibson[1,2*], Tönu Pullerits[3], Christopher Wood[1], Karel Zidek[3].

[1]School of Inorganic Chemistry, The University of Nottingham, University Park, Nottingham, NG7 2RD.

[2]Now at the School of Chemistry, Newcastle University, Newcastle upon Tyne, NE1 7RU, United Kingdom. E-mail: Elizabeth.gibson@ncl.ac.uk

[3]Department of Chemical Physics, Lund University, Box 124, 22241, Lund, Sweden. E-mail: Tonu.Pullerits@chemphys.lu.se

†These authors contributed equally to this work.

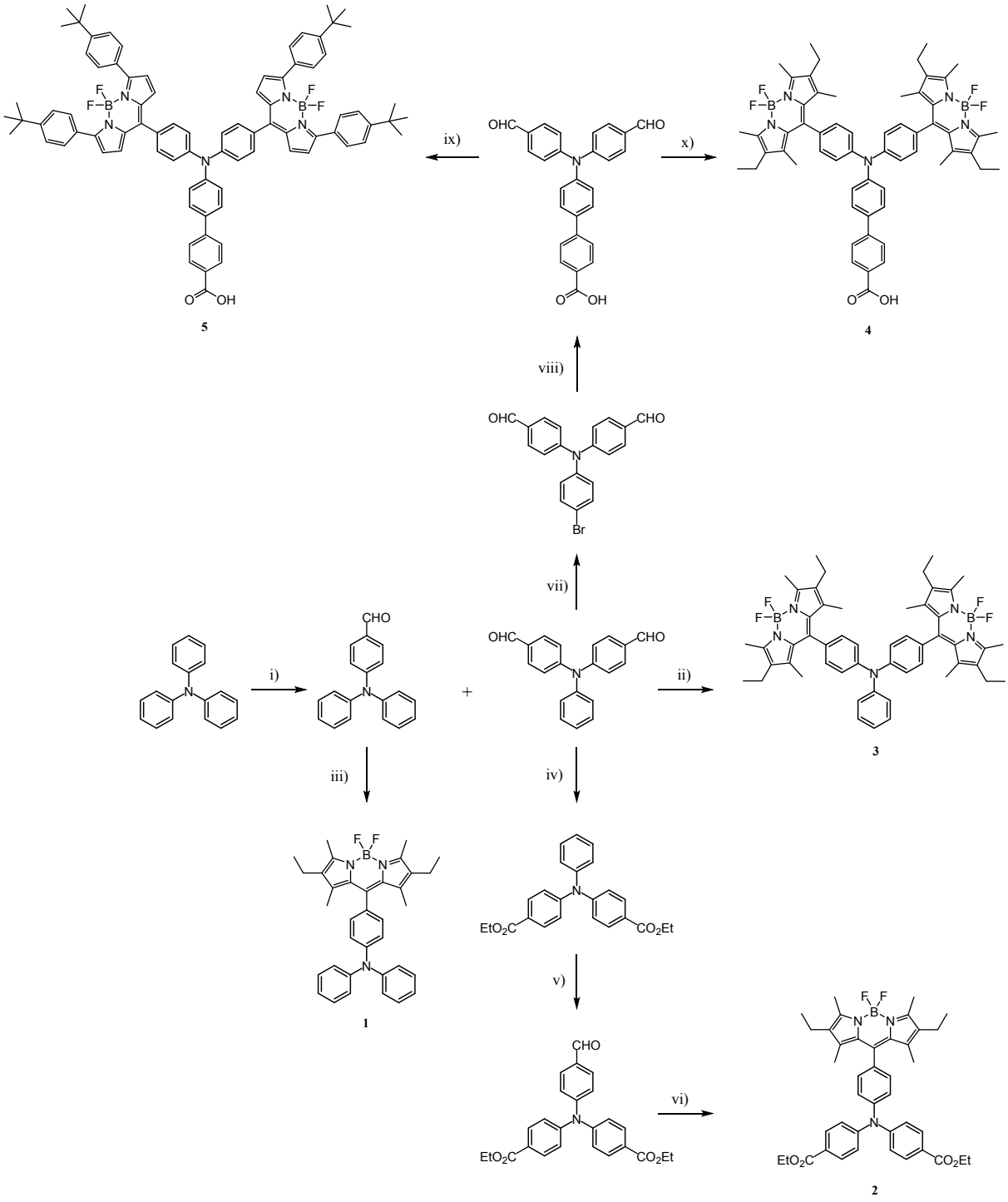

Figure S1 Synthetic route to **1-5**. i) DMF, $POCl_3$, NaOH, 79/11%, ii) 2,4-dimethyl-3-ethylpyrrole, TFA, p-chloranil, N,N-diisopropylethylamine, boron trifluoride diethyl etherate, DCM, 23%, iii) 2,4-dimethyl-3-ethylpyrrole, TFA, p-chloranil, N,N-diisopropylethylamine, boron trifluoride diethyl etherate, DCM, 50%, iv) a: $KMnO_4$, acetone/water (4:1), HCl, 66%, b: MeOH, H_2SO_4, quantitative, v) a: DMF, $POCl_3$, NaOH, / MeOH, H_2SO_4, 19%, vi) 2,4-dimethyl-3-ethylpyrrole, TFA, p-chloranil, N,N-diisopropylethylamine, boron trifluoride diethyl etherate, DCM, 92%, vii) THF, NBS, quantitative, viii) 4-carboxyphenylboronic acid, $Pd(PPh_3)_2Cl_2$, $NaCO_3$, DME/H_2O (3:1), 79%, ix) 2-(4-(tert-butyl)phenyl)-pyrrole, TFA, p-chloranil, N,N-diisopropylethylamine, boron trifluoride diethyl etherate, DCM, 35%, x) 2,4-

dimethyl-3-ethylpyrrole, TFA, p-chloranil, N,N-diisopropylethylamine, boron trifluoride diethyl etherate, DCM, 18%.

Experimental

Full details of the synthesis of **1** to **5** and **Bodipy-CO_2H** are provided in the electronic supplementary material. The synthesis of **6** and **7** have been reported previously.[5,24]

Physical Methods

All products were characterised by ^{1}H NMR and ^{13}C NMR using a Bruker 300 or 400 MHz spectrometer at 25°C; chemical shifts (δ) are reported in parts per million (ppm) from low to high field and referenced to residual non-deuterated solvent. Standard abbreviations indicating multiplicity are used as follows: s = singlet; d = doublet; t = triplet; m = multiplet. All proton assignments are provided in the supporting information. High resolution mass spectrometry (HRMS) was carried out on a high-throughput LC-MS system, based on a Bruker MicroTOF (Time of Flight) mass spectrometer using ElectroSpray Ionisation (ESI). Elemental microanalysis was performed using a CE-440 Elemental Analyzer (Exeter Analytical).

Molecular modelling

All theoretical studies were carried out using Gaussian g03 software[1] on the University of Nottingham HPC (Jupiter) facility. Calculations for optimised geometry and the subsequent energies and plots of the principle molecular orbitals were performed using density functional theory (DFT) using a B3LYP or CAM-B3LYP hybrid functional and a 6-31G(d) basis set. Bond frequencies and subsequent IR data were also gained from study. Principle electronic transitions and subsequent UV-visible spectra were predicted with time dependent density functional theory (TDDFT) using the same functional and basis sets as above. These calculations were performed for the compounds in dichloromethane and acetonitrile using CPCM for the polarisable continuum model (PCM).

Spectroscopic studies

The absorption spectra were measured using an Ocean Optics USB2000 spectrometer. The steady state emission spectra were obtained using an Edinburgh Instruments UC920

spectrometer equipped with M300 monochromators and the lifetimes were recorded using an Edinburgh Instruments EPL-405 laser source and single photon counting.

Transient absorption setup was based on an amplified Ti:sapphire laser (Mai-Tai, Spitfire; both Spectra Physics) providing 80 fs pulses at 800 nm at the rate of 1 kHz. The pulses were split into two beams: excitation pulses (532 nm) were generated by non-collinear optical amplifier (Topas, Light Conversion) and probe pulses (white light supercontinuum) were generated in a thin sapphire plate. The excitation and delayed probe beams were set to overlap in the sample (1 mm quartz cuvette). Consequently the probe beam was dispersed on a photodiode array coupled to a spectrograph (Pascher Instruments). The transient absorption signal was calculated from a difference between spectra of two consecutive probe pulses passing though excited and unexcited sample, respectively. This was maintained by a chopper running at 500 Hz frequency which was synchronized with the laser. Angle between polarizations of excitation and probe beam were set to the so-called magic angle (54.7 degrees) to avoid observation of dynamics connected to transition dipole rotation. The excitation intensity used (80 μJ cm^{-2} (2 x 10^{-14} photons cm^{-2})) did not lead to any visible photodegradation of the samples over the measurement period.

Electrochemical studies

Cyclic voltammetric studies were carried out using an Autolab PGSTAT20 potentiostat. Standard cyclic voltammetry was carried out under an atmosphere of argon using a three-electrode arrangement in a single compartment cell. A glassy carbon working electrode, a Pt wire secondary electrode and a saturated calomel reference electrode, chemically isolated from the test solution *via* a bridge tube containing electrolyte solution and fitted with a porous vycor frit, were used in the cell. The CH_2Cl_2 solutions were 10^{-3} M in test compound and 0.5 M in $[NBu_4][ClO_4]$ as supporting electrolyte. Redox potentials are quoted *versus* the ferrocenium-ferrocene couple used as an internal reference. Compensation for internal resistance was not applied.

The UV-visible spectroelectrochemical experiments were carried out with an optically transparent electrochemical (OTE) cell (modified quartz cuvette, optical pathlength: 0.5 mm). A three-electrode configuration, consisting a Pt/Rh gauze working electrode, a Pt wire secondary electrode (in a fritted PTFE sleeve) and a saturated calomel electrode, chemically isolated from the test solution *via* bridge tube containing electrolyte solution

and terminated in a porous frit, was used in the cell. The potential at the working electrode was controlled by a Sycopel Scientific Ltd. DD10M potentiostat. The UV-visible absorption spectra were recorded on a Perkin Elmer Lambda 16 spectrophotometer. The cavity was purged with dinitrogen and temperature control at the sample was achieved by flowing cooled dinitrogen across the surface of the cell.

Solar cells

NiO precursor solution was prepared by dissolving anhydrous $NiCl_2$ (1 g) and the tri-block co-polymer F108 (poly (ethylene glycol)-*block*-poly (propylene glycol)-*block*-poly (ethylene glycol)) (1 g) in ethanol (6 g) and ultrapure Milli-Q water (5 g). p-DSCs were made by spreading the precursor solution described above onto conducting glass substrates (Pilkington TEC15, sheet resistance 15 Ω/square) using Scotch tape as a spacer (0.2 cm^2 active area), followed by sintering in an oven at 450 °C for 30 min. Undyed NiO films were prepared to a thickness of 1.51 μm, measured using a Bruker DektakXT stylus profileometer and averaged over 3 samples. The NiO electrodes were soaked in an acetonitrile solution of the dye (0.3 mM) for 16 h at room temperature. The dyed NiO electrode was assembled face-to-face with a platinized counter electrode (Pilkington TEC8, sheet resistance 8 Ω/square) using a 30 mm thick thermoplastic frame (Surlyn 1702, Dyesol). The electrolyte, containing LiI (1.0 M) and I_2 (0.5 M or 0.1 M) in acetonitrile, was introduced through a pre-drilled hole in the counter electrode, which was sealed afterwards. The UV-visible absorption spectra of the dyes adsorbed on NiO films were recorded using an Ocean Optics USB2000+VIS-NIR fibre-optic spectrophotometer. Current-voltage measurements were measured using an Ivium CompactStat potentiostat under simulated sunlight from an Oriel VeraSol-2 Class AA LED Solar Simulator, giving light with an intensity of 100 mW cm^{-2}. Incident photon-to-current conversion efficiencies were recorded using monochromatic light from the Oriel 300 W Xe lamp fitted with an AM1.5 filter, using a Cornerstone monochromator and calibrated against a certified reference Si photodiode.

Synthesis

General information

All reagents and solvents (analytical grade) were purchased from Sigma-Aldrich or Fisher Scientific and used without further purification unless stated. Dichloromethane was dried over

calcium hydride and distilled under argon. Methanol was dried over magnesium turnings and iodine and distilled under argon. Silica gel 60 and Alumina were purchased from Sigma-Aldrich.

4-formyltriphenylamine and 4,4'-(phenylamino)bis-[benzaldehyde]

Triphenylamine (10 g, 40 mmol) was dissolved in dry N-Dimethylformamide DMF (100 mL) under argon in a three-necked flask and the solution was cooled at 0°C with stirring. Phosphoryl chloride $POCl_3$ (19.5 mL, 210 mmol, 5.25 eq.) was added slowly to the mixture and then the reaction mixture was warmed to 100°C and stirred for 5 hours under argon. After cooling at room temperature, the mixture was neutralized slowly with a 2M sodium hydroxide solution. After stirring for further 30 minutes, the mixture was extracted with ethylacetate (3 x 200 mL). The organic layer was then dried with Na_2SO_4 and the solvent evaporated. The different products were separated by column chromatography (Si-60, 2:1 heptane:chloroform v/v to chloroform) to afford 4-formyltriphenylamine (8.75 g, 79%) as a beige solid and 4,4'-diformyltriphenylamine (1.07 g, 11 %).

4-formyltriphenylamine

δ_H (300 MHz; $CDCl_3$) 9.82 (1H, s, C*H*O), 7.69 (2H, d, J = 8.7 Hz, phenyl), 7.41-7.30 (4H, m, phenyl), 7.24-7.13 (6H, m, phenyl), 7.03 (2H, d, J = 8.7 Hz, phenyl) ppm.

δ_C (75 MHz; $CDCl_3$) 190.45 (*C*HO), 153.4, 146.2, 131.3, 129.7, 129.1, 126.3, 125.1, 119.4 ppm.

m/z (HR-ESI$^+$) 274.12 (M + H^+, $C_{19}H_{16}NO$ requires 274.12)

4,4'-(phenylamino)bis-[benzaldehyde]

δ_H (300 MHz; $CDCl_3$) 9.91 (1H, s, C*H*O), 7.82-7.76 (2H, m, phenyl), 7.46-7.38 (1H, m, phenyl), 7.31-7.25 (1H, m, phenyl), 7.23-7.16 (3H, m, phenyl) ppm.

δ_C (75 MHz; $CDCl_3$) 190.5 (*C*HO), 152.0, 145.5, 131.3, 131.3, 130.1, 127.1, 126.3, 122.8, ppm.

m/z (HR-ESI$^+$) 302.12 (M + H^+, $C_{20}H_{16}NO_2$ requires 302.12)

1

4-formyltriphenylamine (100 mg, 0.366 mmol) and 2,4-dimethyl-3-ethylpyrrole (0.1 mL, 0.768 mmol, 2.05 eq.) were dissolved in dichloromethane (50 mL) under argon. One drop of trifluoroacetic acid (TFA) was added and the mixture was stirred under argon for 4 hours. Then *p*-chloranil (90 mg, 0.366 mmol) was added and the mixture was stirred under argon for 30 minutes. Then *N*,*N*-diisopropylethylamine (0.5 mL, 2.87 mmol) and boron trifluoride etherate (0.5 mL, 4.05 mmol) were added and the mixture was stirred under argon for 2 hours. After the evaporation of the solvent, the residue was filtered through a small silica gel column (dichloromethane). The first two fractions containing the product were combined and the solvent was evaporated. Pure **1** (100 mg, 0.183 mmol, 50%) was obtained after a second column chromatography purification step (Si-60, 3:1 to 1:1 dichloromethane:pentane v/v).

ν_{max} (MeCN) /cm^{-1} 3067w, 2975m, 2940w, 2880w, 1595w, 1550s, 1518w, 1482s, 1410w, 1328s, 1280s.

ν_{max} (CH_2Cl_2) /cm^{-1} 3020m, 2923m, 2875w, 1595m, 1537s, 1517m, 1482s, 1328m, 1164w, 1120w, 1066w, 9780m.

δ_H (400 MHz; $CDCl_3$) 7.35-7.30 (4H, m, phenyl), 7.23-7.19 (2H, m, phenyl), 7.18-7.13 (6H, m, phenyl), 7.12-7.06 (2H, m, phenyl), 2.56 (6H, s, CH_3 on 1 and 10), 2.36 (4H, q, J = 7.5 Hz, CH_2), 1.53 (6H, s, CH_3 on 3 and 7), 1.03 (6H, t, J = 7.5 Hz, CH_2CH_3) ppm.

δ_C (75 MHz; $CDCl_3$) 153.5, 148.4, 147.45, 140.3, 138.3, 132.7, 131.05, 129.4, 129.3, 129.2, 124.6, 123.6, 123.3, 17.1 (CH_2), 14.7 (CH_2CH_3), 12.5 (CH_3 on 1 and 10), 11.9 (CH_3 on 3 and 7) ppm.

m/z (HR-ESI$^+$) 548.30 (M + H$^+$, $C_{35}H_{37}BF_2N_3$ requires 548.30)

λmax(CH_3CN)/nm 303 (ε, dm^3 mol^{-1} cm^{-1} 19800), 379 (5550), 396 (sh, 5250), 495 (sh, 11150), 525 (53800).

4,4'-(phenylamino)bis[benzoic acid]

4,4'-diformyltriphenylamine (1.0 g, 3.32 mmol) was dissolved in a mixture acetone/water (40/10 mL) and the solution was heated at 60°C with stirring. Potassium permanganate (2.6 g, 16.45 mmol, 5 eq.) was added portionwise to the mixture during one hour and the reaction mixture was warmed to 60°C and stirred for 5 hours. After evaporation of acetone, water (40mL) was added to the residue and the mixture was filtrated. The filtrate was then acidified

by slow addition of concentrated hydrochloric acid. The white precipitate was filtered and dried under vacuum to afford 4,4'-(phenylamino)bis[benzoic acid] (725 mg, 66%).

δ_H (d_6-DMSO; 300MHz) 7.86 (4H, d, J = 8.4 Hz, phenyl), 7.47-7.36 (2H, m, phenyl), 7.28-7.19 (1H, m, phenyl), 7.19-7.11 (2H, m, phenyl), 7.05 (4H, d, J = 8.4 Hz, phenyl) ppm.

δ_C (75 MHz; DMSO) 167.3 (*C*OOH), 150.8, 146.1, 131.45, 130.6, 126.9, 126.0, 125.15, 122.6 ppm.

m/z (HR-ESI$^+$) 334.11 (M + H$^+$, $C_{20}H_{16}NO_4$ requires 334.11)

Dimethyl-4,4'-(phenylamino)bis[benzoate]

4,4'-(phenylamino)bis[benzoic acid] (0.40 g, 1.20 mmol) was dissolved in a mixture of dry methanol (8 mL, 198 mmol) and sulphuric acid (0.2 mL). The solution was heated to reflux with a calcium chloride trap for 6 hours. After evaporation of the solvent, the residue was dissolved in a mixture of chloroform (30 mL) and water (20 mL). The mixture was neutralized with aqueous sodium hydrogen carbonate. The organic layer was washed three times with water and dried over anhydrous magnesium sulphate. The evaporation of the solvent gave dimethyl-4,4'-(phenylamino)bis[benzoate] as a yellow oil in quantitative yield (435 mg)

δ_H (300 MHz; $CDCl_3$) 7.97-7.89 (4H, m, phenyl), 7.40-7.32 (2H, m, phenyl), 7.24-7.06 (7H, m, phenyl), 3.90 (6H, s, COOCH_3) ppm.

δ_C (75 MHz, $CDCl_3$) 166.6 (*C*0OCH_3), 151.0, 146.1, 131.0, 129.9, 126.55, 125.4, 124.15, 122.4, 51.95 (C0O*C*H_3) ppm.

m/z (HR-ESI$^+$) 362.14 (M + H$^+$, $C_{22}H_{20}NO_4$ requires 362.14)

Dimethyl-4,4'-[(4-formylphenyl)amino]bis[benzoate]

Dimethyl-4,4'-(phenylamino)bis[benzoate] (294 mg, 0.813 mmol) was dissolved in dry DMF (5 ml) under argon. Phosphoryl chloride (1.5 mL, 16.1 mmol, 20 eq) was then added slowly at 0°C under argon. The mixture was heated to 100°C for 24 hours. Ice was added to the cooled mixture, which was then neutralized by slow adding of 2M NaOH. After an extraction with chloroform (4 × 50 mL), the solvent was evaporated to obtain a mixture of different products.

This mixture was reacted with dry methanol (4 mL) and sulfuric acid (0.2 mL) at reflux overnight to recover the ester groups. After evaporation of the methanol, the residue was dissolved in a mixture of water and chloroform and neutralized with sodium hydrogencarbonate. The organic layer was then washed three times with water, dried on magnesium sulphate and evaporated. The residue was purified by column chromatography (Si-60 1:1 pentane:dichloromethane v/v to dichloromethane) to obtain dimethyl-4,4'-[(4-formylphenyl)amino]bis[benzoate] as a yellow oil (60 mg, 19%).

δ_H (300 MHz; $CDCl_3$) 9.91 (1H, s, C*H*O), 8.03-7.96 (4H, m, phenyl), 7.83-7.76 (2H, m, phenyl), 7.23-7.13 (6H, m, phenyl), 3.92 (6H, s, COOCH_3) ppm.

δ_C NMR (75MHz, $CDCl_3$) 190.5 (*C*HO), 166.3, 151.7, 150.05, 131.7, 131.4, 131.3, 126.1, 124.4, 123.35, 52.14 ppm.

m/z (HR-ESI$^+$) 390.13 (M + H^+, $C_{23}H_{20}NO_5$ requires 390.13), 412.12 (M + Na^+, $C_{23}H_{19}NNaO_5$ requires 390.13).

2

Dimethyl-4,4'-[(4-formylphenyl)amino]bis[benzoate] (30.5 mg, 78.3 µmol) and 2,4-dimethyl-3-ethylpyrrole (24 µL, 0.172 mmol, 2.2 eq.) were dissolved under argon in dry dichloromethane (1 mL). One drop of trifluoroacetic acid (TFA) was added and the mixture was stirred under argon for 4.5 h. Then a suspension of *p*-chloranil (20 mg, 78.3 µmol) in dichloromethane (1 mL) was added and the mixture was stirred under argon for one hour. Then N,N-diisopropylethylamine (0.3 mL, 1.72 mmol) and boron trifluoride etherate (0.3 mL, 2.43 mmol) were added and the mixture was stirred under argon for one hour. After evaporation of the solvent, the residue was separated by two successive column chromatography steps (deactivated alumina 150, grade III, 1:1 pentane:dichloromethane v/v) to give **2** (48 mg, 92%).

ν_{max} (MeCN) /cm^{-1} 3062s, 2976w, 2940w, 2880w, 1740s, 1600s, 1544s, 1514m, 1483m, 1442 m, 1410w, 1326s, 1280s.

ν_{max} (CH_2Cl_2) /cm^{-1} 2930m, 2872w, 1720s, 1596s, 1537s, 1516m, 1482m, 1320s, 1198s, 1218m, 1068m, 983m.

δ_H (300 MHz; $CDCl_3$) 7.98 (4H, d, *J* = 8.7 Hz, phenyl), 7.29 (4H, s, phenyl), 7.14 (4H, d, *J* = 8.7 Hz, phenyl), 3.93 (6H, s, CO_2CH_3), 2.56 (6H, s, CH_3 on 1 and 10), 2.36 (4H, q, *J* = 7.5 Hz, CH_2), 1.50 (6H, s, CH_3 on 3 and 7), 1.03 (6H, t, *J* = 7.5 Hz, CH_2CH_3) ppm.

δ_C NMR (75 MHz, $CDCl_3$) 166.5 (CO_2CH_3), 154.0, 150.7, 146.7, 139.25, 138.0, 133.0, 132.5, 131.2, 130.8, 130.0, 126.6, 124.7, 122.7, 52.05 (CO_2CH_3), 17.1 (CH_2), 14.65 (CH_2CH_3), 12.5 (CH_3 on 1 and 10), 11.9 (CH_3 on 3 and 7) ppm.

m/z (HR-ESI$^+$) 664.32 (M + H^+, $C_{39}H_{41}BF_2N_3O_4$ requires 664.32).

303 379 (5550), 396 (sh, 5250), 495 (sh, 11150), 525 (53800).

λmax(CH_3CN)/nm 330 (ε, $dm^3\ mol^{-1}\ cm^{-1}$ 34800), 351 (sh, 28300), 399 (sh, 6350), 497 (sh, 17900), 526 (53200).

Elem. Anal.: Found: C, 69.32; H, 6.25; N, 6.10. $C_{39}H_{40}BF_2N_3O_4$•CH_3OH requires C, 69.07; H, 6.38; N, 6.04%.

3

4,4'-(phenylamino)bis-[benzaldehyde] (100 mg, 0.332 mmol) and 2,4-dimethyl-3-ethylpyrrole (0.19 mL, 1.41 mmol, 4.2 eq.) were dissolved in dry dichloromethane (5 mL) under argon. One drop of trifluoroacetic acid (TFA) was added and the mixture was stirred under argon for 4 hours 30. Then *p*-chloranil (163 mg, 0.663 mmol, 2 eq.) was added and the mixture was stirred under argon for 1 hour. Then *N*,*N*-diisopropylethylamine (0.5 mL, 2.87 mmol) and boron trifluoride etherate (0.5 mL, 4.05 mmol) were added and the mixture was stirred under argon for 2 hours. After the evaporation of the solvent, the residue was filtered though a small silica gel column (Si-60, dichloromethane). The first fractions, containing the product, were combined and the solvent evaporated and **3** (65 mg, 23%) was isolated using a second column chromatography step (Si-60 3:1 to 1:1 dichloromethane:pentane v/v).

ν_{max} (CH_2Cl_2) /cm^{-1} 2932m, 2874m, 1597w, 1537s, 1513w, 1484m, 1328m, 1197s, 1169m, 1114m, 1067w 977m.

δ_H (400 MHz; $CDCl_3$) 7.40-7.35 (2H, m, phenyl), 7.23-7.13 (11H, m, phenyl), 2.57 (12H, s, CH_3 on 1 and 10), 2.36 (8H, q, *J* = 7.6 Hz, CH_2), 1.54 (12H, s, CH_3 on 3 and 7), 1.04 (12H, t, *J* = 7.6 Hz, CH_2CH_3) ppm.

δ_C NMR (100 MHz, $CDCl_3$) 153.7, 147.9, 147.1, 140.0, 138.2, 132.8, 131.0, 130.0, 129.7, 129.5, 125.1, 124.1, 123.95, 17.1 (*C*H_2), 14.7 (CH_2*C*H_3), 12.5 (*C*H_3 on 1 and 10), 11.9 (*C*H_3 on 3 and 7) ppm.

m/z (HR-ESI$^+$) 850.48 (M + H^+, $C_{52}H_{58}B_2F_4N_5$ requires 850.48), 830.48 (M - F^-, $C_{52}H_{57}B_2F_3N_5$ requires 830.48).

λmax(CH_3CN)/nm 307 (ε, $dm^3\ mol^{-1}\ cm^{-1}$ 16700), 381 (8400), 399 (sh, 7800), 494 (sh, 25000), 525 (78800) nm.

Elem. Anal.: Found: C, 72.01; H, 6.73; N, 7.86. $C_{52}H_{57}B_2F_4N_5 \bullet H_2O$ requires C, 71.98; H, 6.85; N, 8.07%.

4,4'-[(4-bromophenyl)amino]bis-[benzaldehyde]

4,4'-(phenylamino)bis-[benzaldehyde] (500 mg, 1.66 mmol) was dissolved in dry THF (25 mL) under argon. N-bromosuccinimide (NBS) (600 mg, 3.37 mmol) was added under argon at room temperature. The mixture was heated to reflux for 6 hours. The completion of the reaction was monitored by TLC. The solvent was then evaporated and chloroform (40 mL) was added to the residue. The solid was filtered and washed with chloroform. The filtrate was washed with a 10% $NaHCO_3$ aqueous solution and with water. After drying on magnesium sulphate and evaporation of the solvent, the residue was recrystallized in DCM / pentane to afford 4,4'-[(4-bromophenyl)amino]bis-[benzaldehyde] as a yellow solid in quantitative yield (609 mg).

δ_H (400 MHz; $CDCl_3$) 9.84 (1H, s, C*H*O), 7.71 (4H, d, *J* = 8.8 Hz, phenyl), 7.53 (2H, d, *J* = 8.8 Hz, phenyl), 7.21 (4H, d, J = 8.8 Hz, phenyl), 7.08 (4H, d, J = 8.8 Hz, phenyl) ppm.

δ_C NMR (100 MHz, $CDCl_3$) 190.4 (*C*HO), 151.6, 144.7, 133.3, 131.7, 131.4, 128.7, 123.0, 119.2 ppm.

m/z (HR-ESI$^+$) 380.03 (M + H^+, $C_{20}H_{15}BrNO_2$ requires 380.03), 402.01 (M + Na^+, $C_{20}H_{14}BrNNaO_2$ requires 402.01).

4,4'-[4-(4-carboxyphenyl)phenylamino]bis-[benzaldehyde]

4,4'-[(4-bromophenyl)amino]bis-[benzaldehyde] (84 mg, 2.21 × 10^{-4} mol), 4-carboxyphenylboronic acid (120 mg, 7.23 × 10^{-4} mol), bis(triphenylphosphine)palladium(II) dichloride (8 mg, 1.14 × 10^{-5} mol, 0.05 eq.) and sodium carbonate (70 mg, 6.60 × 10^{-4} mol, 3 eq.) were loaded in a Schlenk tube purged with nitrogen. H_2O (1 mL) and then 1,2-dimethoxyethane DME (3 mL) were added and the mixture was heated to reflux overnight under nitrogen. After cooling, ethyl acetate (20 mL) and water (10 mL) was added and the mixture was acidified with diluted 0.1 M hydrochloric acid until slightly acidic pH. The organic phase was extracted with ethyl acetate (3 × 20 mL) and washed with water (3 × 5 mL), dried on $MgSO_4$ and evaporated. The product was quickly purified by silica gel flash column chromatography with a gradient of methanol in DCM as eluent to afford 110 mg of 4,4'-[4-(4-carboxyphenyl)phenylamino]bis-[benzaldehyde] as a yellow solid in 79% yield.

δ_H (300 MHz; $CDCl_3$) 9.95 (1H, s, C*H*O), 8.23 (2H, d, *J* = 8.2 Hz, phenyl), 7.84 (4H, d, *J* = 8.7 Hz, phenyl), 7.73 (2H, d, *J* = 8.2 Hz, phenyl), 7.69 (2H, d, *J* = 8.7 Hz, phenyl), 7.26-7.32 (6H, m, phenyl) ppm.

δ_C NMR (100 MHz, $CDCl_3$)190.6, 151.8, 145.7, 145.0, 137.3, 131.6, 131.4, 128.9, 126.9, 123.2 ppm.

m/z (HR-ESI$^+$) 422.14 (M + H^+, $C_{27}H_{20}NO_4$ requires 422.14).

m/z (HR-ESI$^-$) $^+$) 420.12 (M – H^-, $C_{27}H_{18}NO_4$ requires 420.12).

4

4,4'-[4-(4-carboxyphenyl)phenylamino]bis-[benzaldehyde] (36.4 mg, 8.64 × 10^{-5} mol) was loaded in a Schlenk tube purged with 3 cycles vacuum / nitrogen and dissolved in dry dichloromethane (1 mL). 2,4-dimethyl-3-ethylpyrrole (51 µL, 4.38 × 10^{-4} mol, 4.4 eq.) and then trifluoroacetic acid (2 drops) were added to the solution. The mixture was stirred for 16 hours in the dark under nitrogen. *p*-chloranil (43 mg, 1.73 × 10^{-4} mol, 2.0 eq.) was added under a flux of nitrogen and the mixture was stirred under nitrogen for another 30 minutes. N,N-diisopropylethylamine (0.15 mL, 8.63 × 10^{-4} mol, 10 eq.) was added and the mixture was stirred under nitrogen for another 10 minutes. Finally, boron trifluoride etherate (0.24 mL, 8.08 × 10^{-4} mol, 10 eq.) was added and the mixture was stirred under nitrogen for another 2 hours. Dichloromethane (20 mL) was added to the mixture and the organic layer was washed with water (3 × 10 mL), dried on $MgSO_4$ and evaporated. The residue was purified by silica gel

column chromatography with a dichloromethane / methanol mixture (*v/v* 99.5/0.5). Crystallisation from dichloromethane with addition of pentane afforded 15 mg of pure **4** in 18% yield.

δ_H (300 MHz; $CDCl_3$) 8.21 (2H, d, *J* = 8.5 Hz, phenyl), 7.74 (2H, d, *J* = 8.6 Hz, phenyl), 7.66 (2H, d, *J* = 8.6 Hz, phenyl), 7.23-7.34 (10H, m, phenyl), 2.57 (12H, s, CH_3), 2.37 (8H, q, J = 7.5 Hz, C*H*2CH3), 1.55 (12H, s, CH_3), 1.04 (12H, t, J = 7.5 Hz, CH_2CH_3) ppm.

δ_C NMR (100 MHz, $CDCl_3$) 170.2, 153.8, 147.5, 147.3, 139.7, 138.1, 132.9, 130.9, 130.8, 130.6, 129.7, 128.5, 126.6, 124.6, 124.4, 17.1, 14.6, 12.5, 11.9 ppm.

m/z (TOF-ESI$^+$) 1008.4530 (M + K^+, $C_{59}H_{61}B_2F_4KN_5O_2$ requires 1008.4597).

λmax(CH_3CN)/nm 332 (ε, $dm^3\ mol^{-1}\ cm^{-1}$ 25000), 351 (27000), 493 (sh, 33400), 522 (94400) nm.

λmax($CHCl_2$)/nm 330 (ε, $dm^3\ mol^{-1}\ cm^{-1}$ 19600), 360 (23900), 494 (sh, 26000), 526 (81700) nm.

Bis(4-tert-butylphenyl)iodonium triflate was synthesised according to the method by Bielawski *et al.*[2]

3-Chloroperbenzoic acid (890 mg, 0.012 mol, 4 eq.) and iodine (737 mg, 1.29×10^{-3} mol, 1 eq.) were dissolved in dichloromethane (15 mL) to which *tert*-butylbenzene (4.5 mL, 0.029 mol, 10 eq.) was added. Trifluoromethanesulfonic acid was added dropwise (0.9 mL, 0.01 mol, 4 eq.) and the mixture was stirred at room temperature for 30 minutes. The solution was concentrated under reduced pressure and the addition of pentane resulted in the precipitation of the product to afford 1.2 g of white solid in 76% yield.

δ_H (300 MHz; $CDCl_3$) 7.93 (4H, d, *J* = 8.85 Hz), 7.45 (4H, d, *J* = 8.85 Hz), 1.26 (18H, s) ppm.

m/z (HR-ESI$^+$) 393.11 ([M]$^+$, $C_{21}H_{27}F_3IO_3S$ requires 543.07).

2-(4-(tert-butyl)phenyl)-pyrrole was synthesised according to the method by Wen *et al.*[3]

Bis(4-*tert*-butylphenyl)iodonium triflate (1.2 g, 2.21×10^{-3} mol, 1 eq.) and sodium hydroxide (190 mg, 4.75×10^{-3} mol, 2.15 eq.) were loaded into a Schlenk tube and purged with nitrogen. Pyrrole (5 mL) was added and the reaction mixture was heated at 80°C overnight. After cooling to room temperature, ethyl acetate was added (10 mL), the mixture was washed with water (3 × 5mL) and the organic phase dried using magnesium sulfate. The crude product was then purified by silica gel chromatography (using a 4:1 hexane/ethyl acetate eluent) to afford 168 mg of the product in 38% yield.

δ_H (300 MHz; $CDCl_3$) 7.47 (4H, m), 6.83 (1H, m), 6.47 (1H, m), 6.19 (1H, m), 1.34 (9H, s) ppm.

m/z (HR-ESI$^+$) 200.14 ($[M+H]^+$, $C_{14}H_{18}N$ requires 200.14).

5

4,4'-[4-(4-carboxyphenyl)phenylamino]bis-[benzaldehyde] (75 mg, 1.76×10^{-4} mol) and 2-(4-(tert-butyl)phenyl)-pyrrole (158.4 mg, 7.95×10^{-4} mol, 4.5 eq.) were loaded in a Schlenk tube purged with 3 cycles vacuum / nitrogen and dissolved in dry dichloromethane (2 mL). Trifluoroacetic acid (2 drops) was added to the solution and the mixture was stirred for 16 hours in the dark under nitrogen. *p*-chloranil (85 mg, 3.42×10^{-4} mol, 2.0 eq.) was added under a flux of nitrogen and the mixture was stirred under nitrogen for another 30 minutes. N,N-diisopropylethylamine (0.38 mL, 2.18×10^{-3} mol, 10 eq.) was added and the mixture was stirred under nitrogen for another 10 minutes. Finally, boron trifluoride etherate (0.45 mL, 1.51×10^{-3} mol, 10 eq.) was added and the mixture was stirred under nitrogen for another 2 hours. Dichloromethane (20 mL) was added to the mixture and the organic layer was washed with water (3 × 10 mL), dried on $MgSO_4$ and evaporated. The residue was purified by silica gel column chromatography with a dichloromethane / methanol mixture (*v/v* 99/1). Crystallisation from dichloromethane with addition of pentane afforded 78 mg of pure **5** in 35% yield.

δ_H (700 MHz, $CDCl_3$) 8.23 (2H, d, J = 8.4 Hz, phenyl), 7.89 (8H, d, J = 8.5 Hz, phenyl), 7.77 (2H, d, J = 8.5 Hz, phenyl), 7.73 (2H, d, J = 8.7 Hz, phenyl), 7.62 (4H, d, J = 8.6 Hz, phenyl), 7.49 (8H, d, J = 8.6 Hz, phenyl), 7.43 (2H, d, J = 8.6 Hz, phenyl), 7.39 (4H, d, J = 8.6 Hz, phenyl), 7.05 (4H, d, J = 4.3 Hz, pyrrole), 6.70 (4H, d, J = 4.3 Hz, pyrrole), 1.10 (36H, s, CH_3) ppm.

δ_C NMR (700 MHz, $CDCl_3$) 170.3, 158.5, 152.6, 148.8, 145.6, 145.4, 142.8, 136.2, 130.9, 130.3, 129.8, 129.4, 129.2, 128.8, 128.0, 126.8, 126.2, 125.3, 123.1, 120.9, 34.8, 31.3 ppm.

δ_B NMR (96 MHz; $CDCl_3$) 1.55 (t, J = 30.1 Hz).

δ_F NMR (282 MHz; $CDCl_3$) -132.66 (q, J = 32.2 Hz).

m/z (HR-ESI-) 1272.61 ([M-H]-, $C_{83}H_{77}B_2F4N_5O_2$ requires 1272.61).

λmax(CH_3CN)/nm 305 (ε, $dm^3\ mol^{-1}\ cm^{-1}$ 56384), 350 (39684), 555 (86818) nm.

λmax($CHCl_2$)/nm 308 (ε, $dm^3\ mol^{-1}\ cm^{-1}$ 41488), 351 (28237), 561 (65824) nm.

Bodipy-CO_2H

4-carboxybenzaldehyde (50 mg, $3.33x10^{-4}$ mol) was purged under argon in a Schlenk tube. 2,4-dimethyl-3-ethylpyrrole (0.1 mL, $7.33x10^{-4}$ mol) and dry dichloromethane (2 mL) were then added. Trifluoroacetic acid (one drop) was added and the mixture was stirred under argon at room temperature in the dark for 3 hours. Chloranil (90 mg, $3.66x10^{-4}$ mol) was added under argon and the mixture was stirred for another 45 mn. Diisopropylethylamine (1 mL, $5.74x10^{-3}$ mol) was added and the mixture was stirred under argon for another 30 mn. Finally, boron trifluoride etherate (0.83 mL, $6.73x10^{-3}$ mol) was added and the mixture was stirred under argon for another hour. Dichloromethane (10 mL) was added to the mixture and the organic layer was washed with water (3x 5 mL), dried on $MgSO_4$ and evaporated. The product was purified by silica gel column chromatography with a gradient of methanol in dichloromethane as eluent to afford 72 mg of the product in 51% yield.

NMR ($CDCl_3$, 300MHz, 25°C): δ 8.25 (d, *J* = 8.4 Hz, 2H, H_{Ar}), 7.45 (d, *J* = 8.4 Hz, 2H, H_{Ar}), 2.54 (s, 6H, H_{Me}), 2.30 (q, *J* = 7.5 Hz, 4H, H_{CH2CH3}), 1.27 (s, 6H, H_{Ar}), 0.98 (t, *J* = 7.5 Hz, 6H, H_{CH2CH3}) ppm.

^{13}C NMR ($CDCl_3$, 300MHz, 25°C): δ 171.8 (C_{COOH}), 156.4, 154.5, 141.8, 138.6, 138.2, 133.3, 131.1, 130.3, 129.0, 17.2, 14.7, 12.7, 12.0 ppm.

m/z (HR-ESI+) 425.22 ([M+H]+, $C_{24}H_{28}BF_2N_2O_2$ requires 425.22).

λmax(CH_3CN)/nm 521 (69828) nm.

λmax($CHCl_2$)/nm 528 (51964) nm.

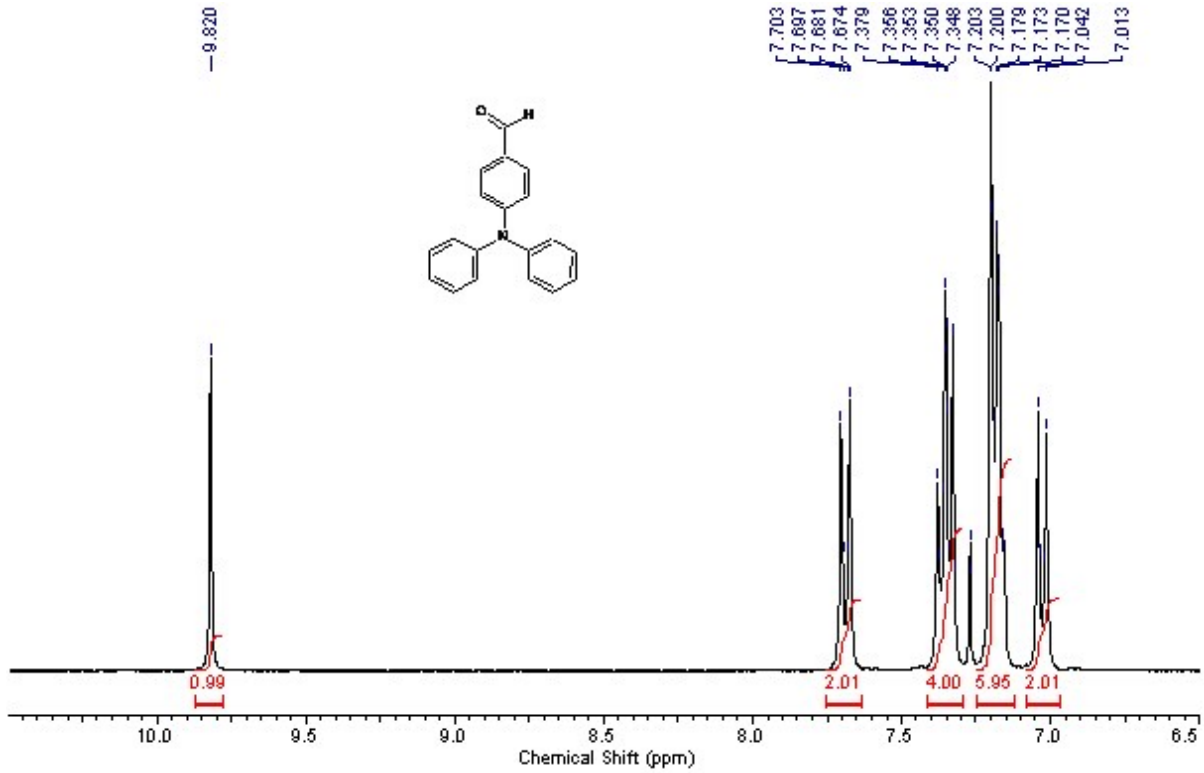

Figure S2 ^{1}H NMR ($CDCl_3$, 300MHz, 25°C) - 4-formyltriphenylamine

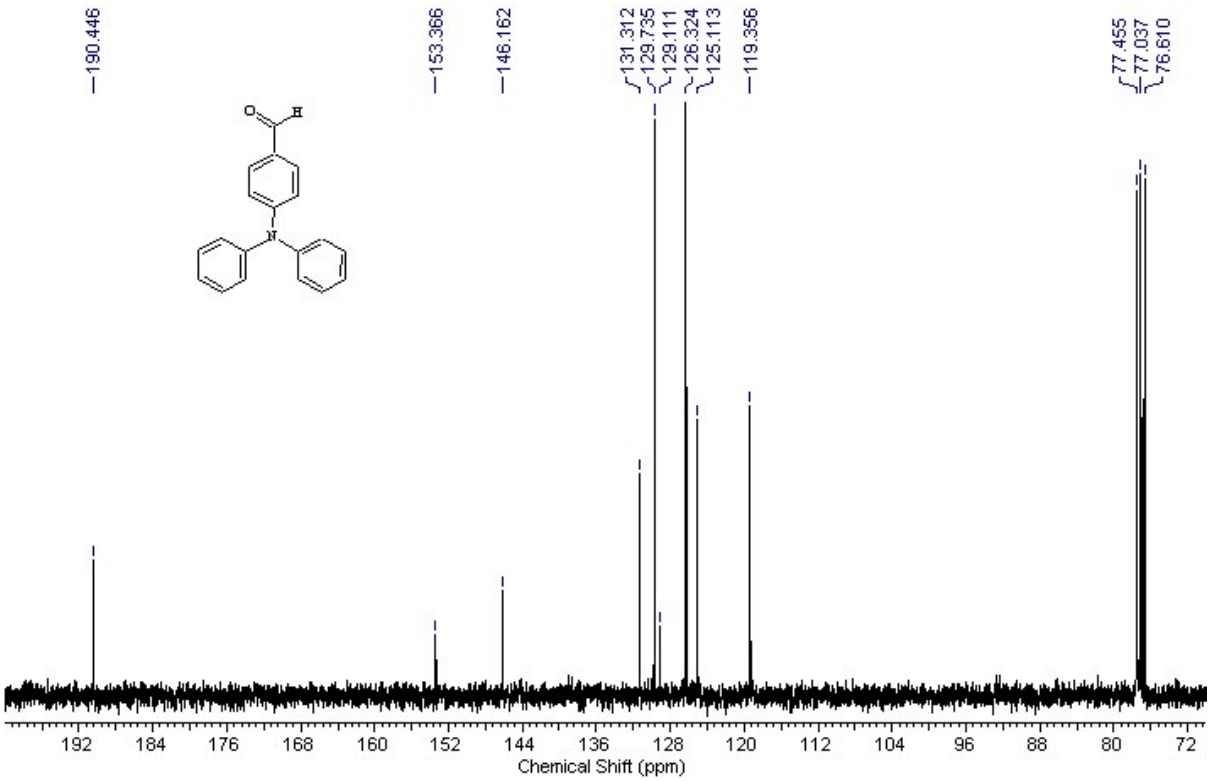

Figure S3 ^{13}C NMR ($CDCl_3$, 300MHz, 25°C) - 4-formyltriphenylamine

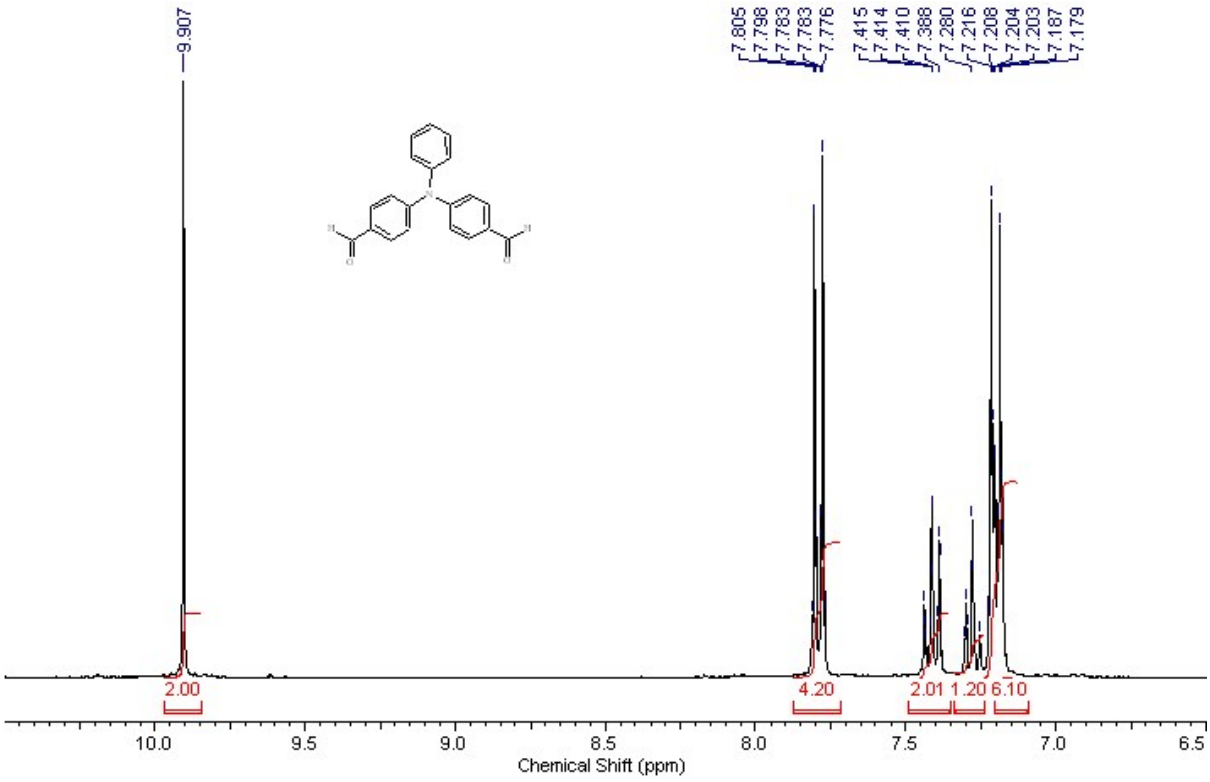

Figure S4 ^{1}H NMR ($CDCl_3$, 300MHz, 25°C) - 4,4'-(phenylamino)bis-benzaldehyde

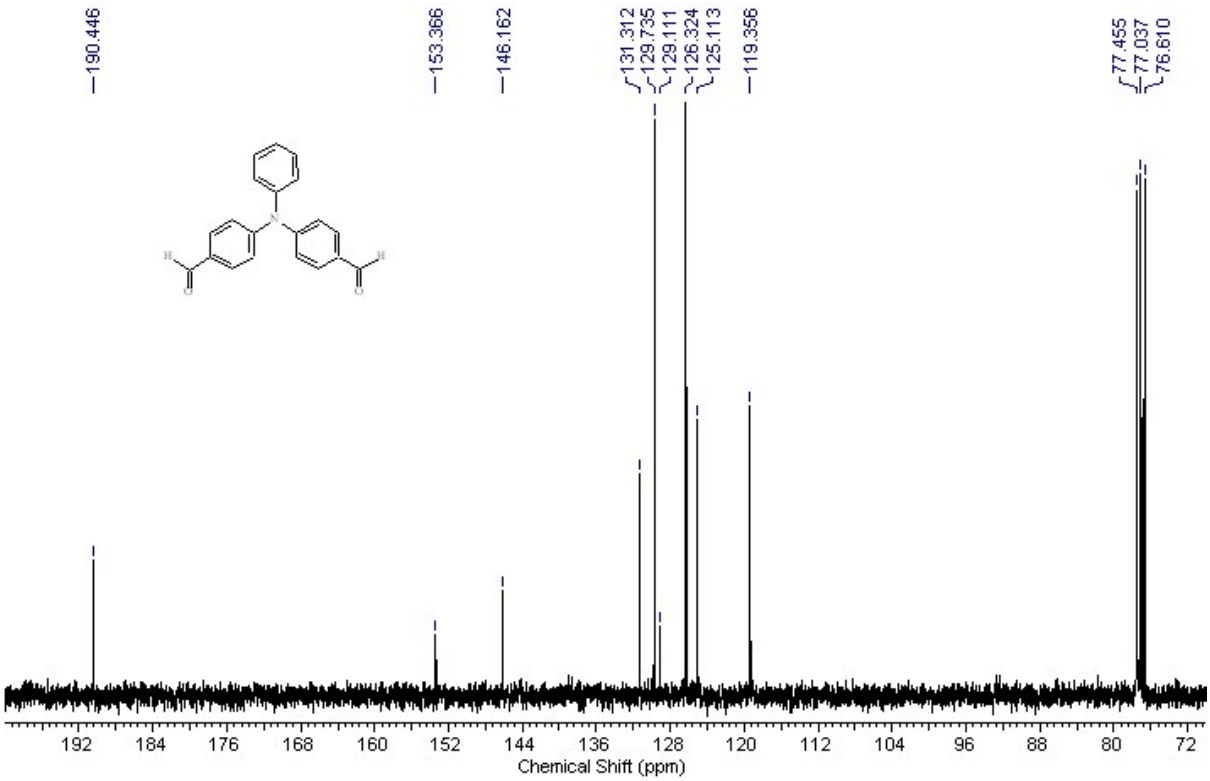

Figure S5 ^{13}C NMR ($CDCl_3$, 300MHz, 25°C) - 4,4'-(phenylamino)bis-benzaldehyde

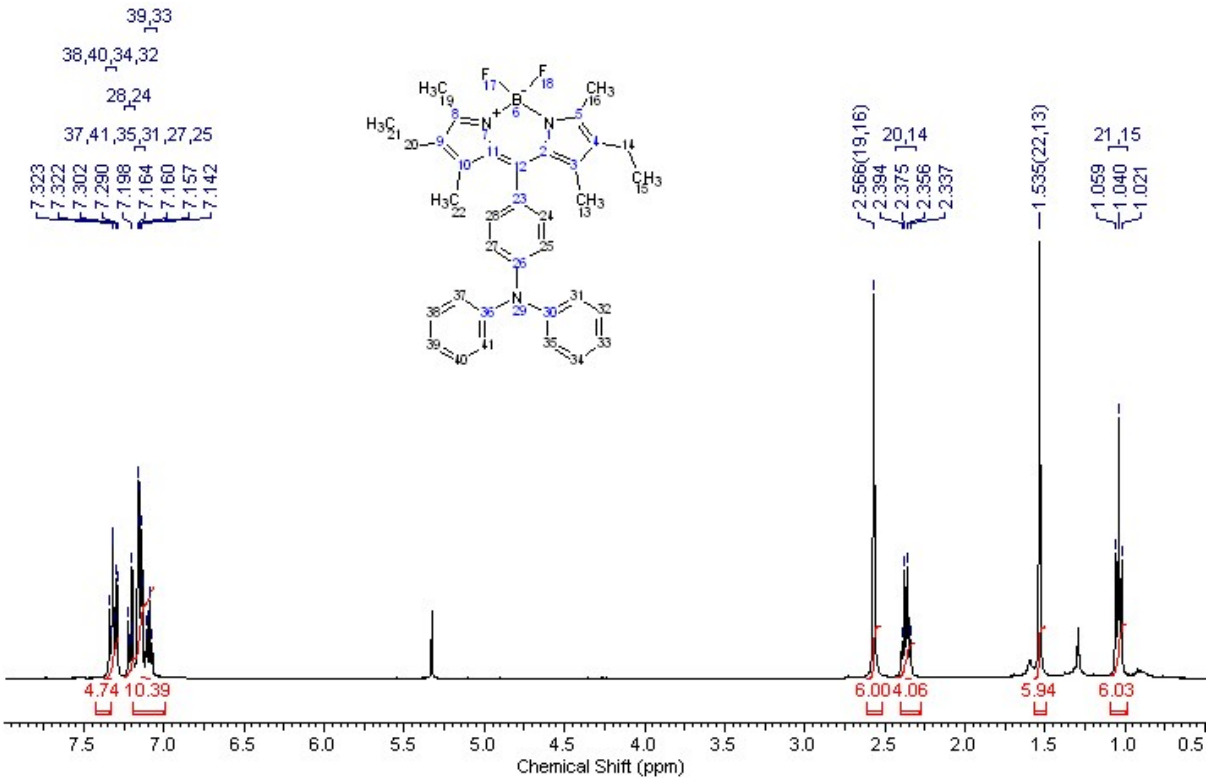

Figure S6 ^{1}H NMR ($CDCl_3$, 400MHz, 25°C) – **1**

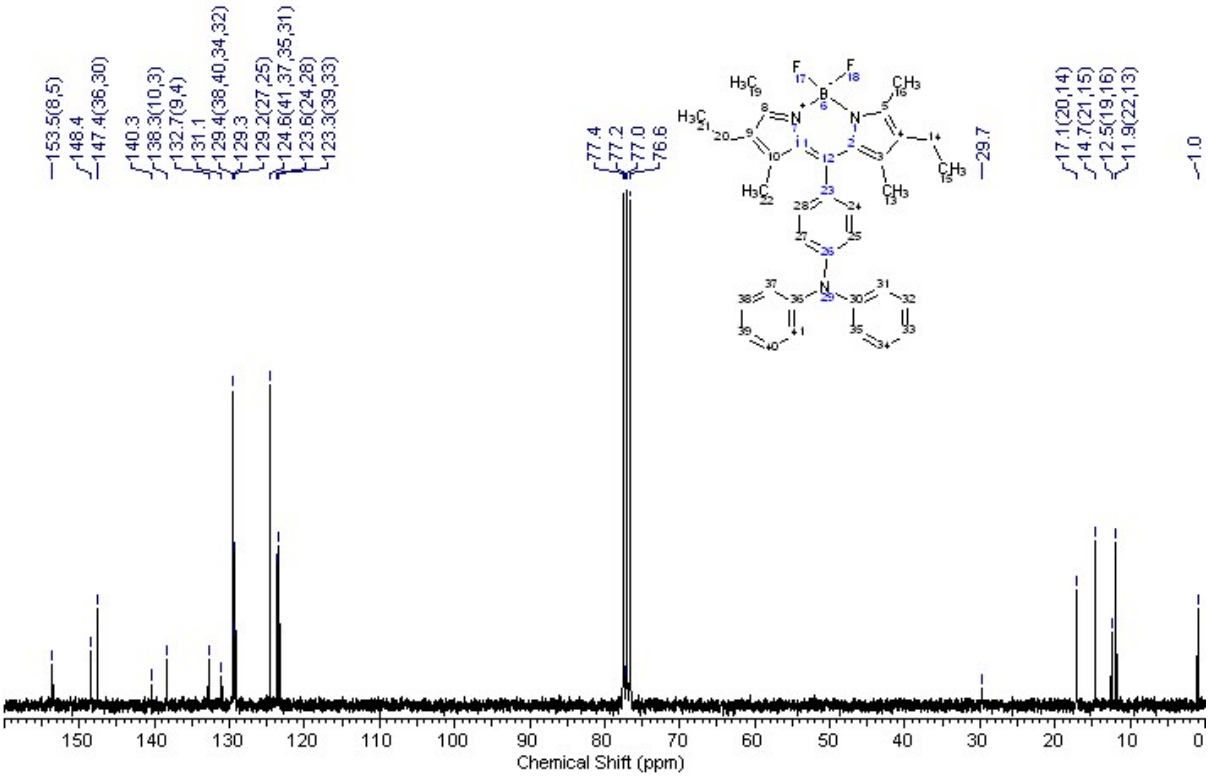

Figure S7 ^{13}C NMR ($CDCl_3$, 300MHz, 25°C) – **1**

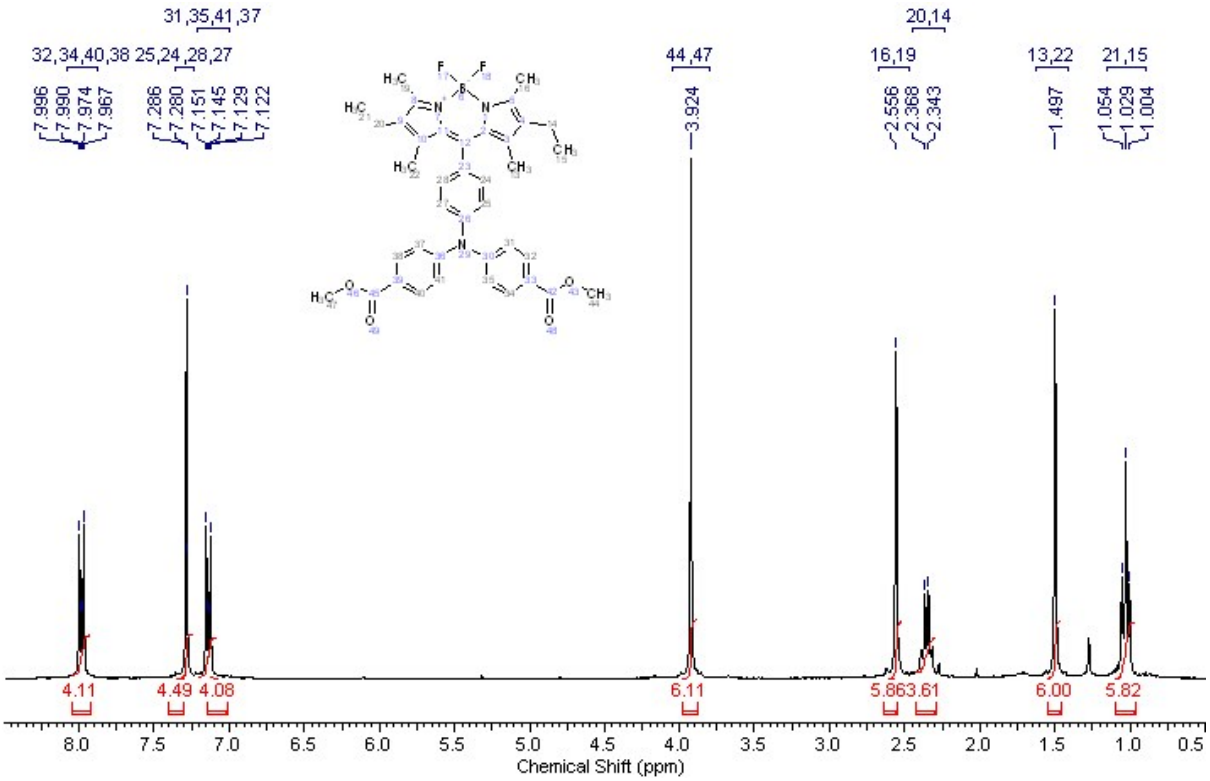

Figure S8 ^{1}H NMR ($CDCl_3$, 300MHz, 25°C) –**2**

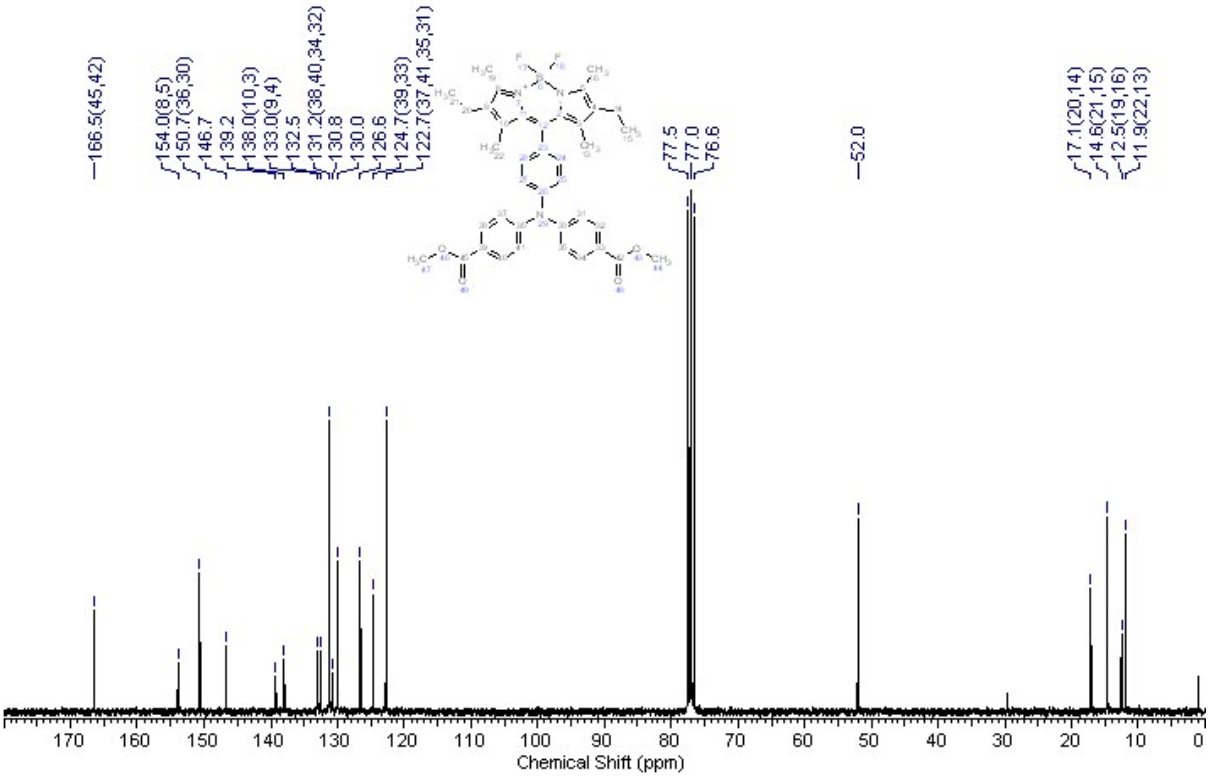

Figure S9 ^{13}C NMR ($CDCl_3$, 300MHz, 25°C) – **2**

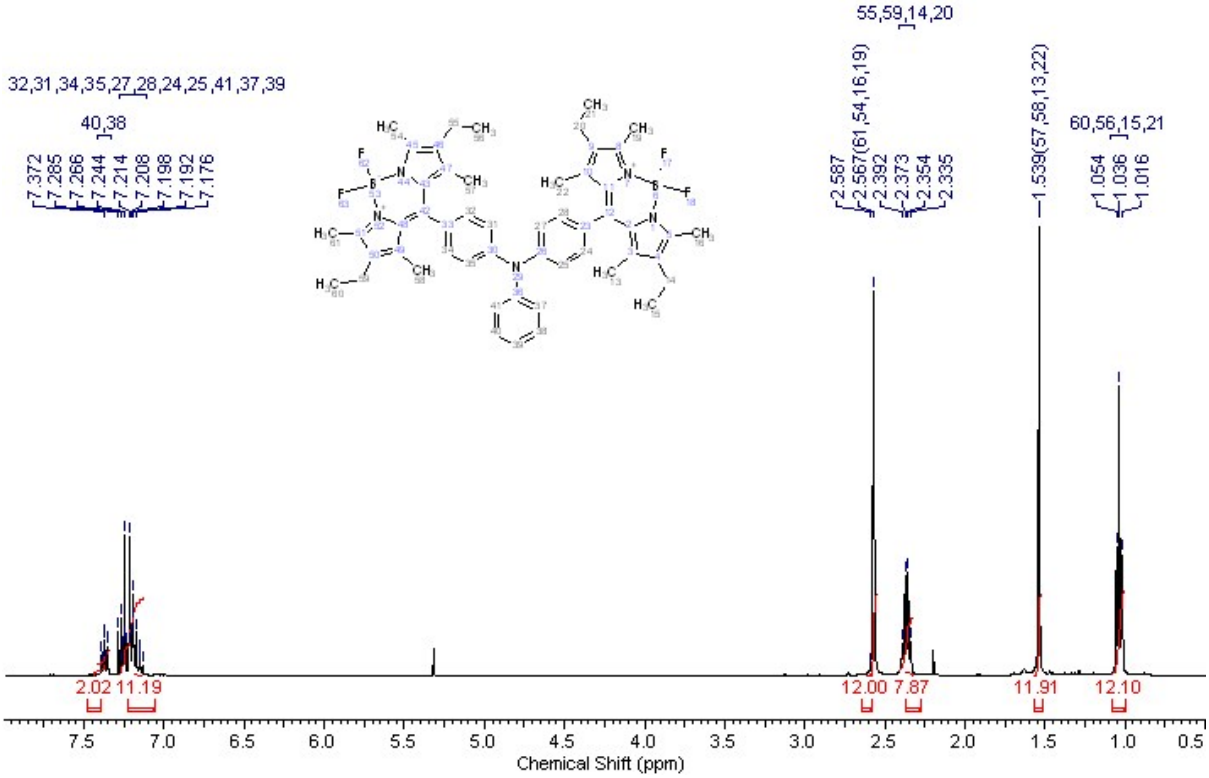

Figure S10 ^{1}H NMR ($CDCl_3$, 400MHz, 25°C) – **3**

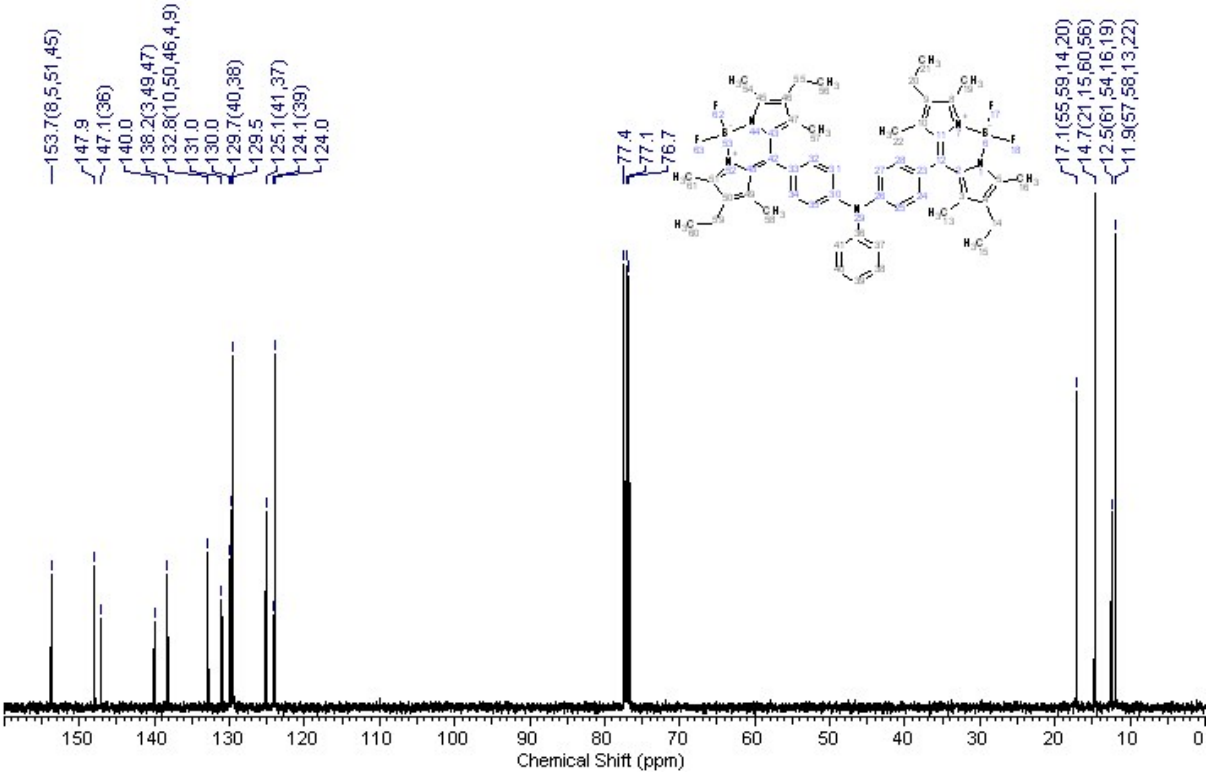

Figure S11 ^{13}C NMR ($CDCl_3$, 400MHz, 25°C) – **3**

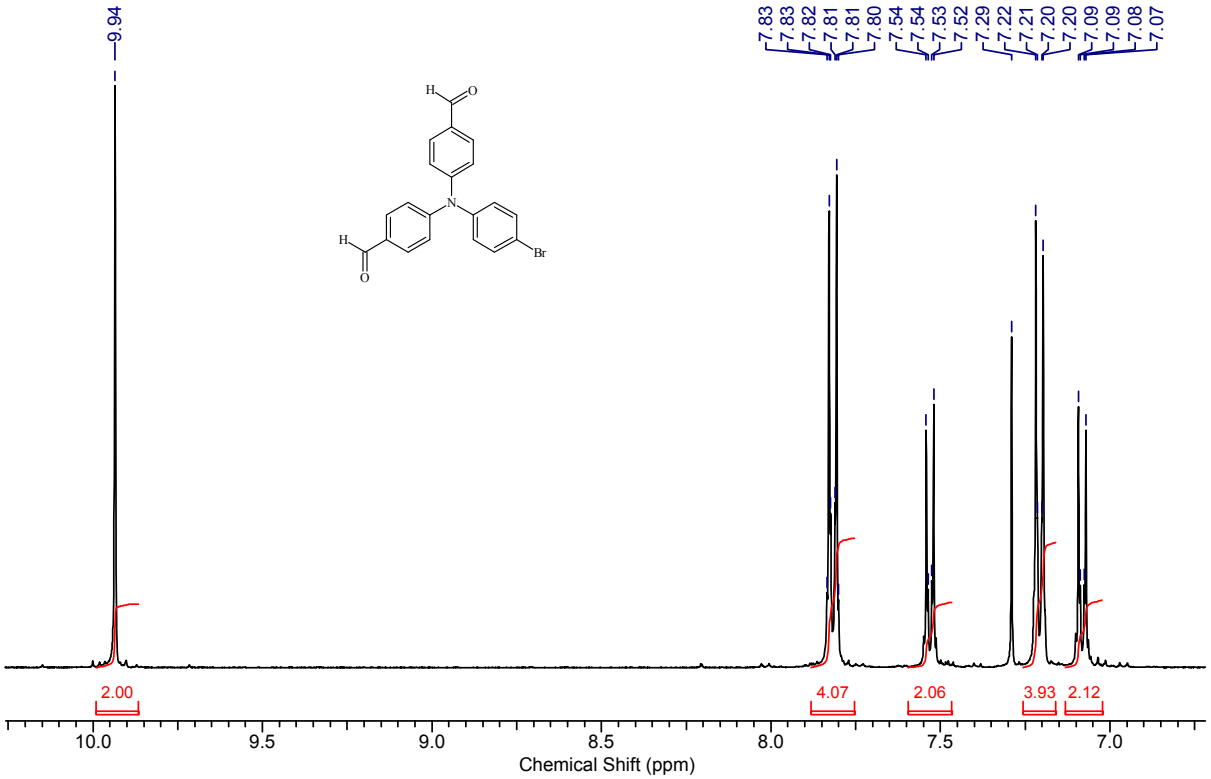

Figure S12 ^{1}H NMR ($CDCl_3$, 300MHz, 25°C) - *4,4'-[(4-bromophenyl)amino]bis-[benzaldehyde]*

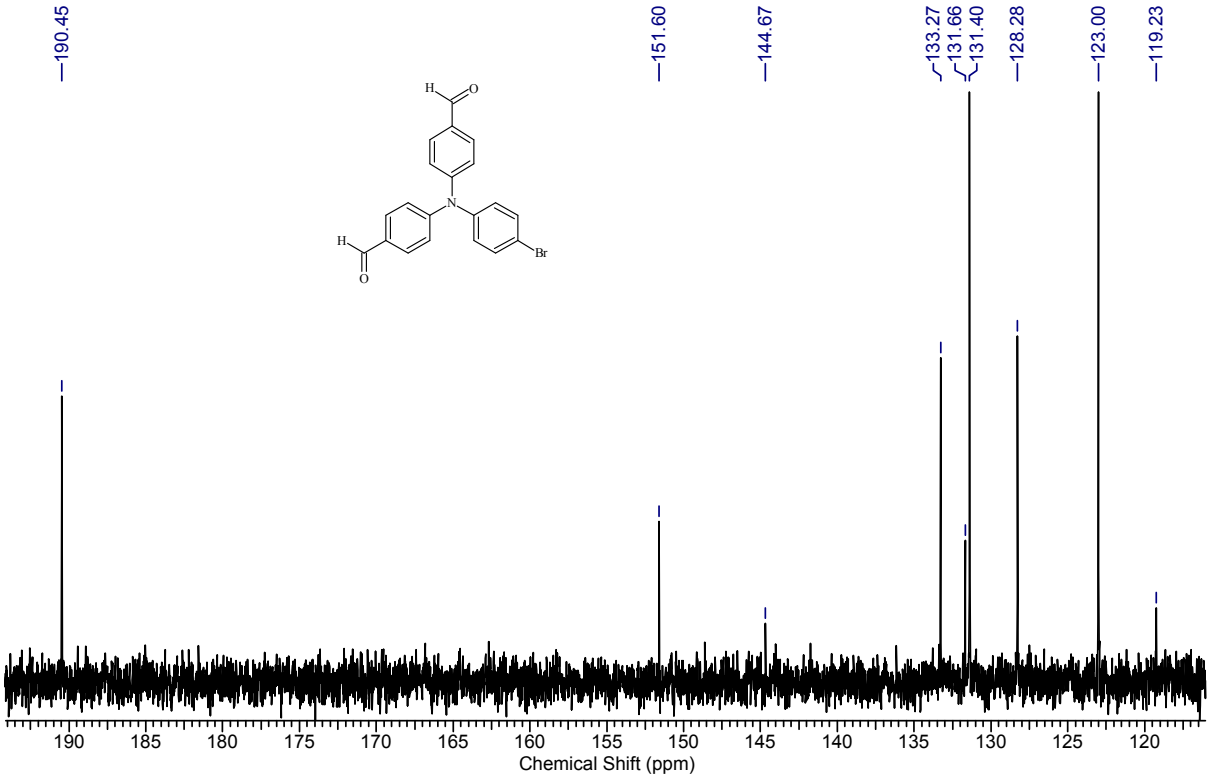

Figure S13 ^{13}C NMR ($CDCl_3$, 300MHz, 25°C) - *4,4'-[(4-bromophenyl)amino]bis-[benzaldehyde]*

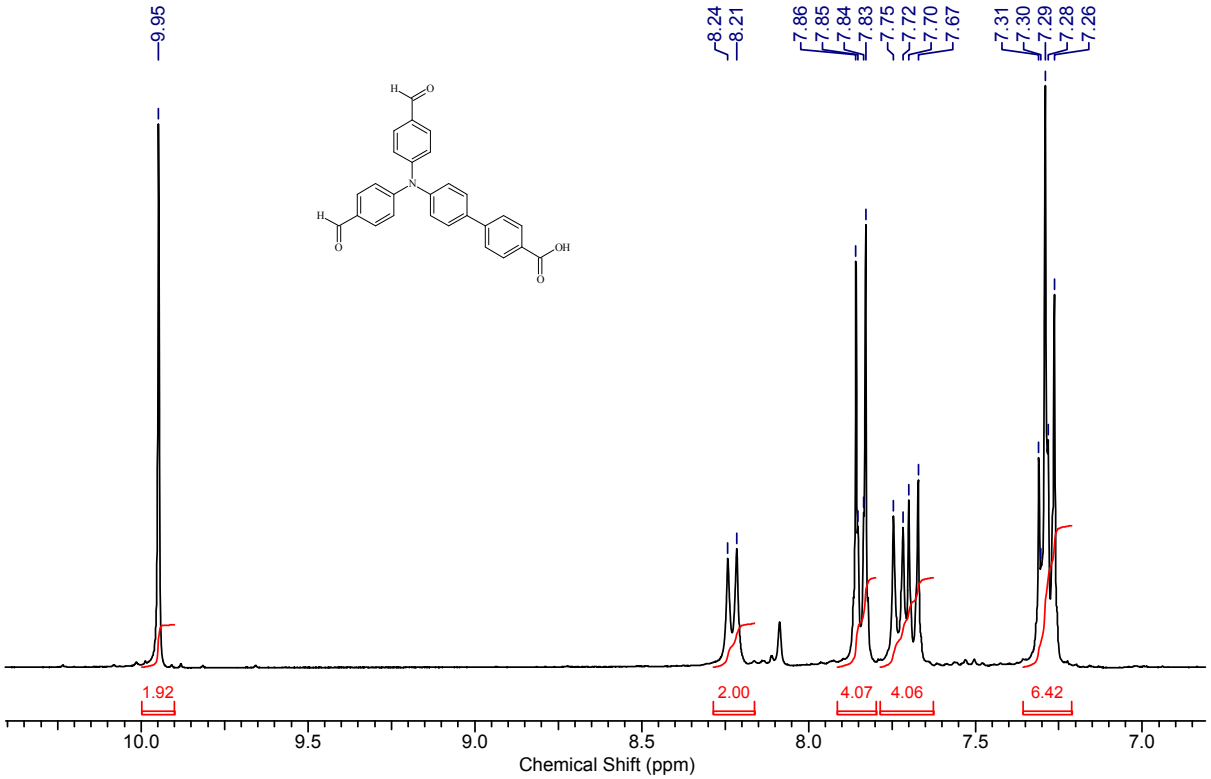

Figure S14 ^{1}H NMR ($CDCl_3$, 300MHz, 25°C) - 4,4'-[4-(4-carboxyphenyl)phenylamino]bis-[benzaldehyde]

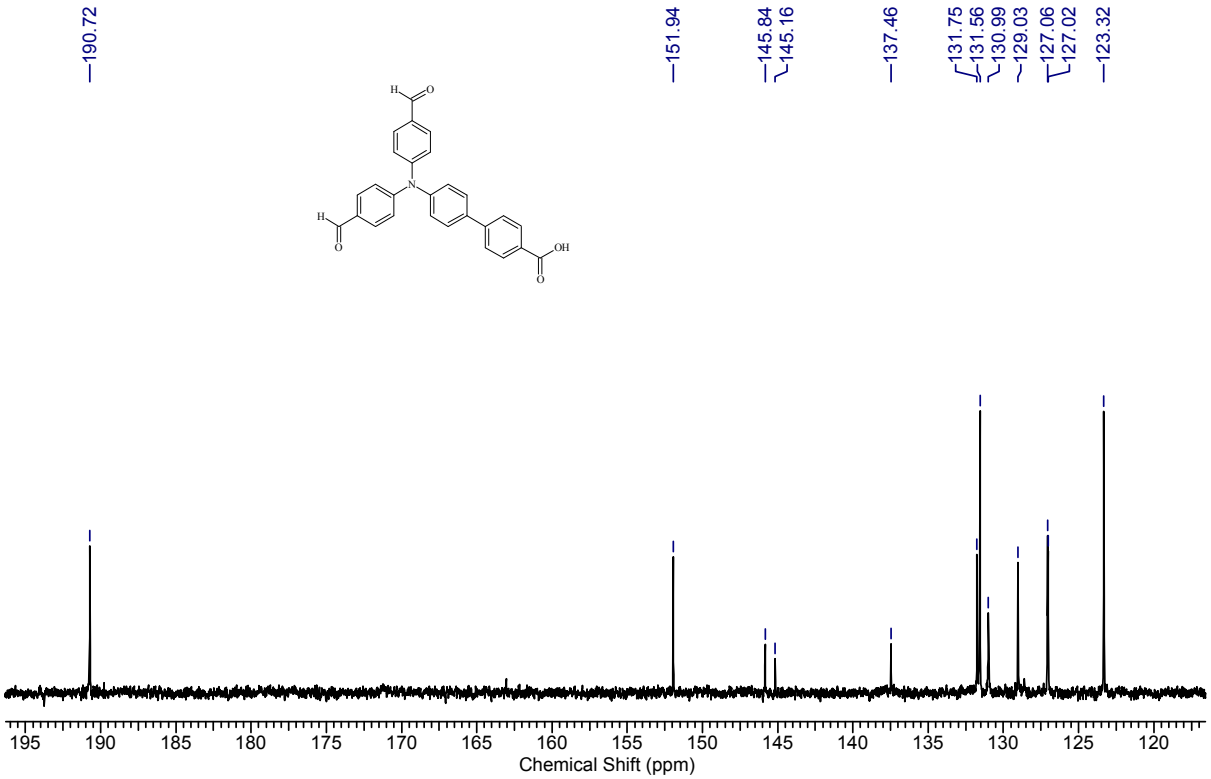

Figure S15 ^{13}C NMR ($CDCl_3$, 300MHz, 25°C) - 4,4'-[4-(4-carboxyphenyl)phenylamino]bis-[benzaldehyde]

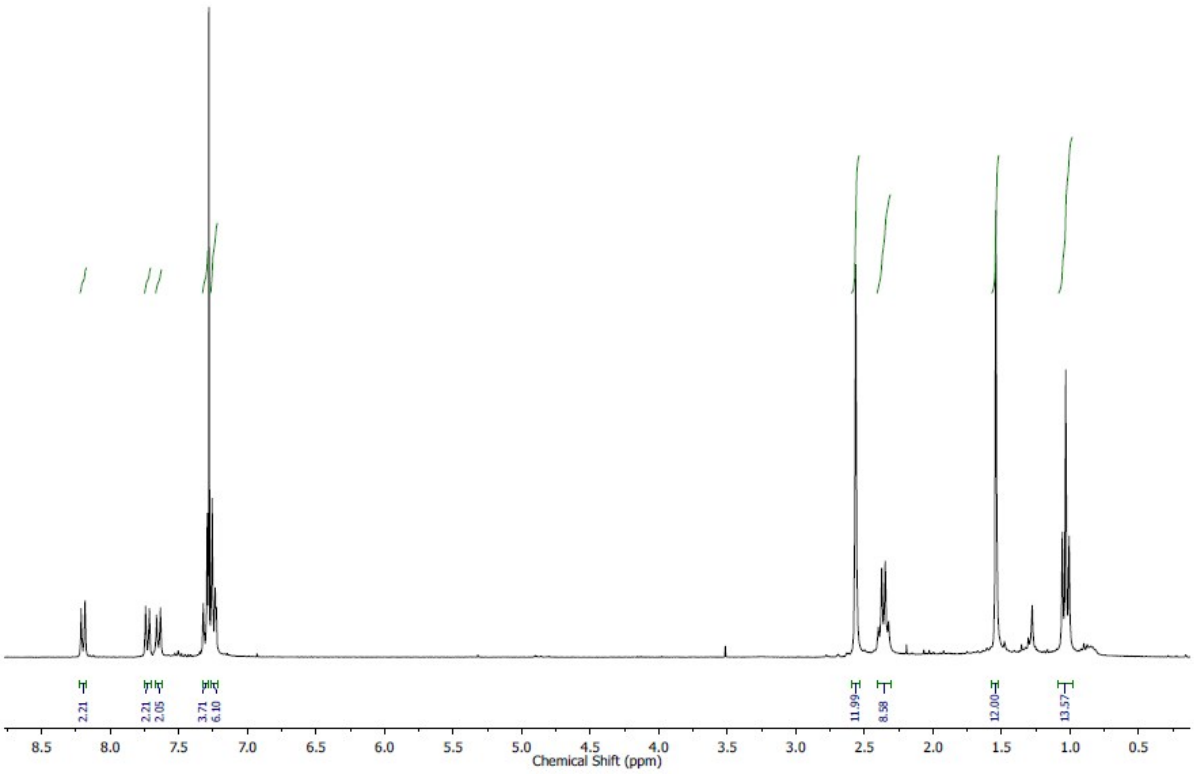

Figure S16 ^{1}H NMR ($CDCl_3$, 300MHz, 25°C) – **4**

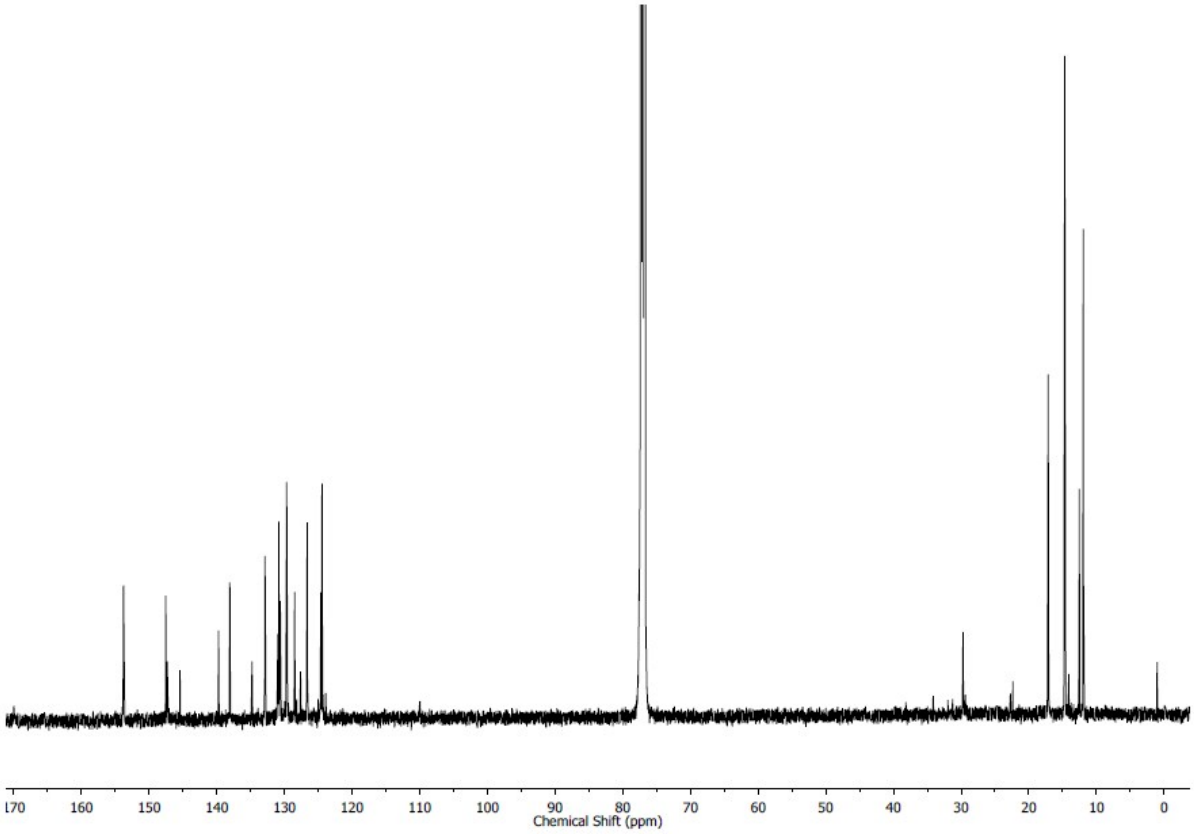

Figure S17 ^{13}C NMR ($CDCl_3$, 300MHz, 25°C) - **4**

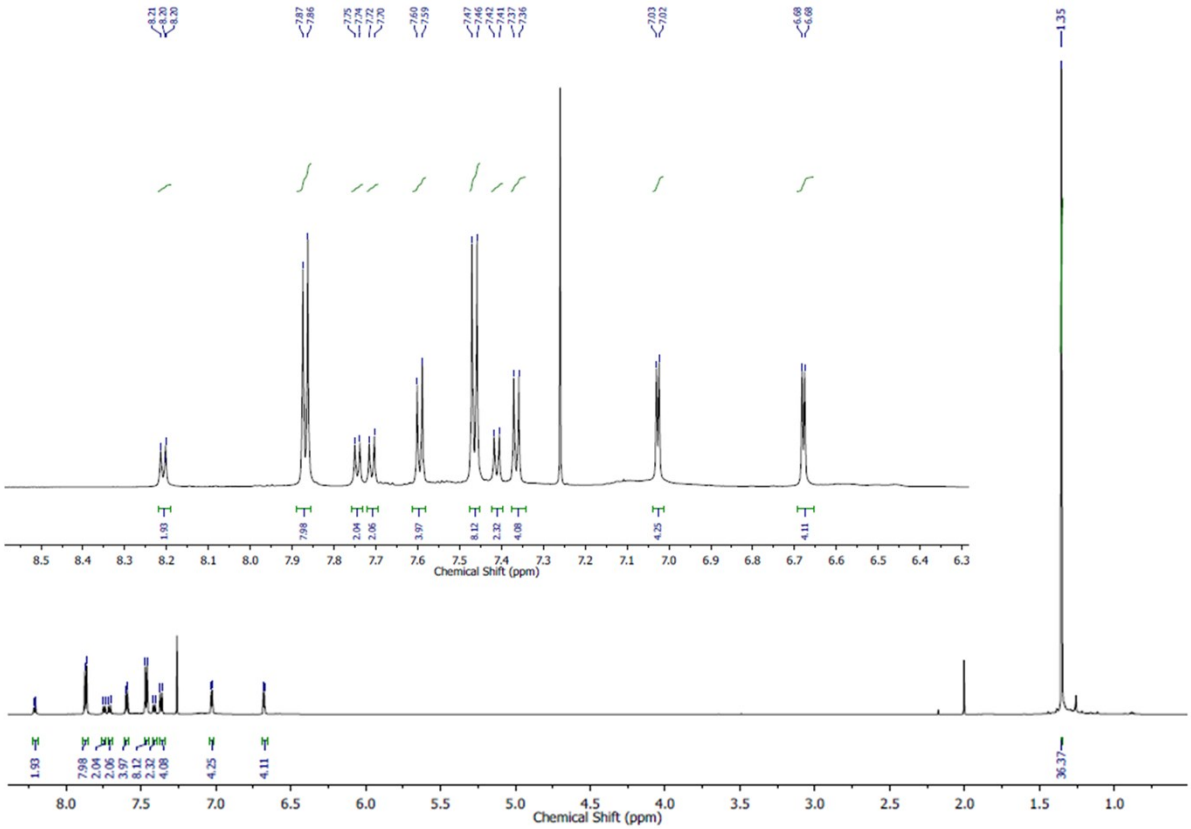

Figure S18 ^{1}H NMR ($CDCl_3$, 700MHz, 25°C) – **5**

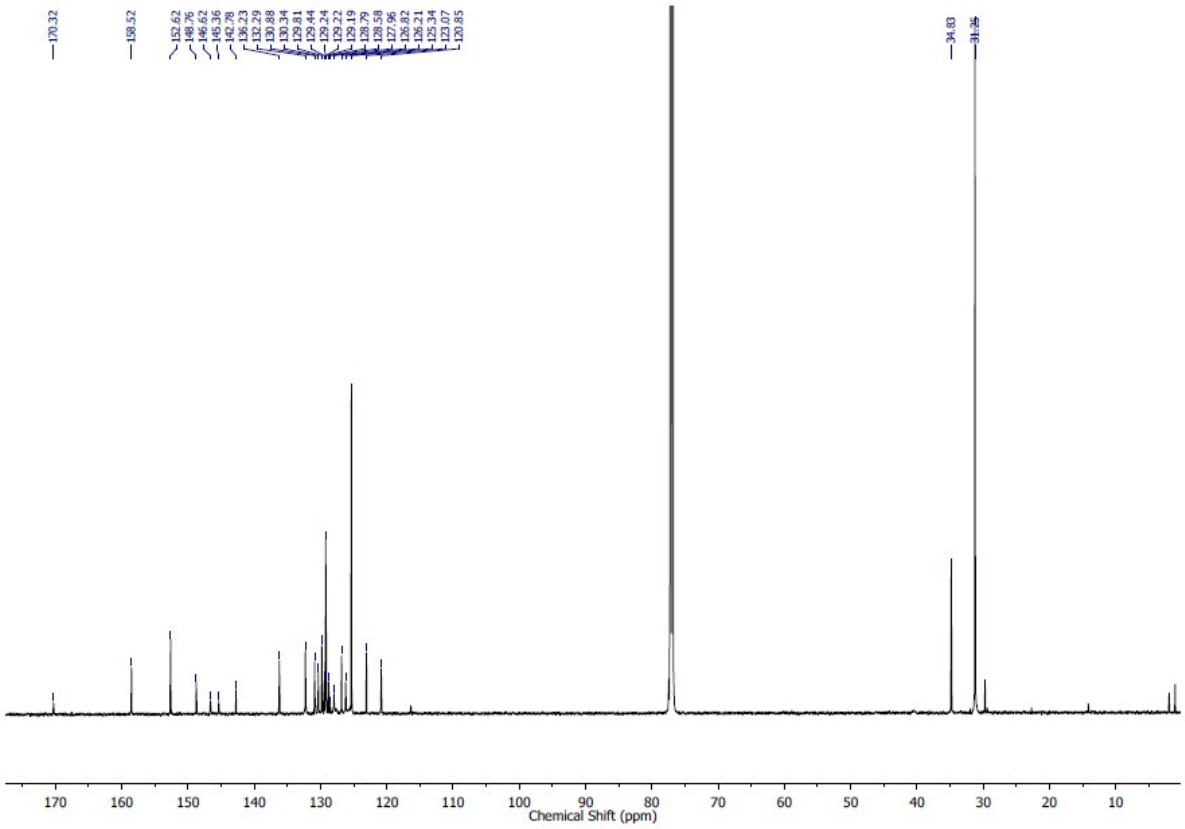

Figure S19 ^{13}C NMR ($CDCl_3$, 700MHz, 25°C) – **5**

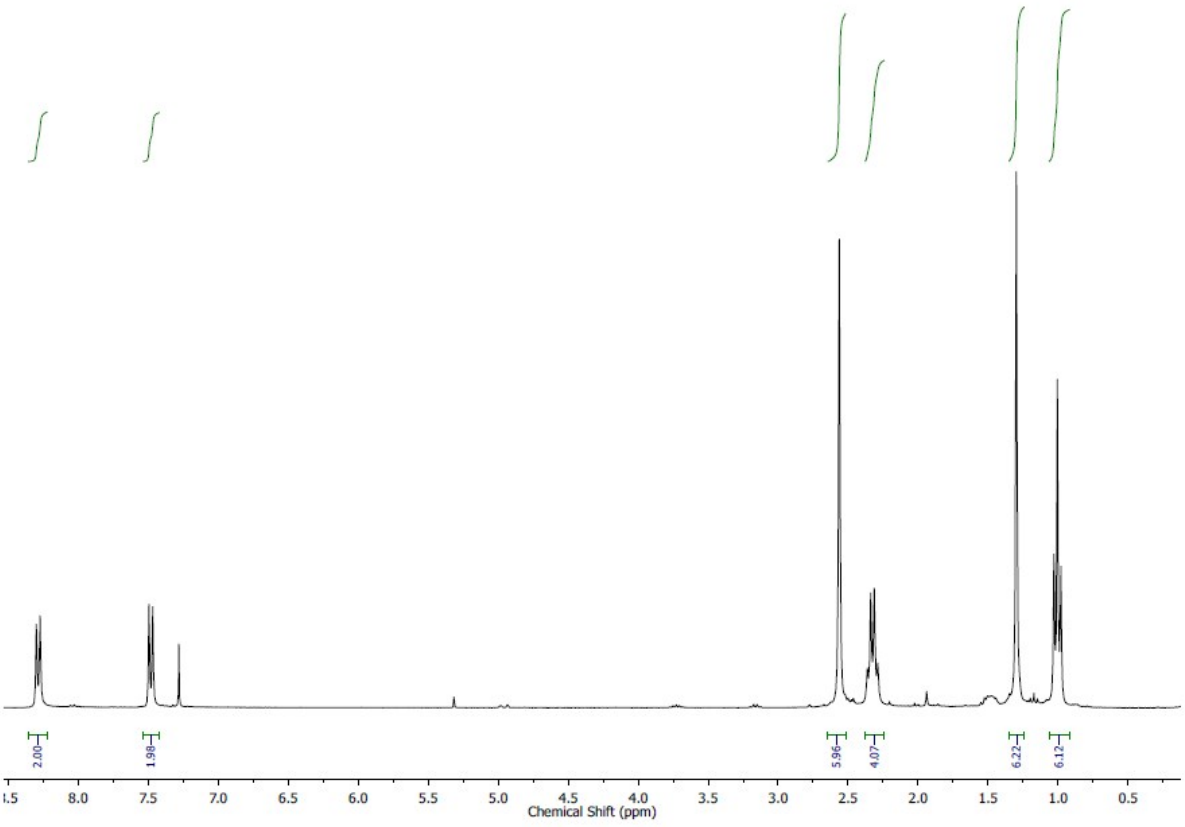

Figure S20 ^{1}H NMR ($CDCl_3$, 300MHz, 25°C) – **Bodipy-CO_2H**

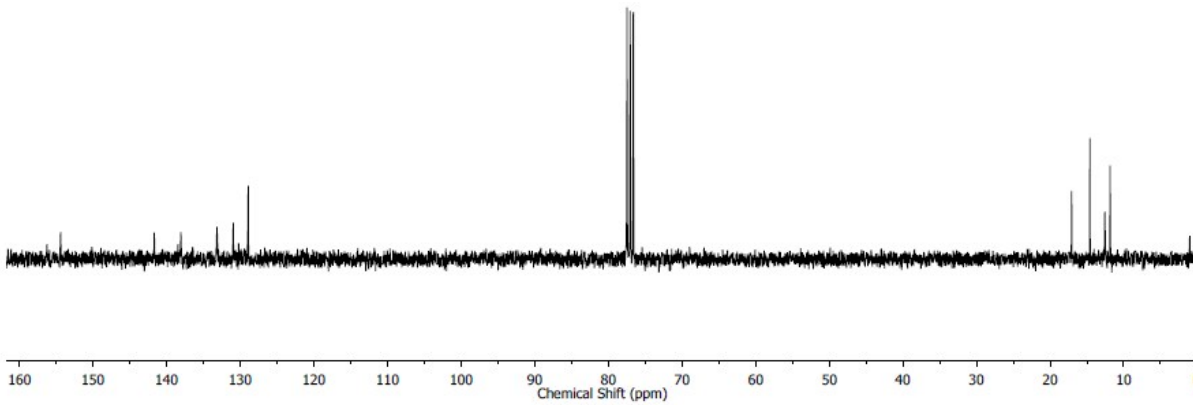

Figure S21 ^{13}C NMR ($CDCl_3$, 300MHz, 25°C) – **Bodipy-CO_2H**

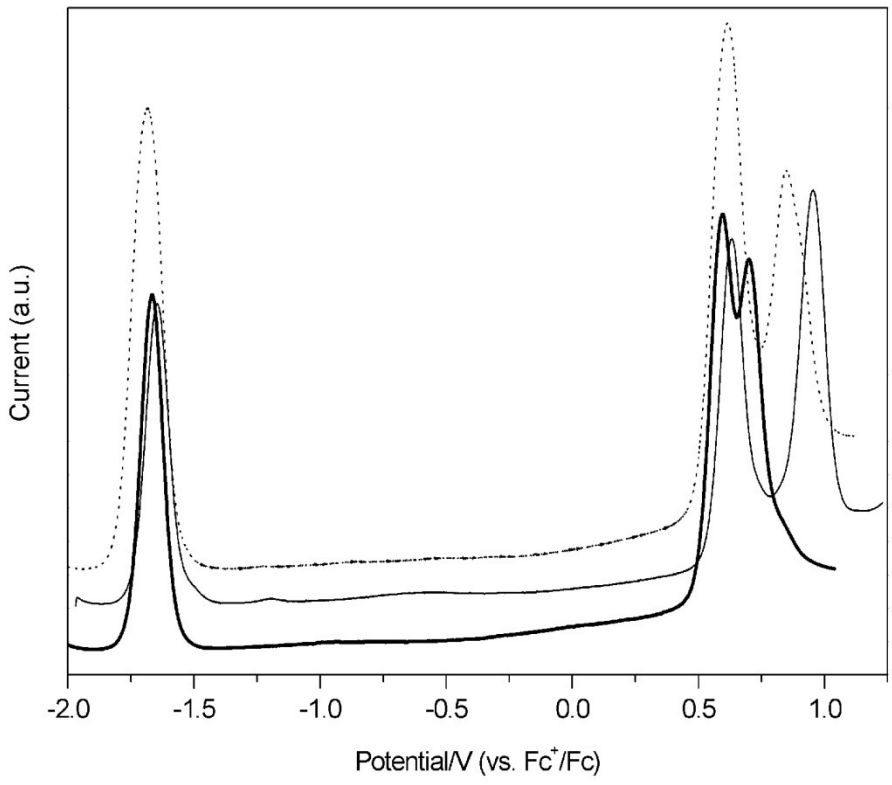

Figure S22 Square wave voltammograms recorded for **1** (thick solid line), **2** (thin solid line) and **3** (dotted line) in CH_2Cl_2 containing $[Bu_4N][ClO_4]$ (0.5 M)

Table S1 Square Wave Voltammetry data for **1-3**.

	1st reduction	1st oxidation	2nd oxidation
1	-1.68	+0.58	+0.69
2	-1.63	+0.63	+0.94
3	-1.68	+0.61	+0.84

Potentials reported vs. Fc^{+}/Fc

Table S2 Selected bond angles calculated for dyes **4-7.**

	Triphenylamine C-N-C	Dipyrromethene C=C-C=C	Bodipy N-B-N	bodipy F–B–F	Bodipy-spacer
4	119.73-121.195°	179.82-179.88°	106.75-106.80°	109.45-109.49°	89°, 85°
5	119.6-120.7°	176.3°,	107.8°;	111.2°	52°, 54°
6	119.02-120.53°	176.63°	106.72°	109.54°	84.41-85.02º
7	119.36-120.34°	175.32°,	107.66°;	111.31°	44.55-44.72°, 47.84-48.24°

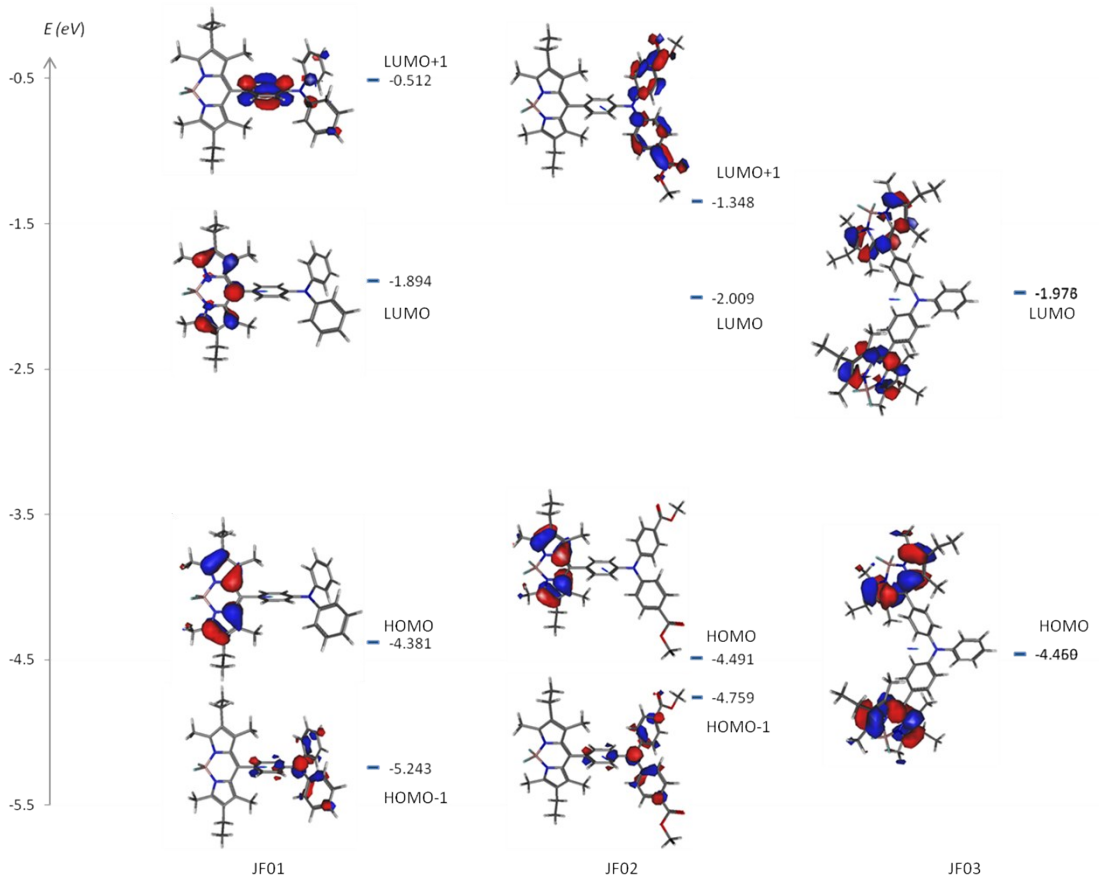

Figure S23 Calculated energy level diagram for **1**, **2** and **3** in vacuum.

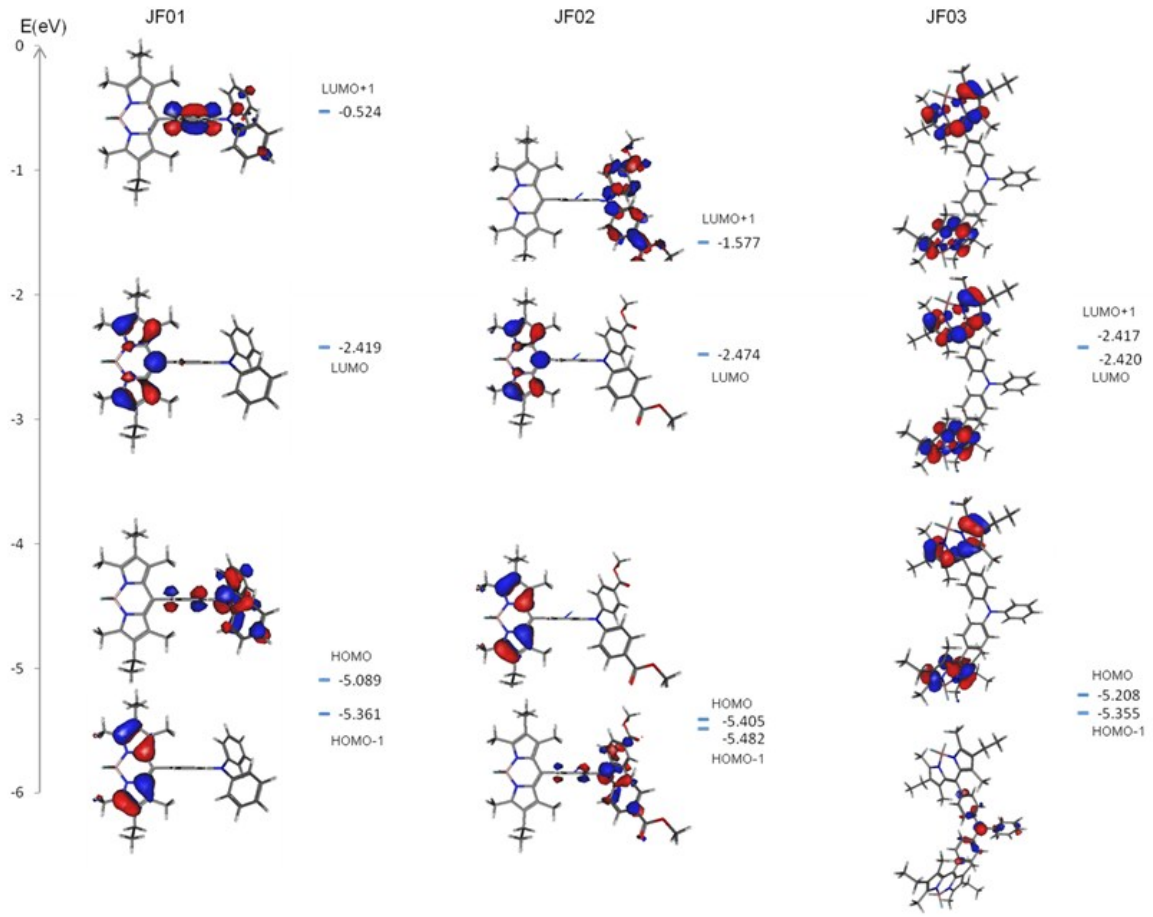

Figure S24 Calculated energy level diagram for **1**, **2** and **3** in dichloromethane. In the case of **1**, the calculated electron density of the HOMO is localised solely on the triphenylamine and the electron density of the HOMO–1 is located exclusively on the dipyrromethene. For **2** the electron-withdrawing nature of the ethyl ester lowers the calculated energy of the orbitals located on the triphenylamine by 392 meV so that the order is reversed and the HOMO is located on the dipyrromethene and the HOMO–1 is located on the triphenylamine. The calculated isodensity plots for **3** are similar to **1**, with electron density of the HOMO–1 and HOMO–2 distributed over each dipyrromethene moiety.

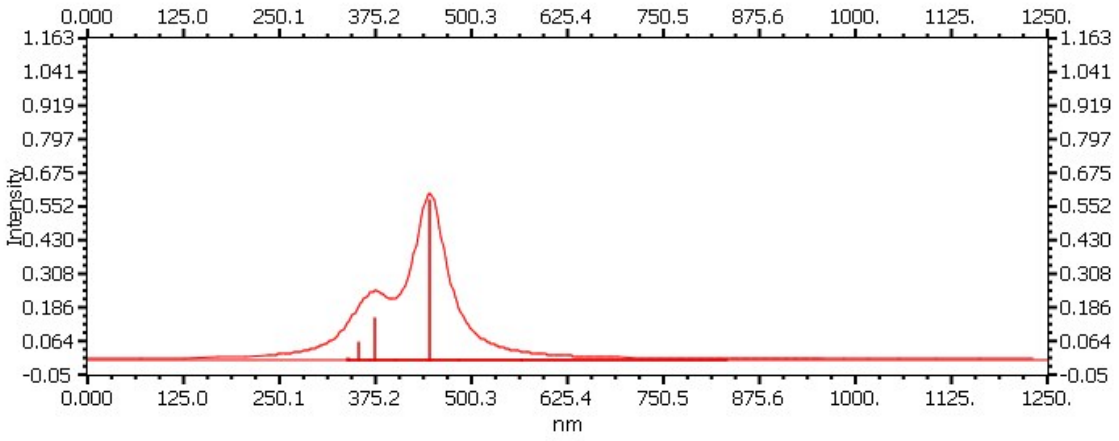

A. **1** 6 singlet and 6 triplet transitions

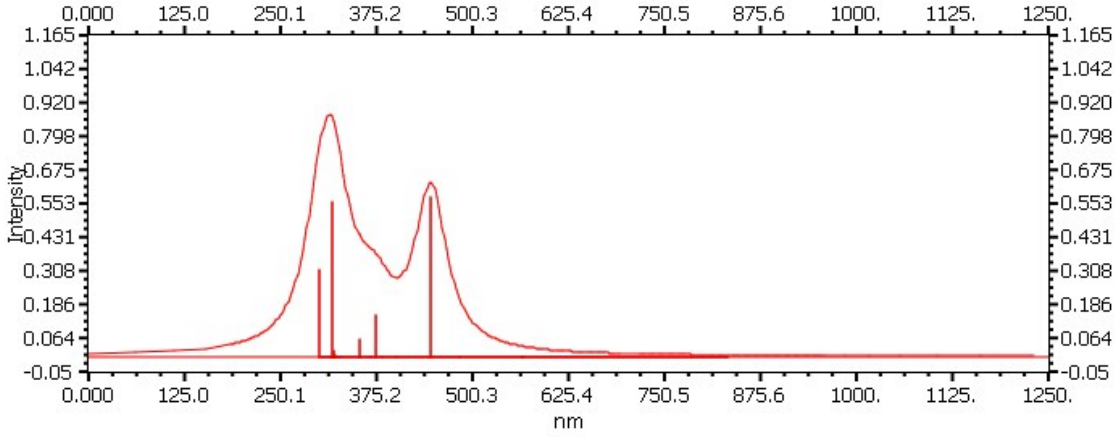

B. **1** 10 singlet and 10 triplet transitions

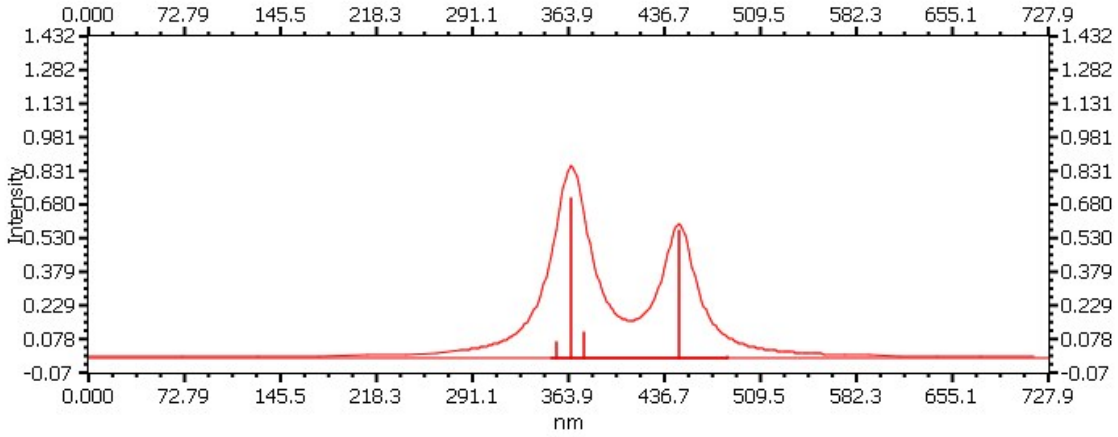

C. **2** 6 singlet and 6 triplet transitions

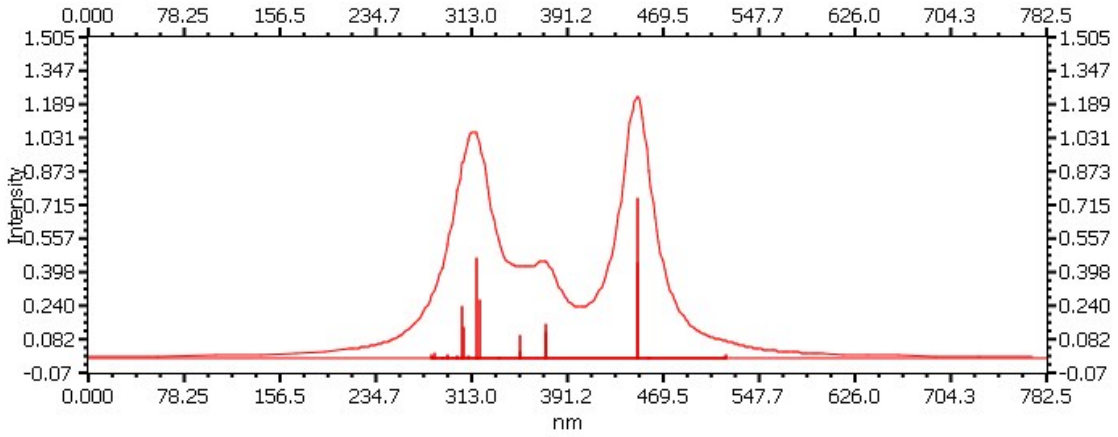

D. **3** 30 singlet transitions

Figure S25 Predicted electronic absorption spectra determined by TD-DFT (PCM TD) in dichloromethane solvent (Lorentzian lineshape). The lowest energy singlet excitations, $S_0 \rightarrow S_1$, appearing at 447 nm (**1**) and 448 nm (**2** and **3**), correspond to HOMO-1→LUMO (**1**) and HOMO-LUMO (**2**) and HOMO-1→LUMO and HOMO-2→LUMO+1 (**3)** transitions localised on the bodipy and are therefore π-π* in character. An excitation energy of 366 nm was calculated for the HOMO-1→LUMO+1 transition ($S_0 \rightarrow S_2$) for **2** which is triphenylamine centred, but no transitions from orbitals on the triphenylamine to orbitals on the bodipy with strong oscillator strengths were calculated, confirming that the two components are fully decoupled. The absence of charge-transfer character is likely to be due to the methyl substituents hindering the rotation of the bodipy around the aniline. The oscillator strength for this transition is significantly higher for **3** (0.7528) than for **1** (0.5819) and **2** (0.5686) on account of the joint contribution of both bodipy moieties to the transition.

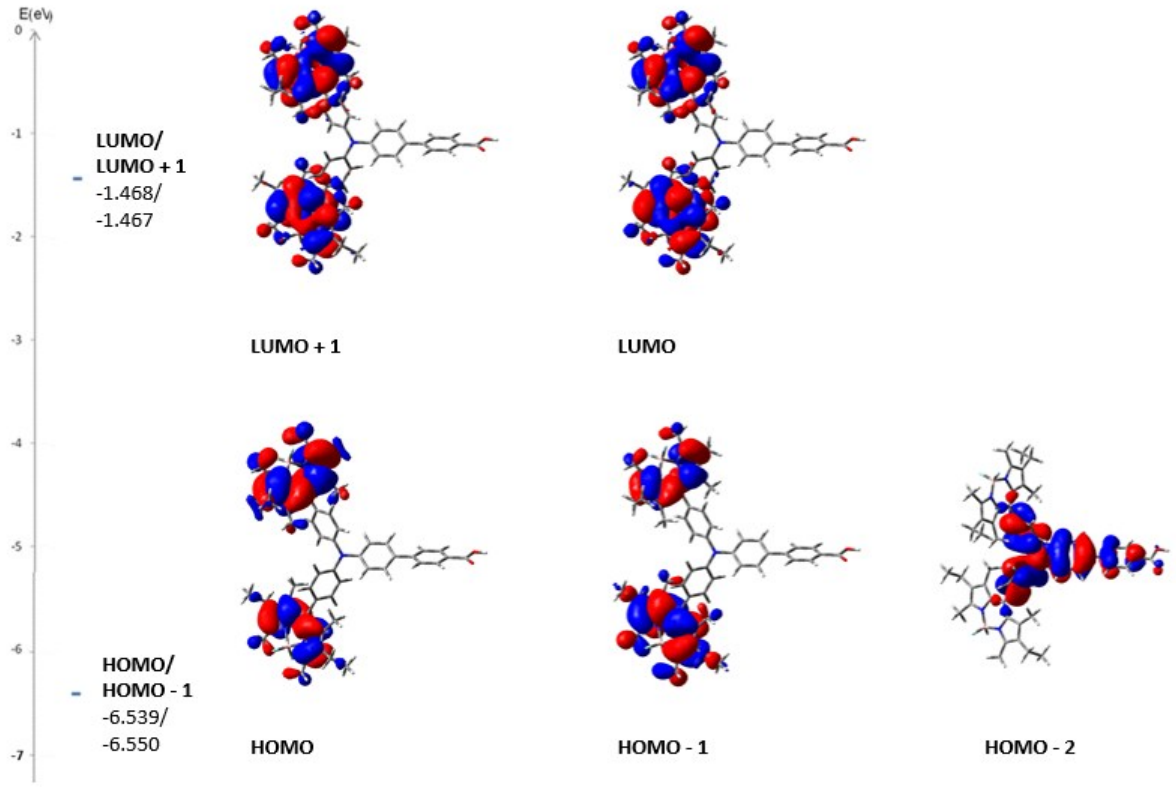

Figure S26 Calculated energy level diagram for **4** in dichloromethane (calculated using CAM-B3LYP/6-31G(d).

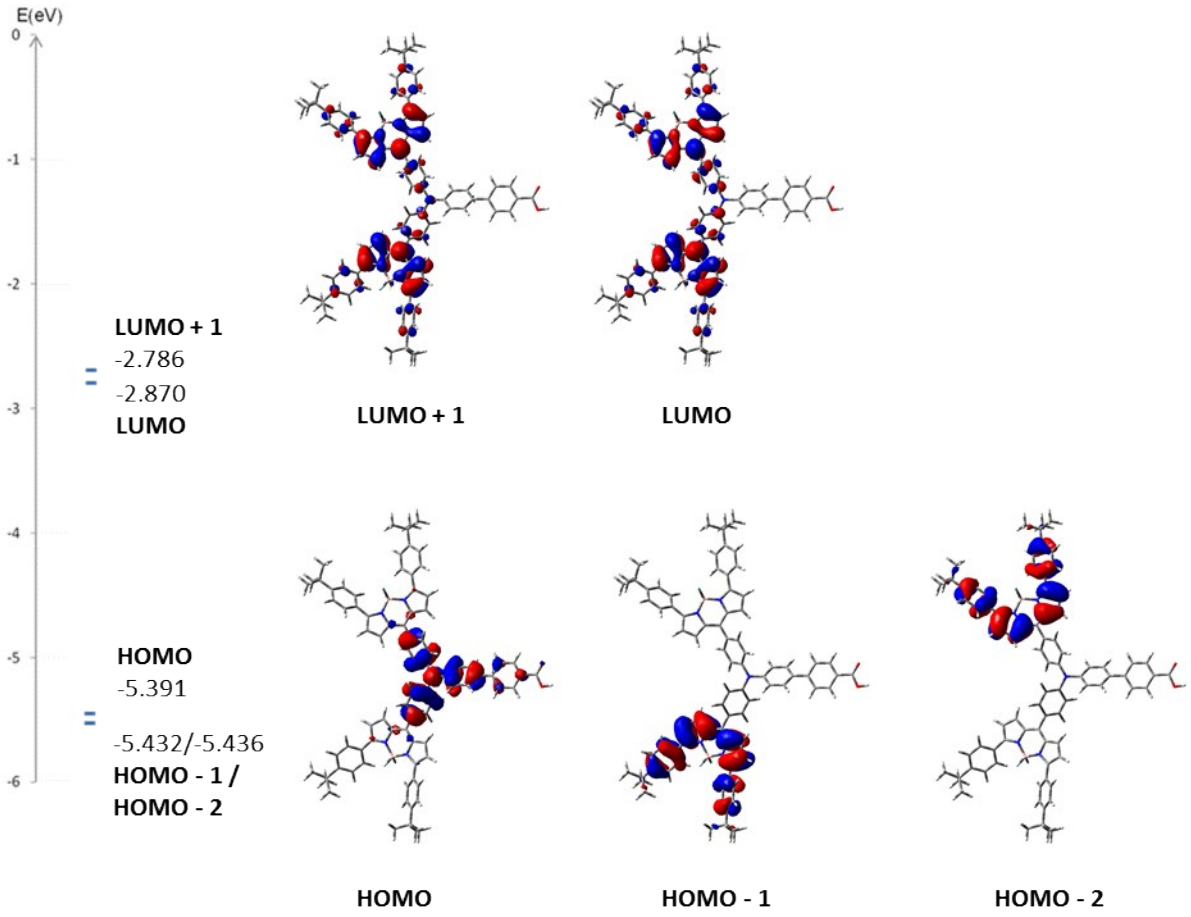

Figure S27 Calculated energy level diagram for **5** in dichloromethane (calculated using B3LYP/6-31G(d).

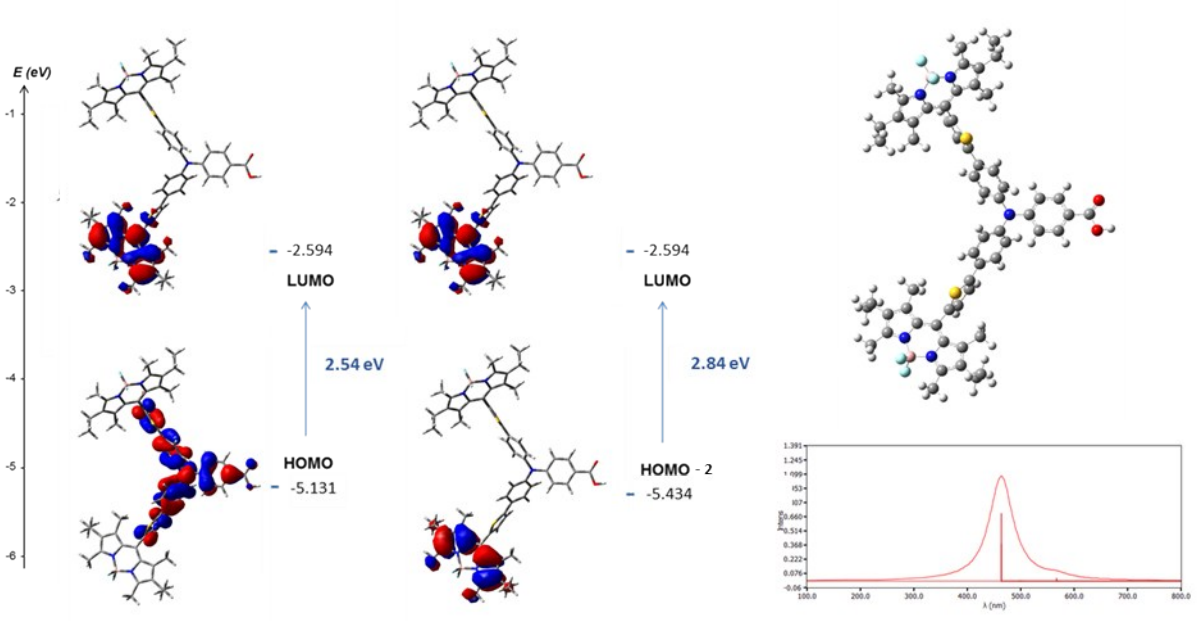

Figure S28. Optimised geometry and calculated principle energy transitions for **6** determined by DFT and TD-DFT (in dichloromethane solvent, calculated using CAM-B3LYP/6-31G(d)).

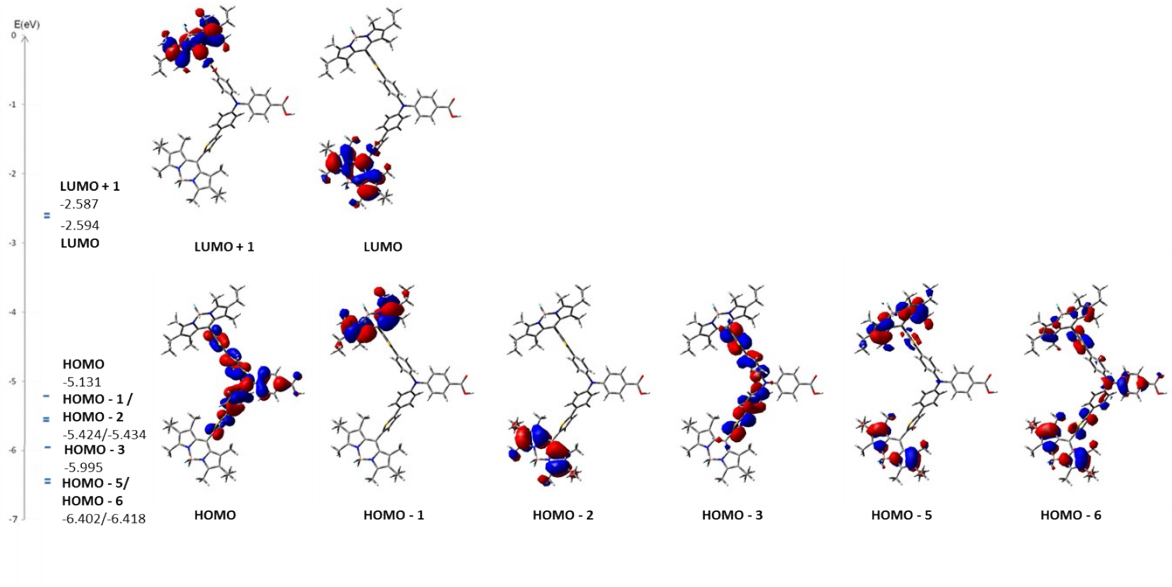

Figure S29 Calculated energy level diagram for **6** in dichloromethane (calculated using B3LYP/6-31G(d).

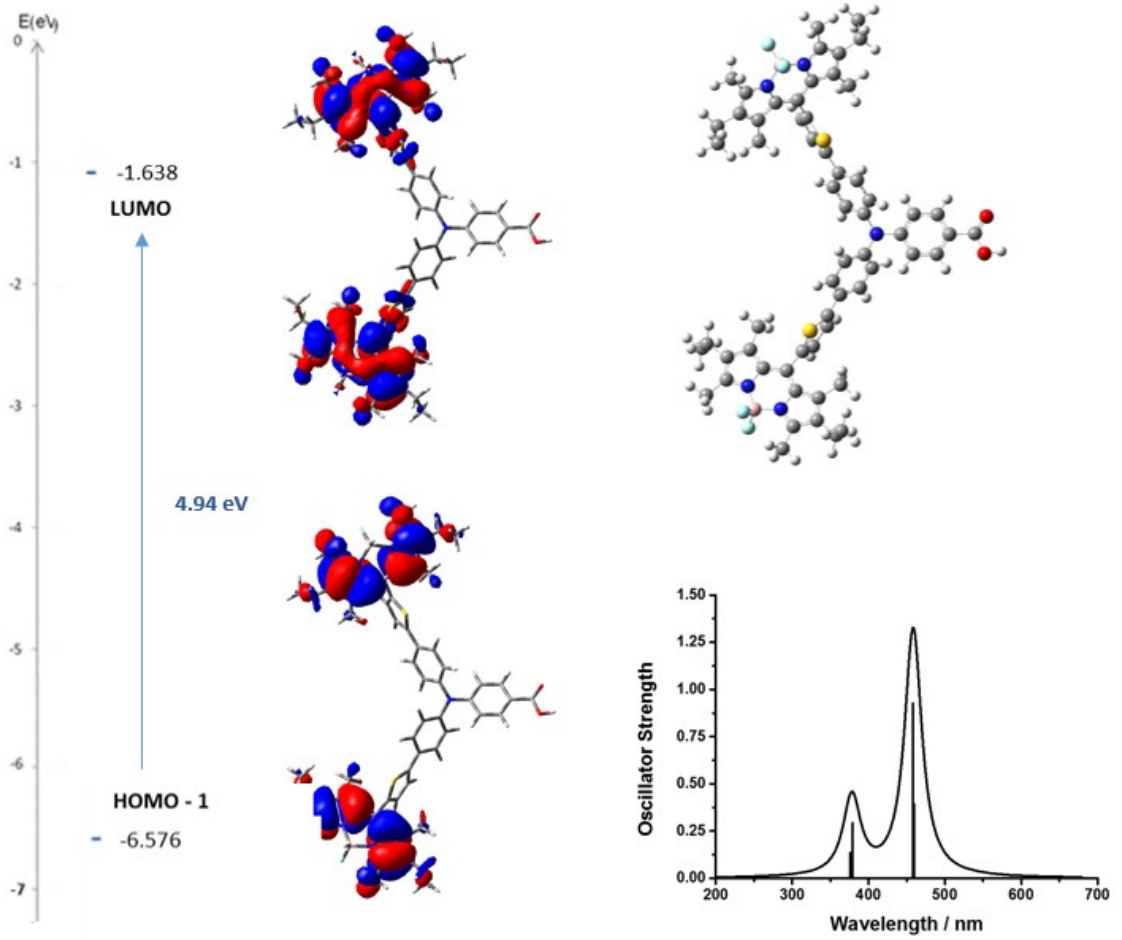

Figure S30 Optimised geometry and calculated principle energy transitions for **6** determined by DFT and TD-DFT (in dichloromethane solvent) using CAM-B3LYP/6-31G(d).

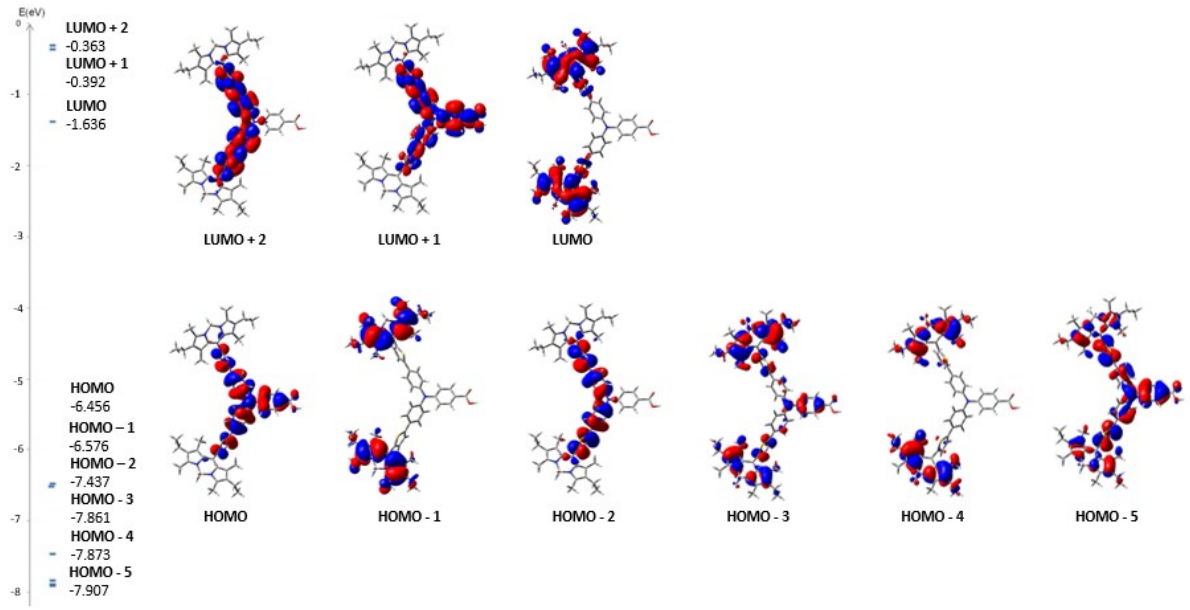

Figure S31 Calculated energy level diagram for **6** using CAM-B3LYP/6-31G(d).

.

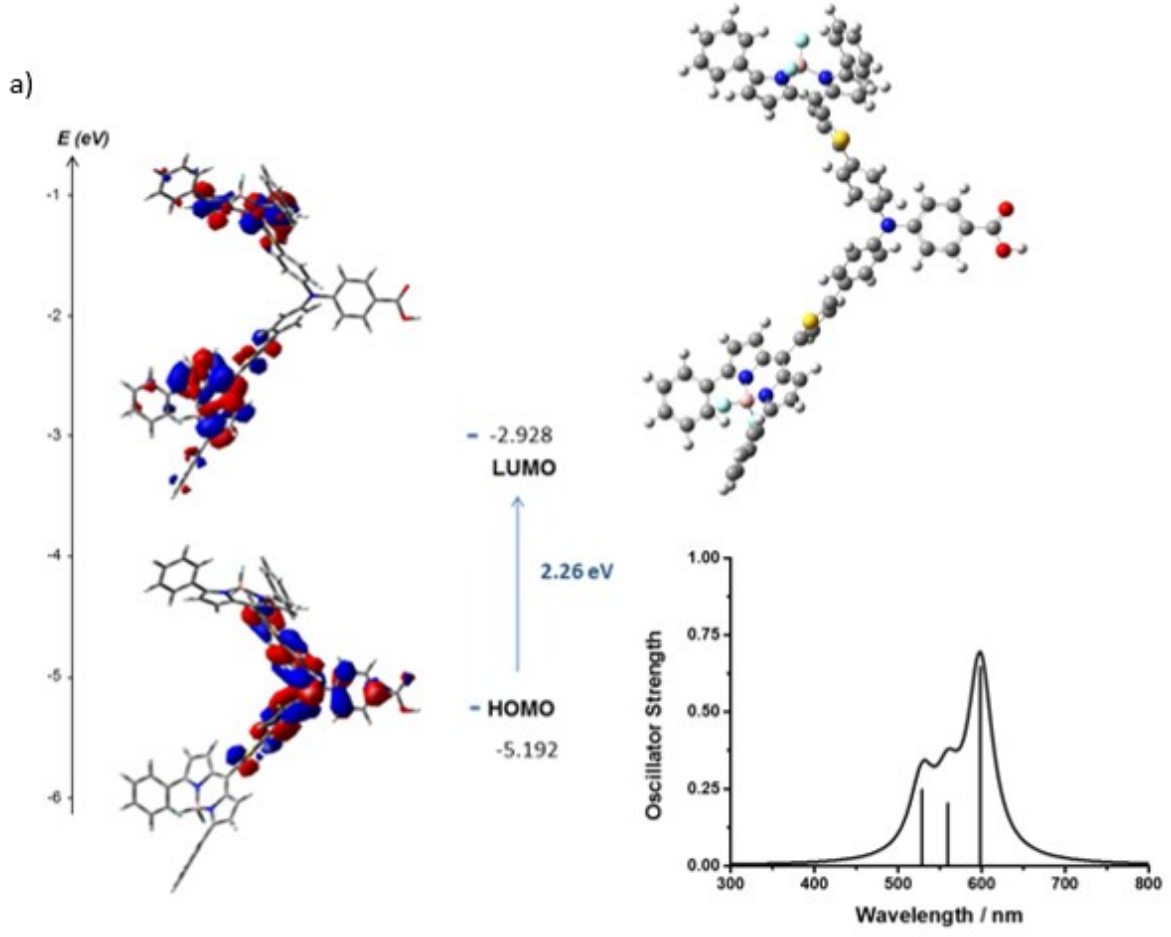

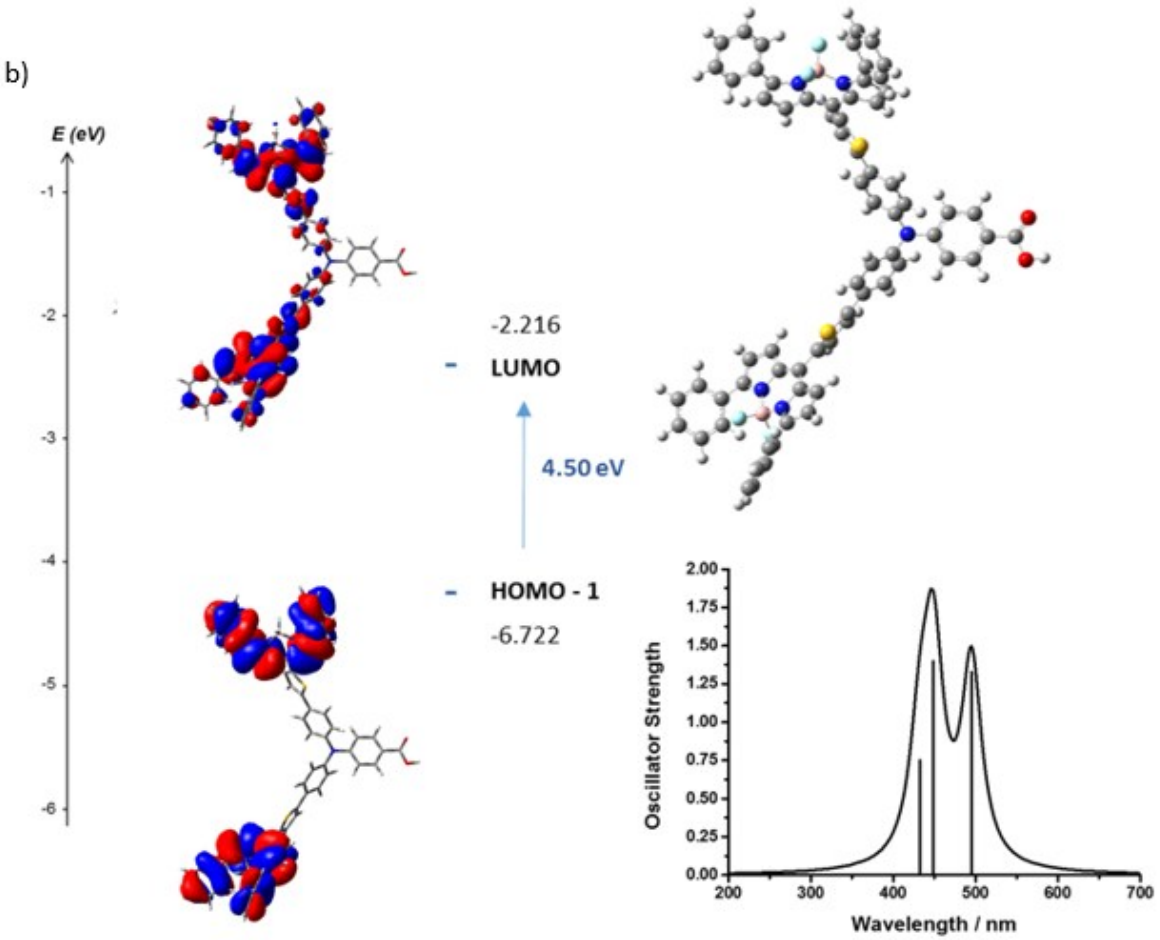

Figure S32 Optimised geometry and calculated principle energy transitions for **7** determined by DFT and TD-DFT (in dichloromethane solvent, CPCM solvation model) using a: B3LYP/6-31G(d) and b: CAM-B3LYP/6-31G(d).

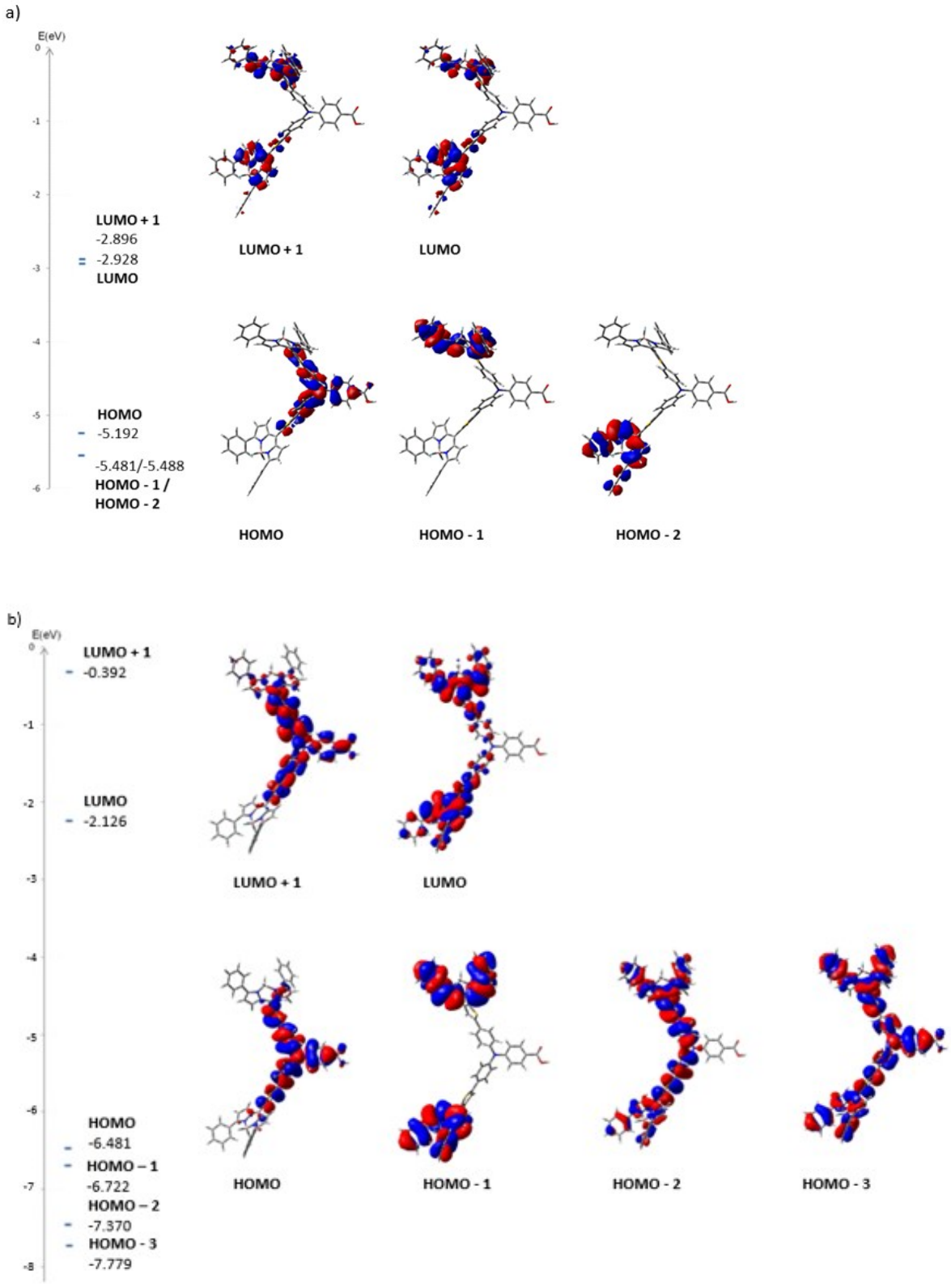

Figure S33 Calculated energy level diagram for **7** in dichloromethane using a: B3LYP/6-31G(d) and b: CAM-B3LYP/6-31G(d).

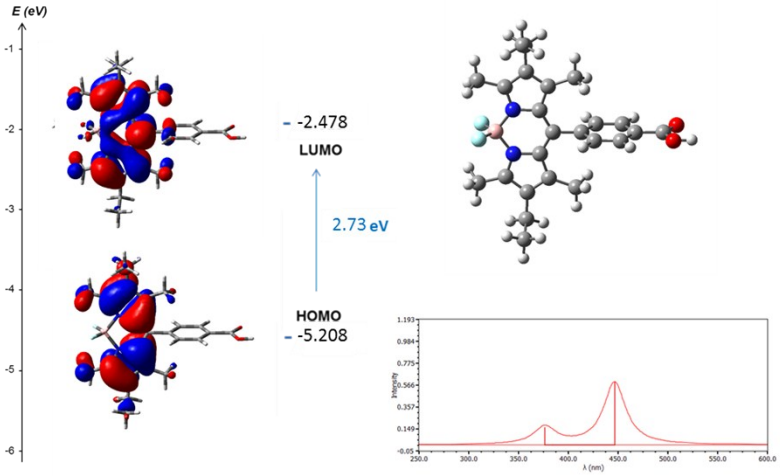

Figure S34 Optimised geometry and calculated principle energy transitions for **Bodipy-CO_2H** determined by DFT and TD-DFT (in dichloromethane solvent, calculated using B3LYP/6-31G(d).

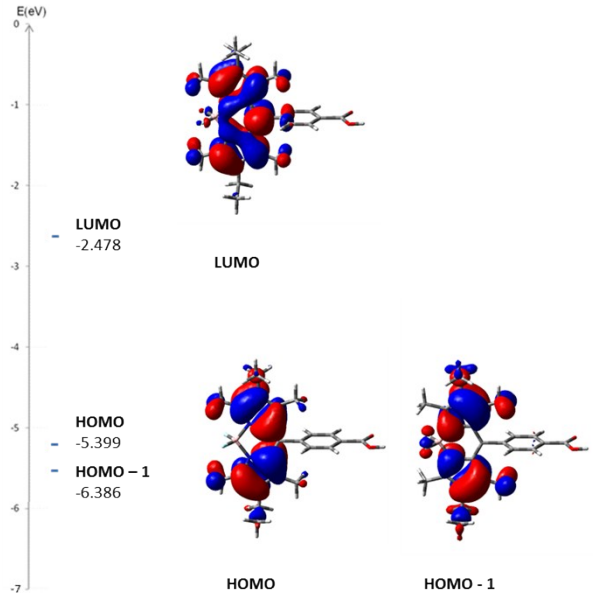

Figure S35 Calculated energy level diagram for **Bodipy-CO_2H** in dichloromethane, calculated using B3LYP/6-31G(d).

Table S3 Calculated principle (singlet) energy transitions determined by TD-DFT for **1-7** and **Bodipy-CO_2H** and their contributions to the electronic spectra in dichloromethane solvent. All transitions were calculated using B3LYP/6-31G(d) unless otherwise stated. [a]Calculated using CAM-B3LYP/6-31G(d).

Dye	Energy /eV (oscillator strength)	λ /nm	Composition	Contribution (%)
1	2.77 (0.5819)	447	HOMO-2→LUMO	7
			HOMO-1→LUMO	70
	3.30 (0.1478)	375	HOMO-2→LUMO	84
			HOMO-1→LUMO	4
	3.50 (0.0643)	354	HOMO-3→LUMO	90
	2.77 (0.5686)	448	HOMO-2→LUMO	6.6
			HOMO→LUMO	69
	3.30 (0.1131)	376	HOMO-2→LUMO	83
			HOMO→LUMO	3.7
	3.38 (0.7164)	366	HOMO-1→LUMO+1	90
3	2.77 (0.7528)	449	HOMO-1→LUMO	45
			HOMO-2→LUMO+1	50
	3.32 (0.1594)	374	HOMO-3→LUMO	35
			HOMO-4→LUMO+1	36
4[a]	2.78 (0.4343)	446	HOMO-1→LUMO	45
			HOMO→LUMO+1	47
	2.78 (0.8999)	445	HOMO-1→LUMO	46
			HOMO-1→LUMO	5
			HOMO-1→LUMO	44
	3.47 (0.0224)	357	HOMO-1→LUMO	67
	3.70 (0.0464)	335	HOMO-2→LUMO	48
5	2.09 (0.6505)	592	HOMO→LUMO	99
	2.23 (0.1990)	554	HOMO→LUMO+1	99
	2.34 (0.2488)	529	HOMO-1→LUMO	77

6[a]	2.69 (0.9390)	459	HOMO-1→LUMO	84
	2.70 (0.9257)	458	HOMO-1→LUMO	55
	3.27 (0.2925)	379	HOMO-5→LUMO	3
			HOMO→LUMO	30
			HOMO→LUMO+2	3
	3.29 (0.1342)	376	HOMO→LUMO	52
7	1.92 (0.6845)	645	HOMO→LUMO	95
	2.00 (0.2467)	618	HOMO→LUMO+1	95
	2.36 (0.2470)	525	HOMO-1→LUMO	13
			HOMO-1→LUMO+1	2
			HOMO-2→LUMO	44
Bodipy-CO_2H	2.77 (0.5965)	447	HOMO-1→LUMO	7
			HOMO→LUMO	94
	3.22 (0.1675)	385	HOMO-1→LUMO	92

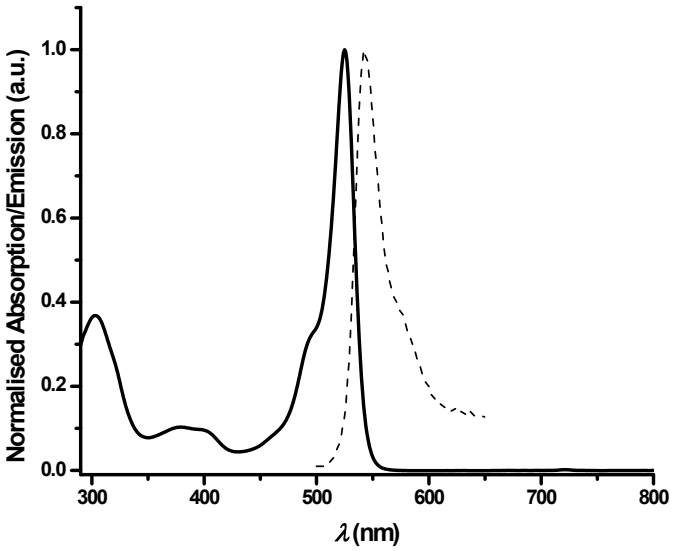

Figure S36 Normalised absorption and emission spectra for **1** in dichloromethane.

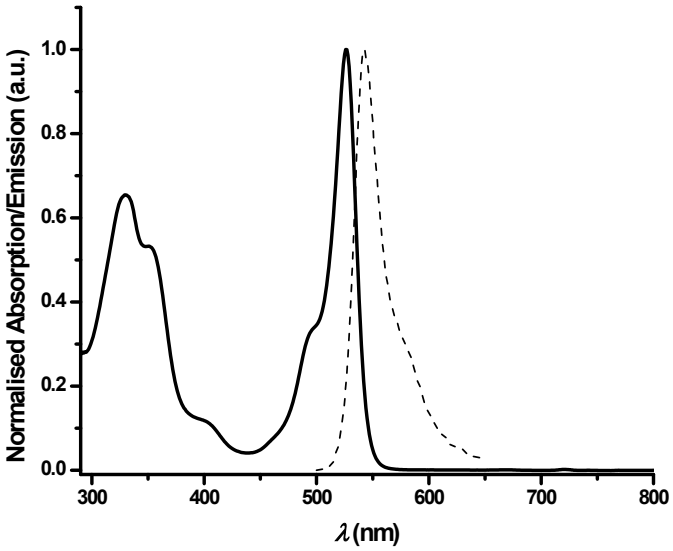

Figure S37 Normalised absorption and emission spectra for **2** in dichloromethane.

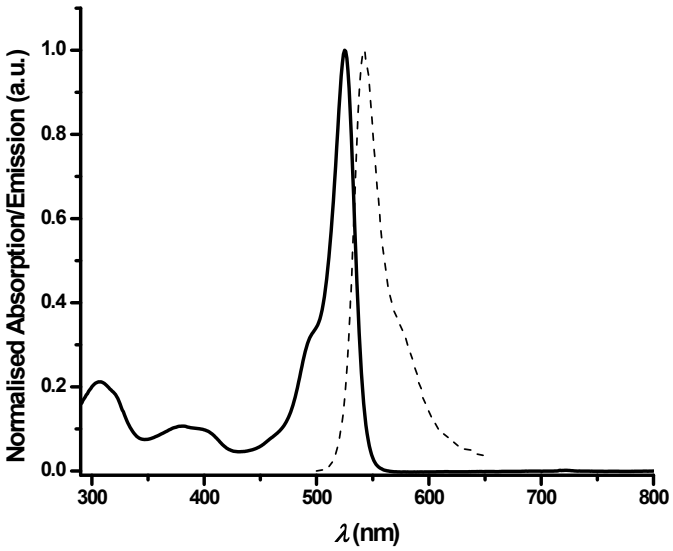

Figure S38 Normalised absorption and emission spectra for **3** in dichloromethane.

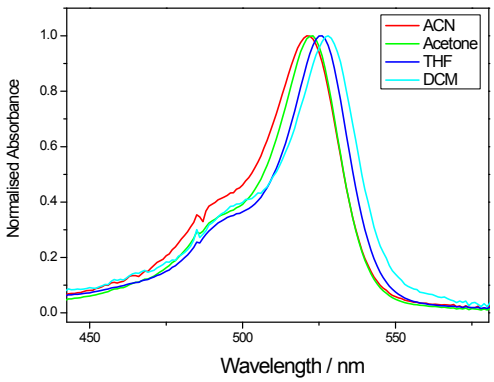

Figure S39 Normalised absorption spectra for **Bodipy-CO_2H** in different solvents.

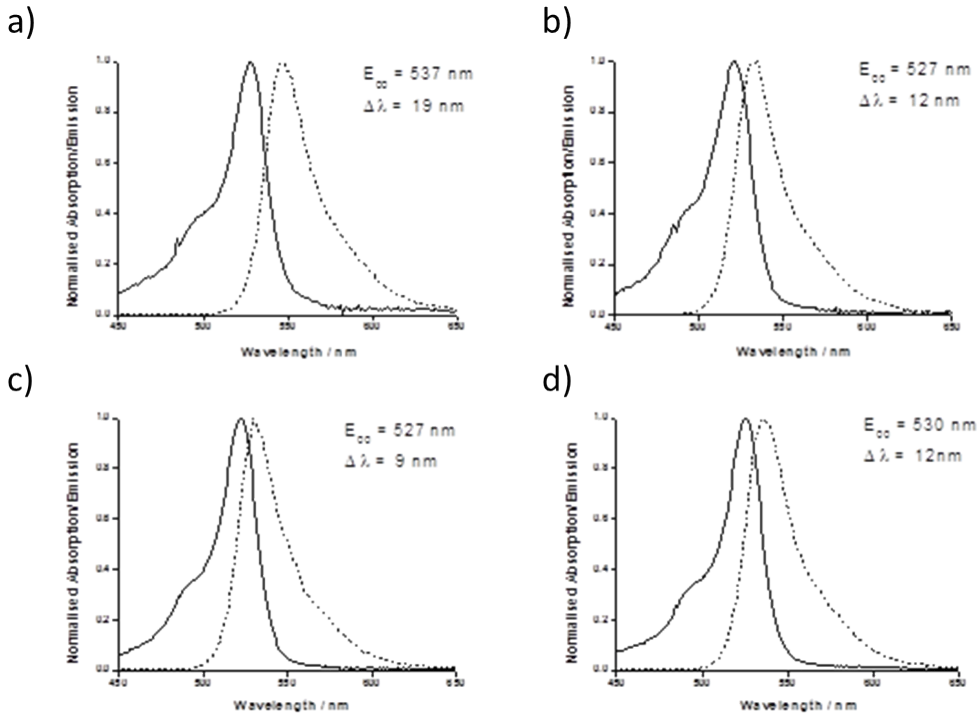

Figure S40 Normalised absorption and emission spectra (λ_{ex} = 400 nm) of **Bodipy-CO_2H** in a) CH_2Cl_2, b) CH_3CN, c) acetone and d) THF.

Table S4 Solvent dependence on the maximum emission wavelength and lifetime of the excited state for **1**, **3**, and **Bodipy-CO_2H**. [a]weakly/non-emissive.

	λ_{em} (nm) ($\Delta\lambda$)				τ_{em} (ns)			
	CH_3CN	$(CH_3)_2CO$	THF	CH_2Cl_2	CH_3CN	$(CH_3)_2CO$	THF	CH_2Cl_2
1	-[a]	536 (14)	537 (13)	543 (17)	3.4	2.9	4.8	5.5
3	530 (10)	530 (8)	535 (12)	544 (19)	1.4	4.0	4.4	5.5
Bodipy-CO_2H	533 (12)	531 (9)	536 (10)	547 (19)	4.7	4.6	3.9	3.3

Table S5 Solvent dependence on the maximum emission wavelength for **4-7**. [a]weakly/non-emissive.

	λ_{em} (nm) ($\Delta\lambda$)			
	CH_3CN	$(CH_3)_2CO$	THF	CH_2Cl_2
4	545 (23)	531 (8)	538 (14)	542 (16)
5	-[a]	586 (26)	602 (37)	600 (39)
6	549 (13)	546 (9)	551 (12)	551 (15)
7	-[a]	583 (21)	-[a]	-[a]

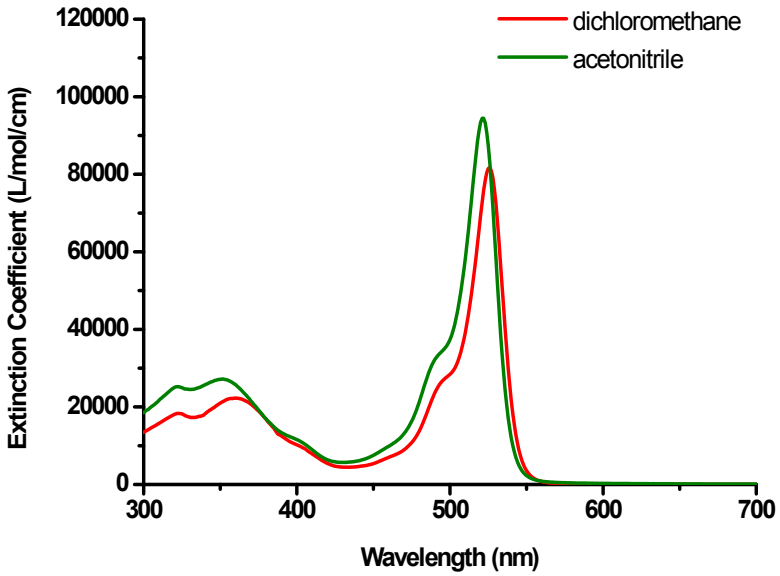

Figure S41 Absorption coefficient *vs.* wavelength of **4** in solution revealing a small hypsochromic shift and a sharpening of both visible and UV bands on switching from dichloromethane to acetonitrile solution.

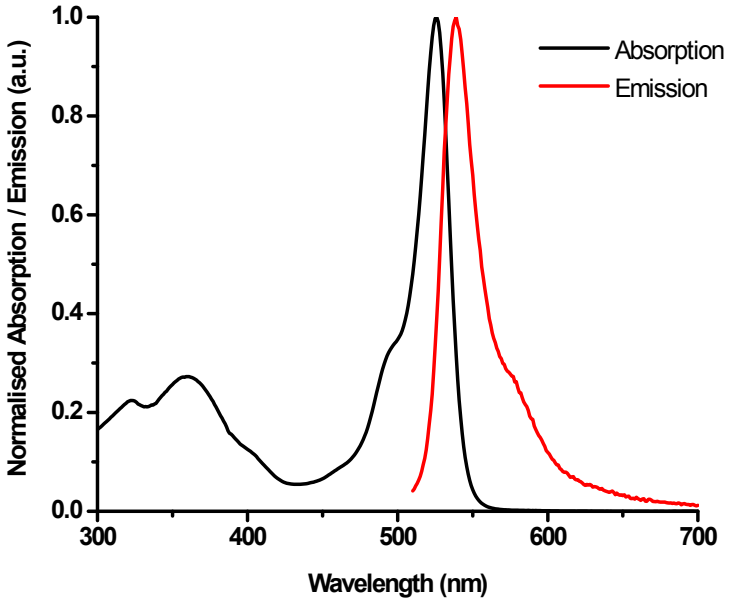

Figure S42 Normalised absorption and emission of **4** in dichloromethane

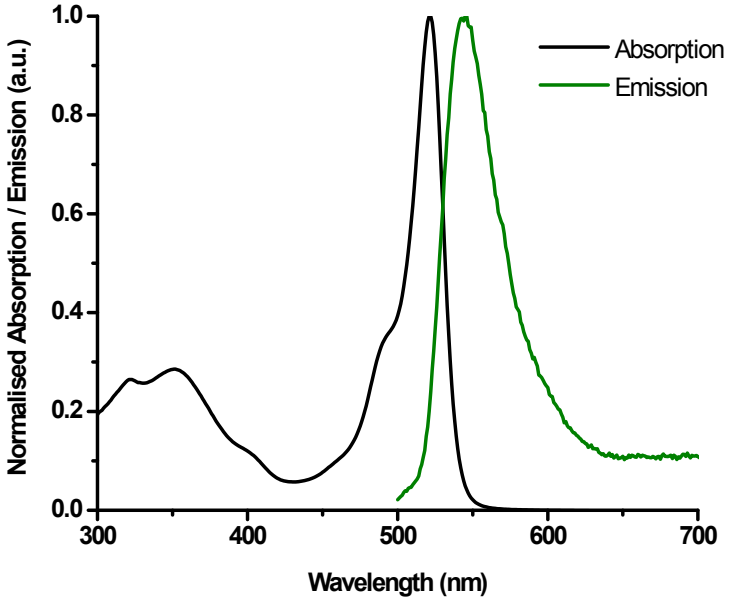

Figure S43 Normalised absorption and emission of **4** in acetonitrile

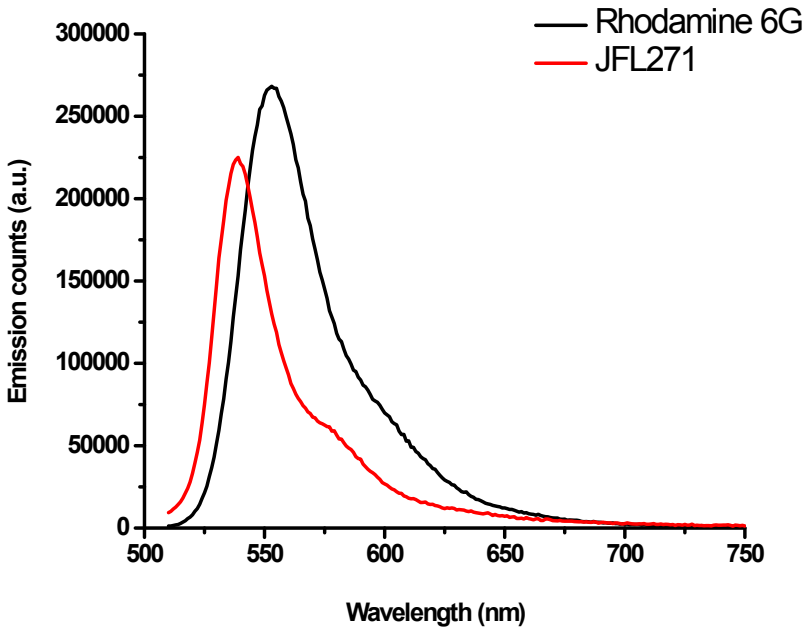

Figure S44 Emission quantum yield measurement of **4** in dichloromethane (obtained yield: 0.38) compared to Rhodamine 6G in ethanol (0.94)

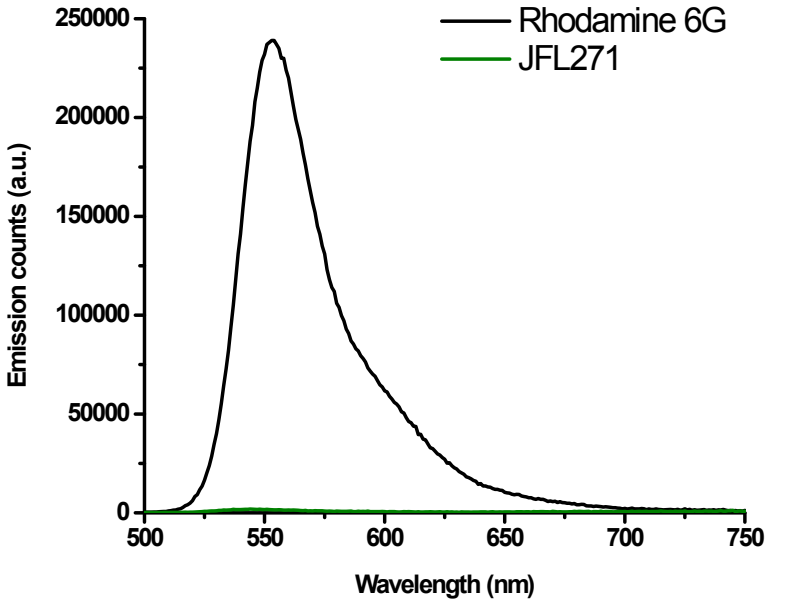

Figure S45 Emission quantum yield measurement of **4** in acetonitrile (obtained yield: 0.02) compared to Rhodamine 6G in ethanol (0.94)

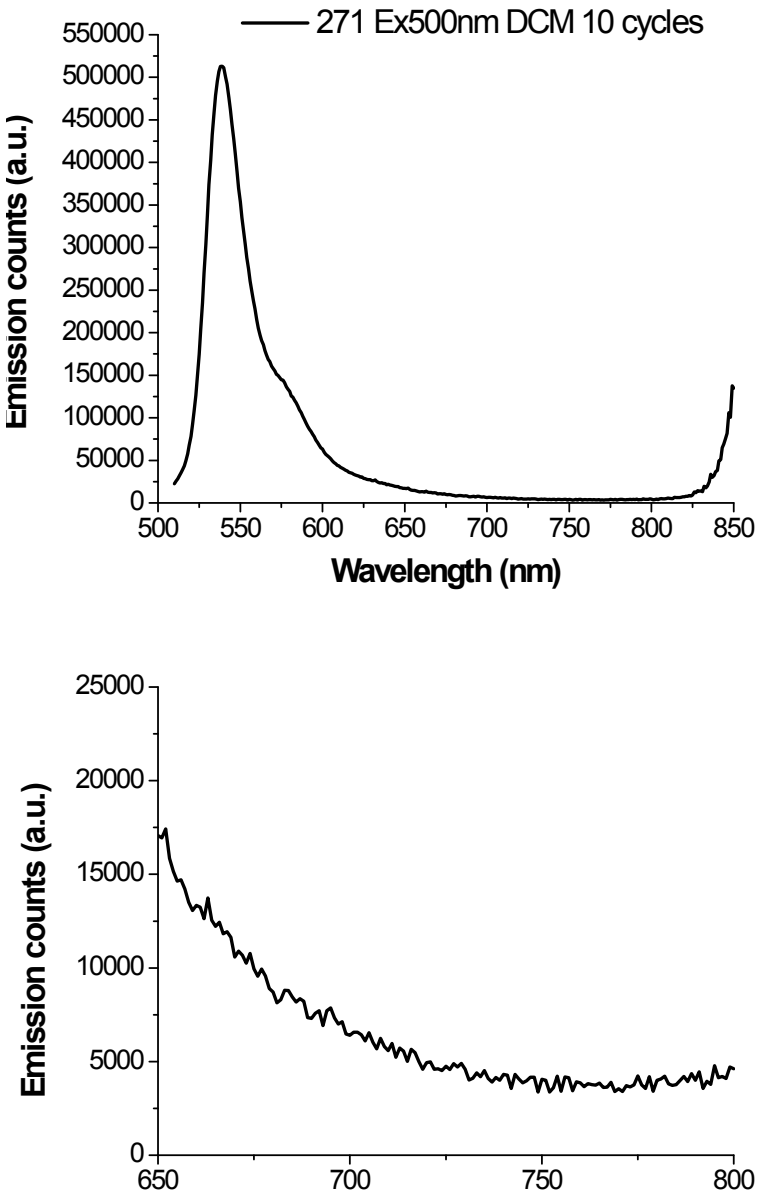

Figure S46 Emission measurement (λ_{ex} = 500 nm) of **4** in dichloromethane with more cycles and on a wider window (down: zoom of the 650 to 800 nm region)

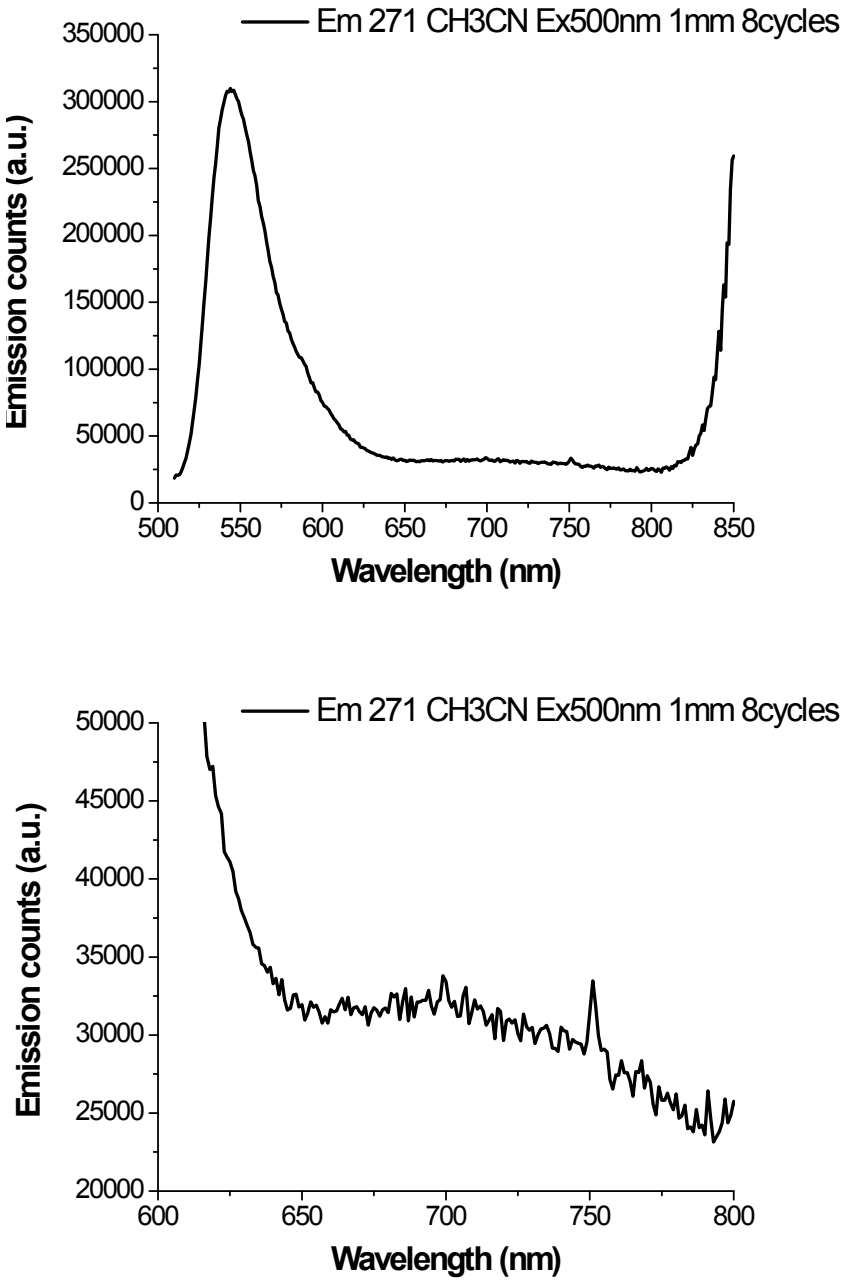

Figure S47 Emission spectrum (λ_{ex} = 500 nm) of **4** in acetonitrile with more cycles and on a wider windows (down: zoom of the 650 to 800 nm region)

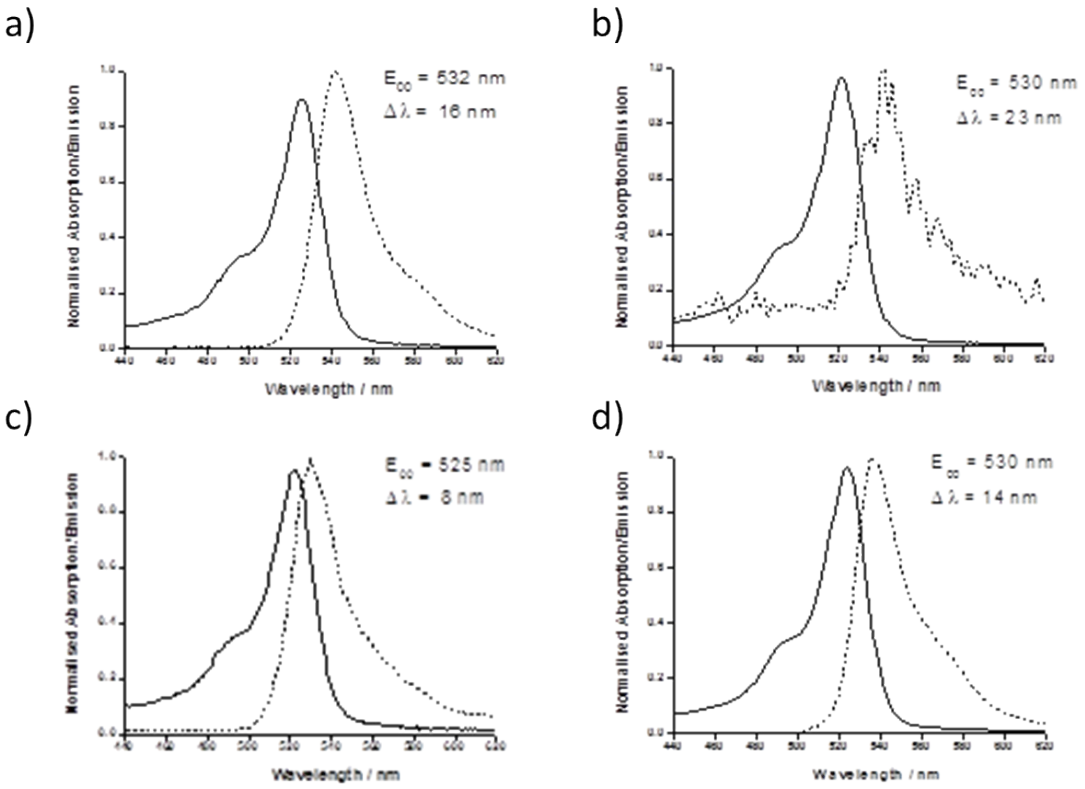

Figure S48 Normalised absorption and emission spectra (λ_{ex} = 400 nm) of **4** in a) CH_2Cl_2, b) CH_3CN, c) acetone and d) THF determined by single photon counting.

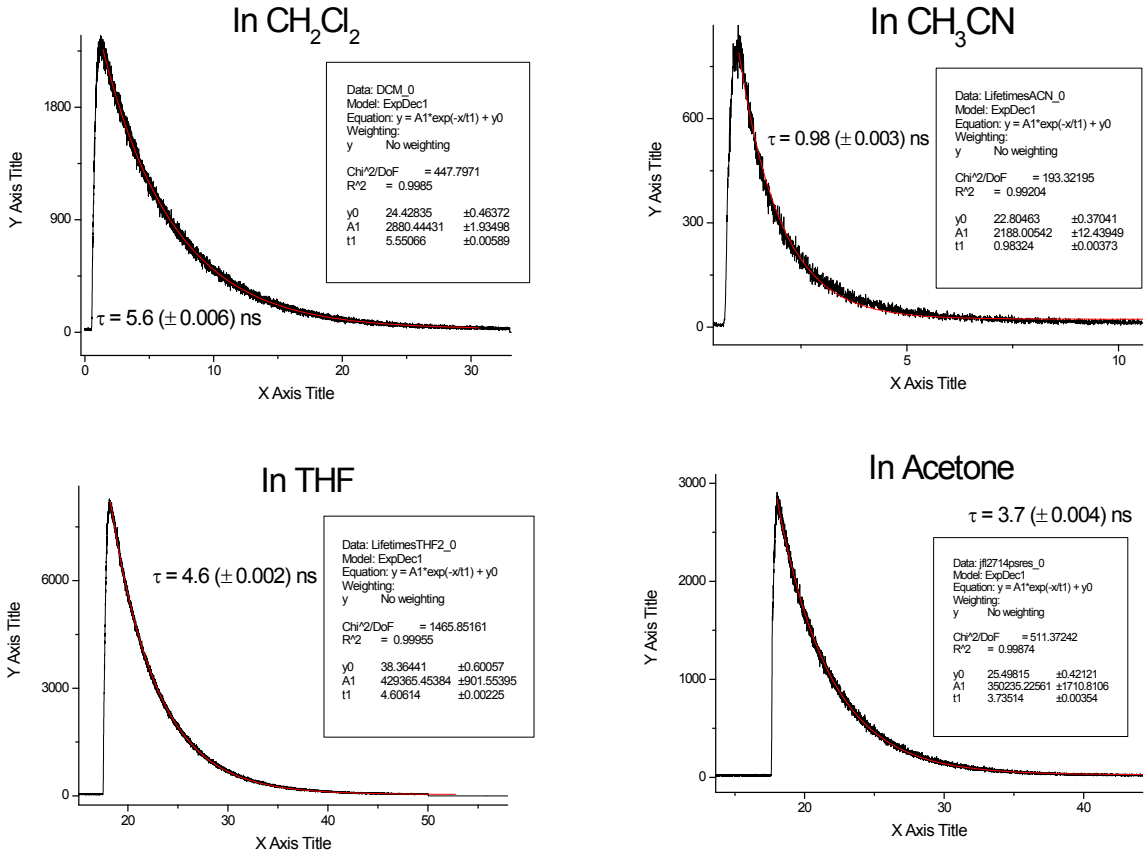

Figure S49 Excited state lifetimes (λ_{ex} = 440 nm) of **4** in CH_2Cl_2, CH_3CN, THF and acetone determined by single photon counting. τ in CH_3CN was within the instrument response time and can be disregarded.

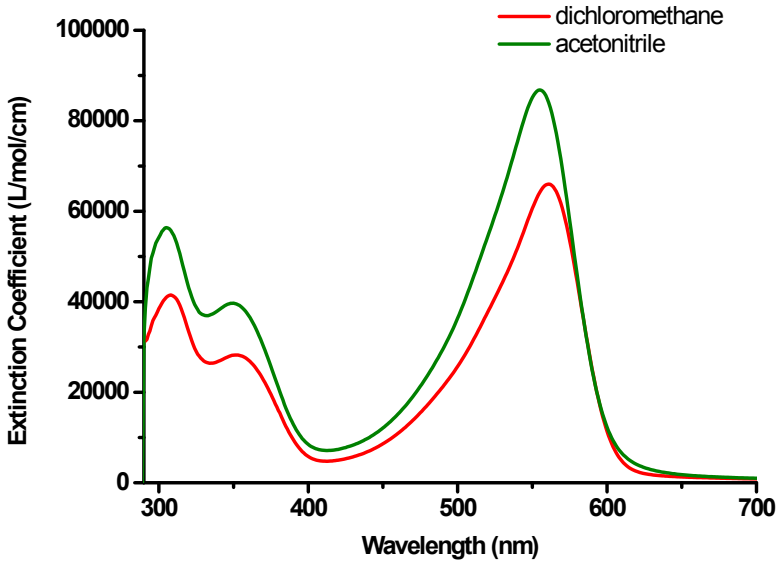

Figure S50 Absorption coefficient of **5** in dichloromethane and acetonitrile.

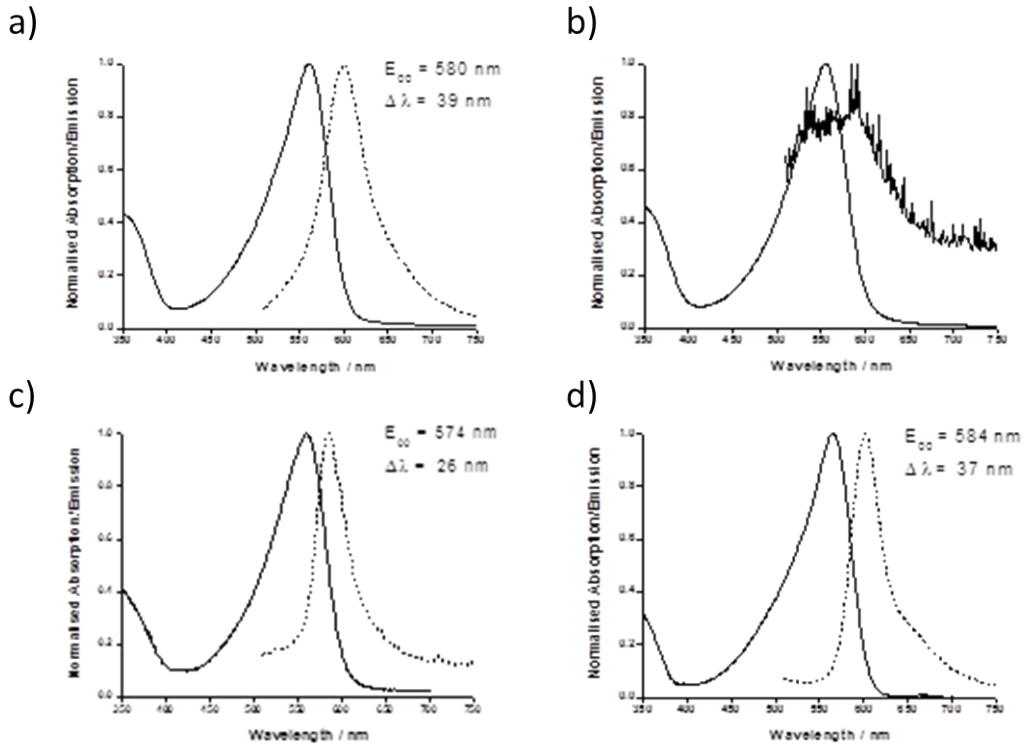

Figure S51 Normalised absorption and emission spectra (λ_{ex} = 500 nm) of **5** in a) CH_2Cl_2, b) CH_3CN, c) acetone and d) THF.

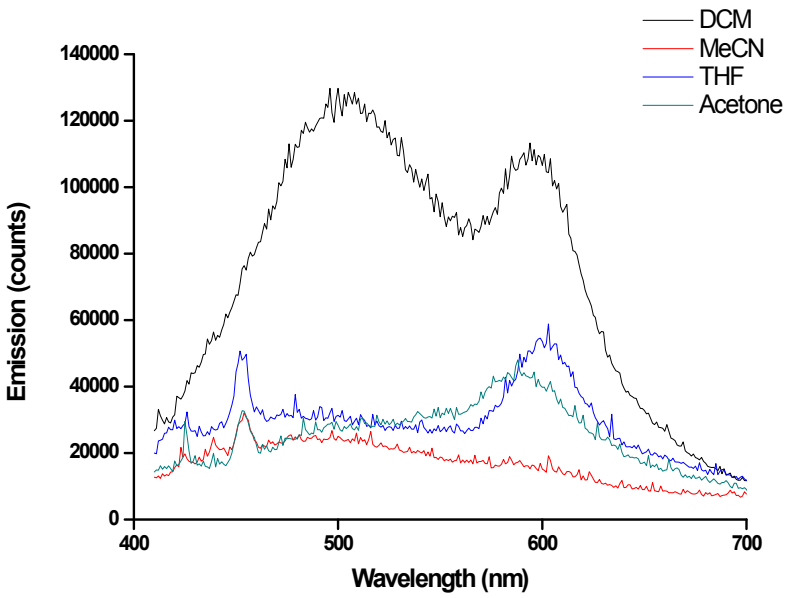

Figure S52 Emission of **5** in various solvents (excitation at 400 nm). The samples were much less emissive compared to excitation at 500 nm.

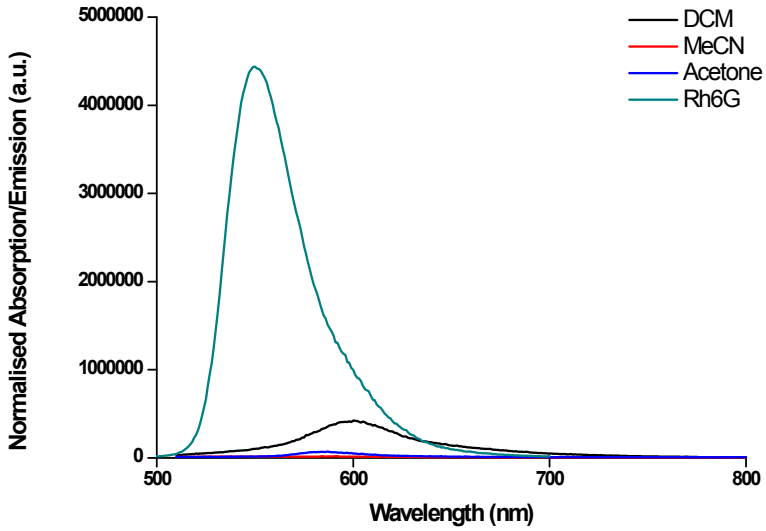

Figure S53 Emission quantum yield measurement of **5** in dichloromethane (obtained yield: 0.15), acetonitrile (obtained yield: 0.02) and acetone (obtained yield: 0.03) compared to Rhodamine 6G in ethanol (0.94).

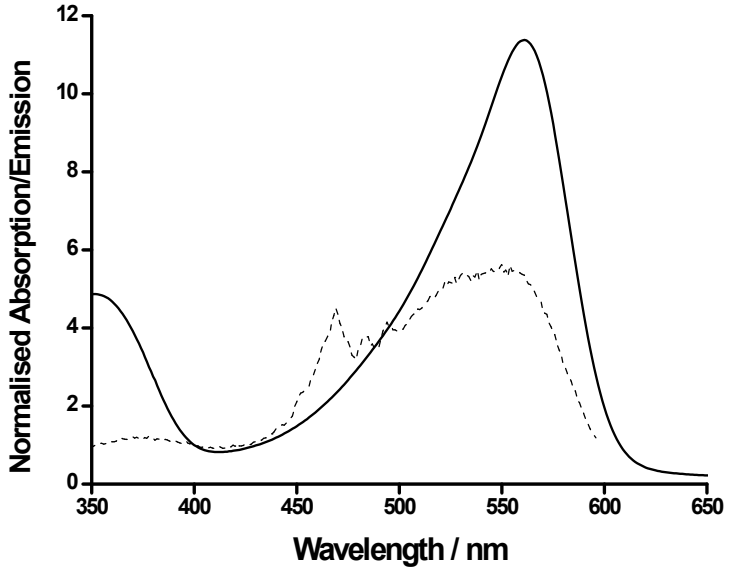

Figure S54 Normalised absorption (solid line) and excitation (dashed line) spectra of **5** in DCM (emission at 600 nm, normalised at 400 nm)

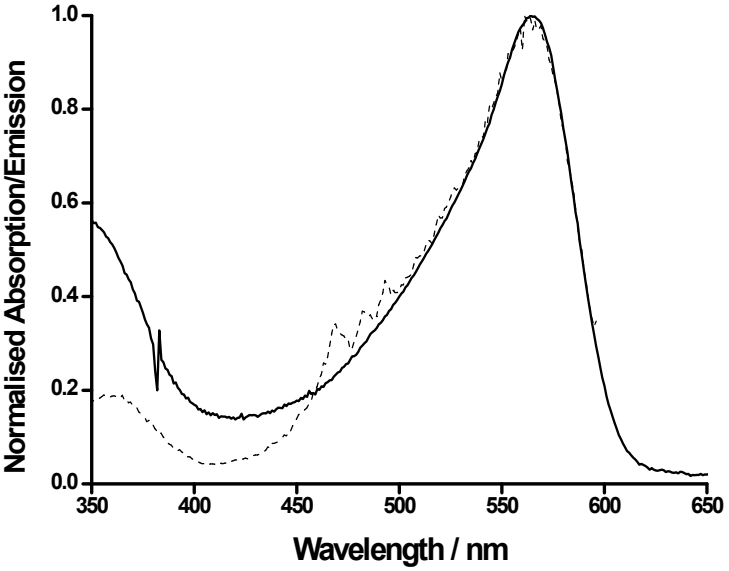

Figure S55 Normalised absorption (solid line) and excitation (dashed line) spectra of **5** in THF (emission at 600 nm, normalised at 560 nm)

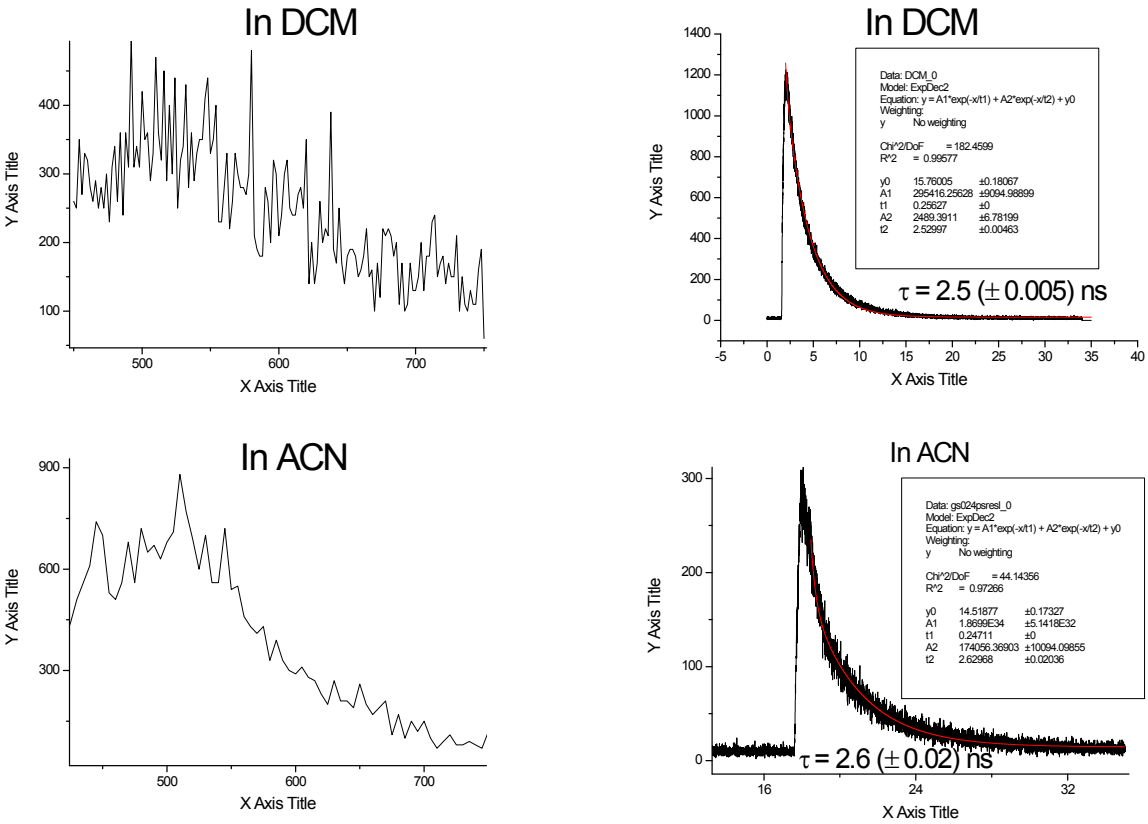

Figure S56 Steady state emission spectra and single photon counting of **5** in acetonitrile and dichloromethane.

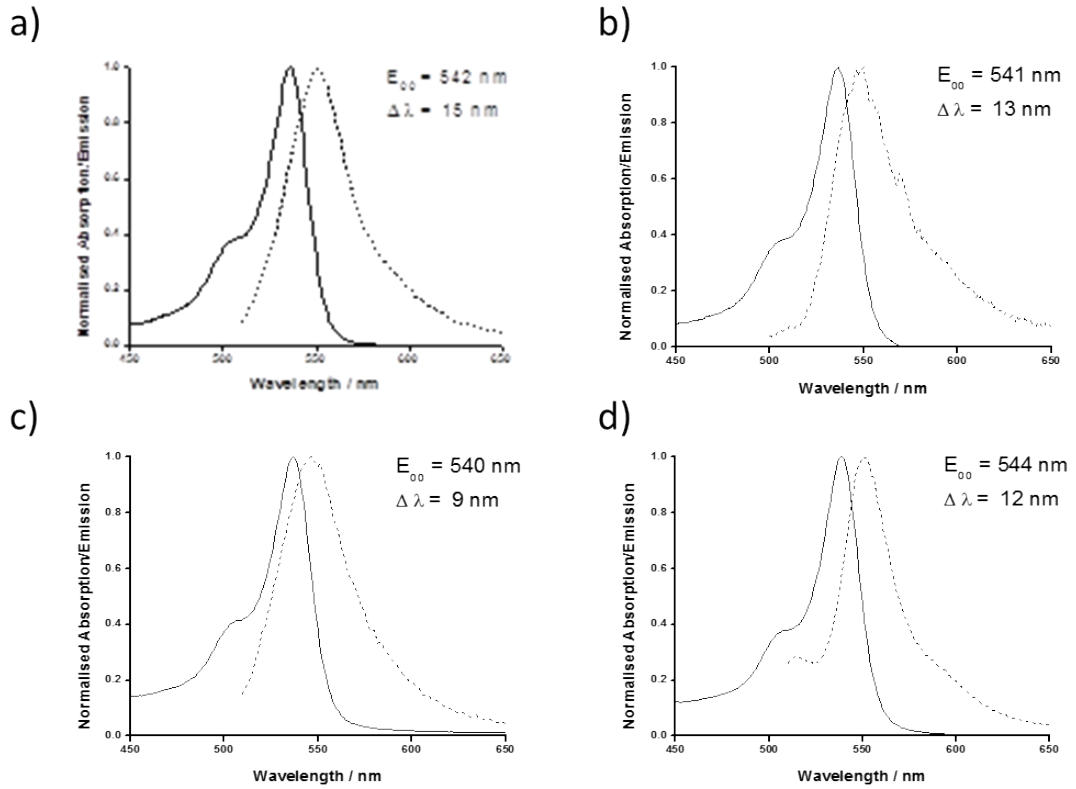

Figure S57 Normalised absorption and emission spectra (λ_{ex} = 500 nm) of **6** in a) CH_2Cl_2, b) CH_3CN, c) acetone and d) THF.

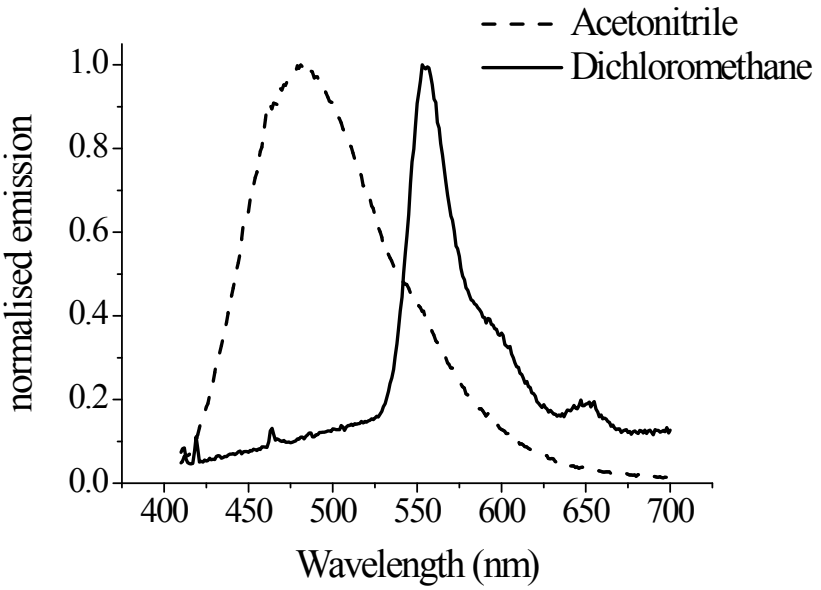

Figure S58 Normalised emission of **6** in acetonitrile (dashed line) and dichloromethane (solid line) (excitation at 406 nm).

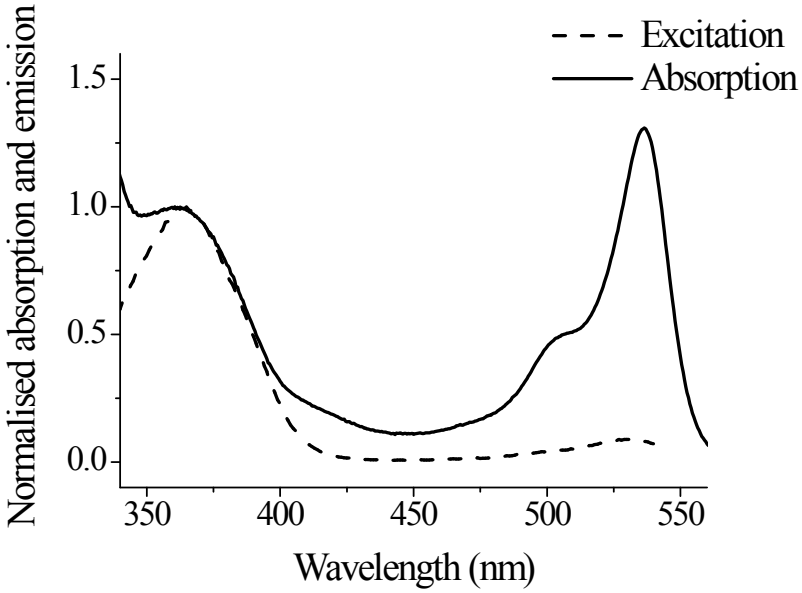

Figure S59 Normalised absorption (solid line) and excitation (dashed line) spectra of **6** in acetonitrile (emission at 550 nm, normalised at 363 nm)

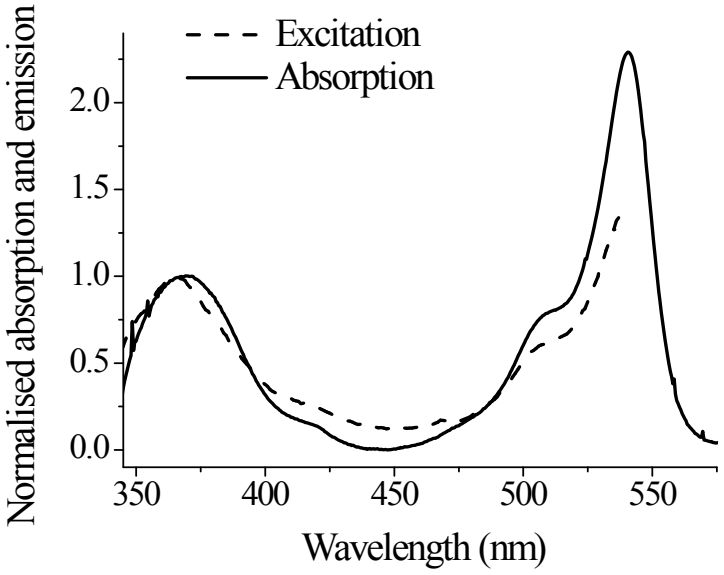

Figure S60 Normalised absorption (solid line) and excitation (dashed line) spectra of **6** in dichloromethane (emission at 550 nm, normalised at 363 nm).

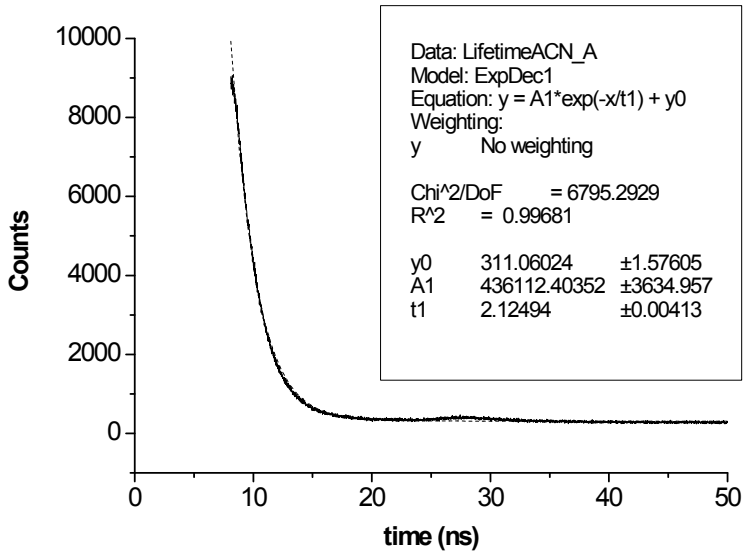

F**igure S61** Emission lifetime measurement of **6** in acetonitrile (excitation at 406 nm)

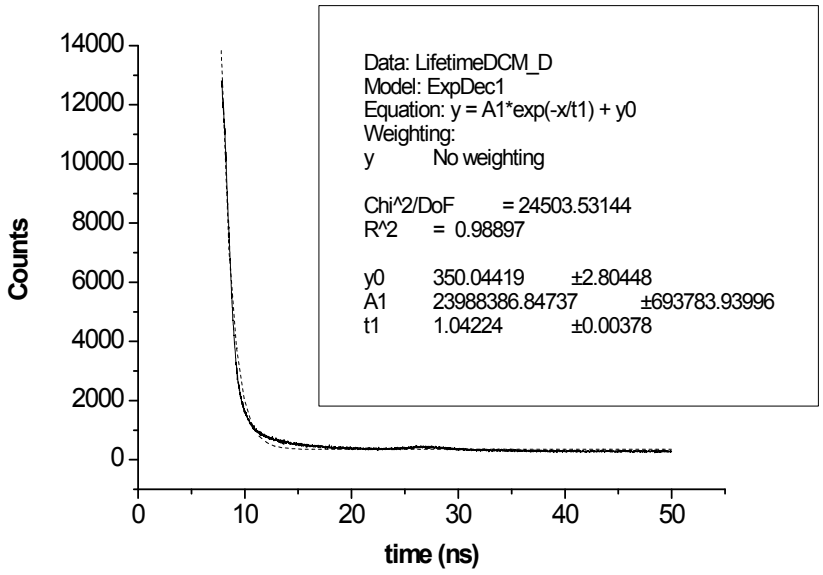

Figure S62 Emission lifetime measurement of **6** in dichloromethane (excitation at 406 nm)

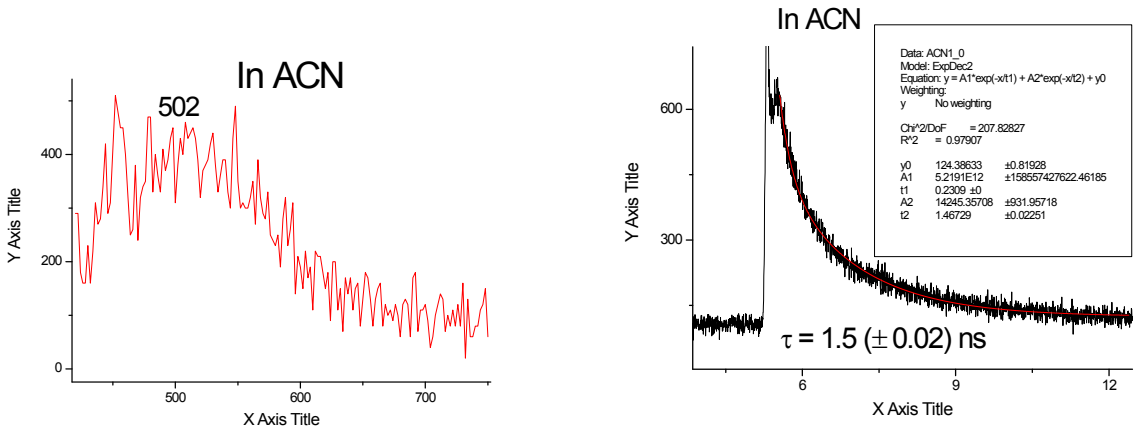

Figure S63 Steady state emission spectra and single photon counting of **7** in acetonitrile. **7** was non emissive (τ < 1 ns, within the instrument response time) in dichloromethane. (λ_{ex} = 400 nm)

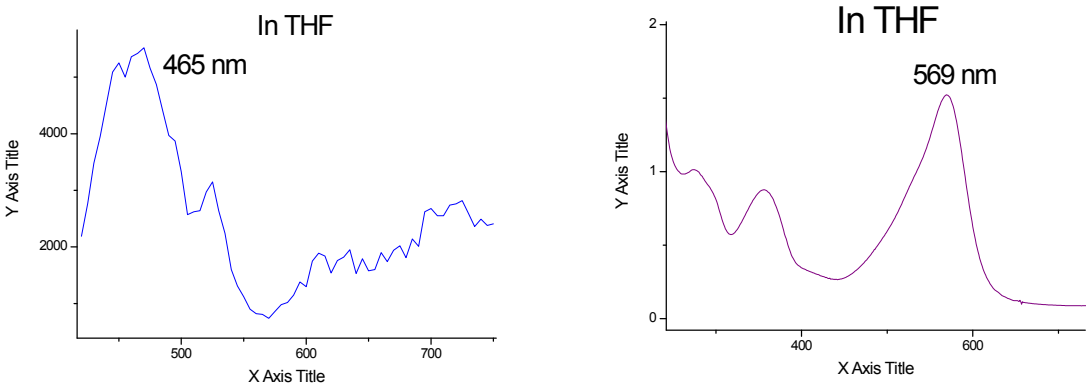

Figure S64 Steady state absorption and emission spectra and single photon counting of **7** in tetrahydrofuran (λ_{ex} = 400 nm).

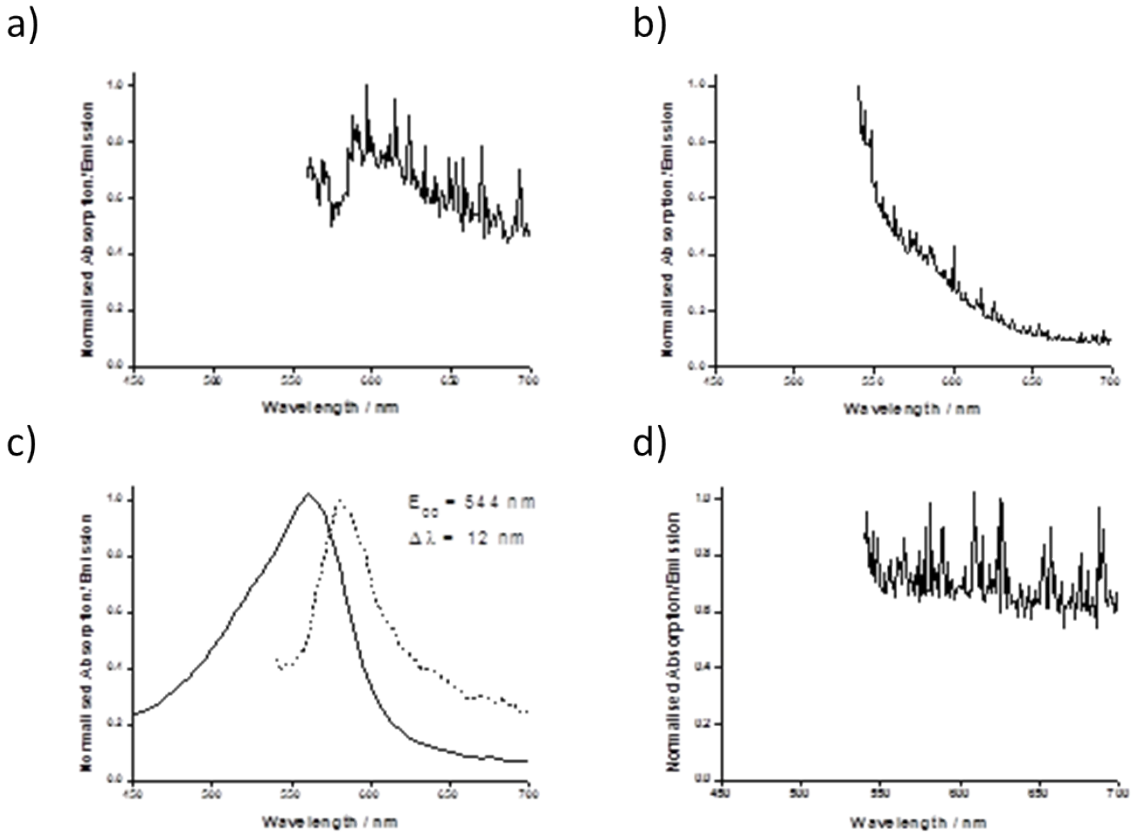

Figure S65 Normalised absorption and emission spectra (λ_{ex} = 530 nm) of **7** in a) CH_2Cl_2, b) CH_3CN, c) acetone and d) THF.

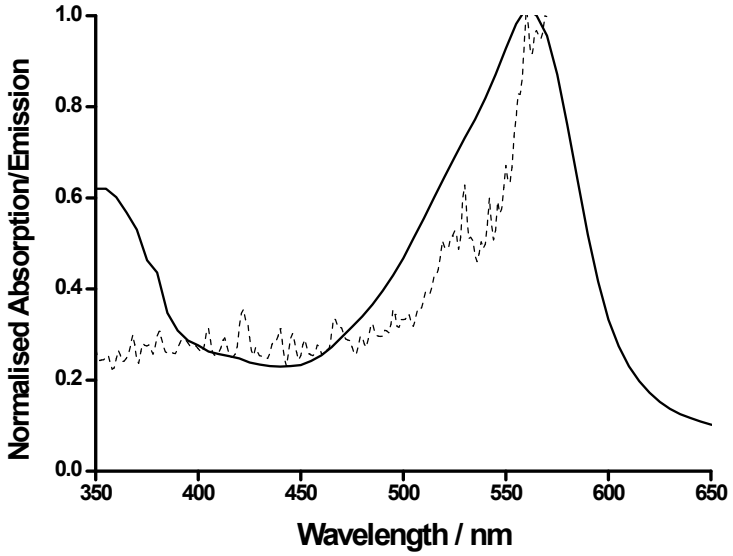

Figure S66 Normalised absorption (solid line) and excitation (dashed line) spectra of **7** in acetone (emission at 800 nm, normalised at 550 nm).

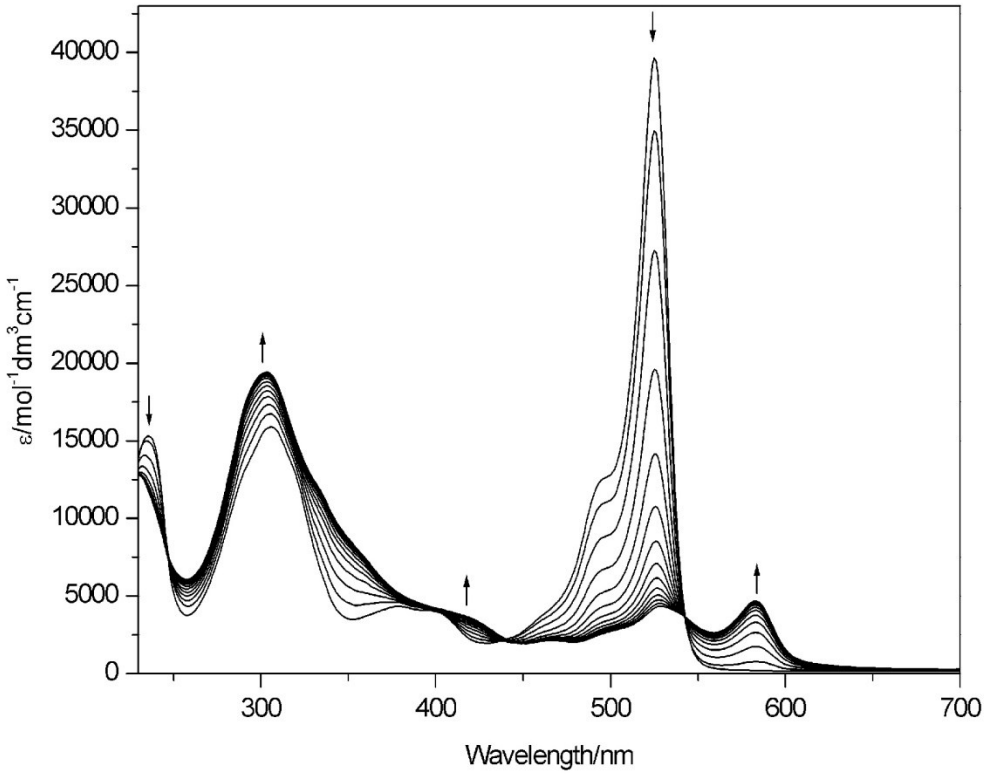

Figure S67 View of UV-visible spectra recorded in CH_2Cl_2 containing $[Bu_4N][ClO_4]$ (0.5 M) using spectroelectrochemical methods for **1** at 248 K showing the inter-conversion of $\mathbf{1}^0$ to $\mathbf{1}^{1-}$. Arrows indicate the progress of the reduction.

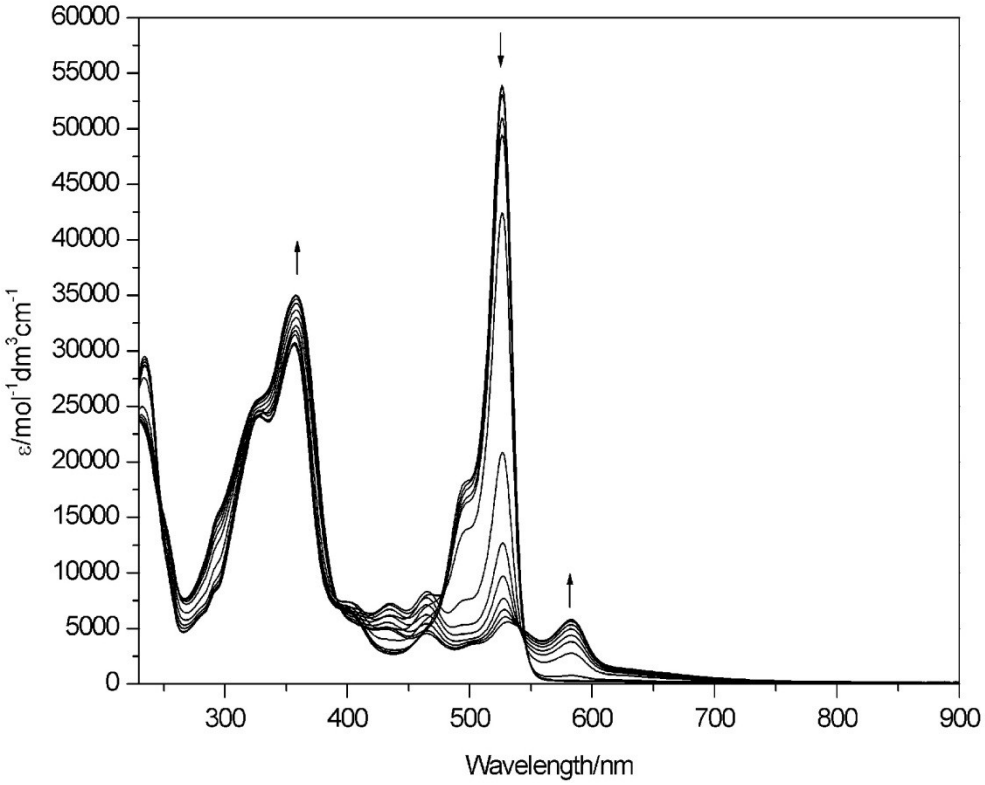

Figure S68 View of UV-visible spectra recorded in CH_2Cl_2 containing $[Bu_4N][ClO_4]$ (0.5 M) using spectroelectrochemical methods for **2** at 248 K showing the inter-conversion of $\mathbf{2}^0$ to $\mathbf{2}^{1-}$. Arrows indicate the progress of the reduction.

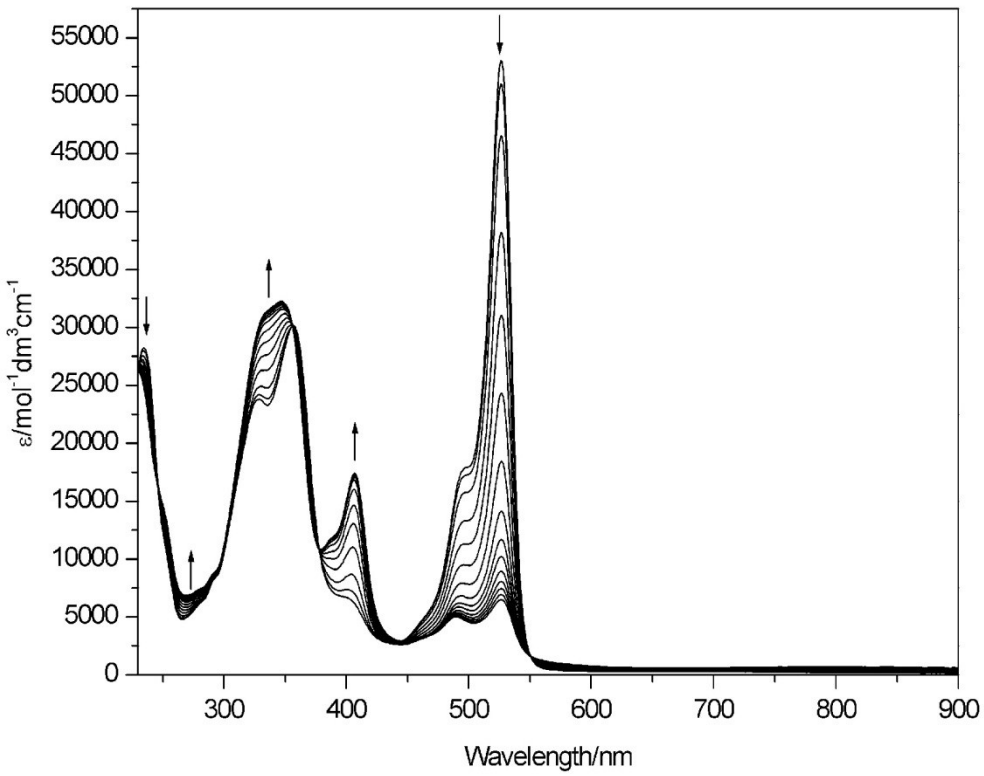

Figure S69 View of UV-visible spectra recorded in CH_2Cl_2 containing $[Bu_4N][ClO_4]$ (0.5 M) using spectroelectrochemical methods for **2** at 248 K showing the inter-conversion of $\mathbf{2}^{0}$ to $\mathbf{2}^{1+}$. Arrows indicate the progress of the oxidation.

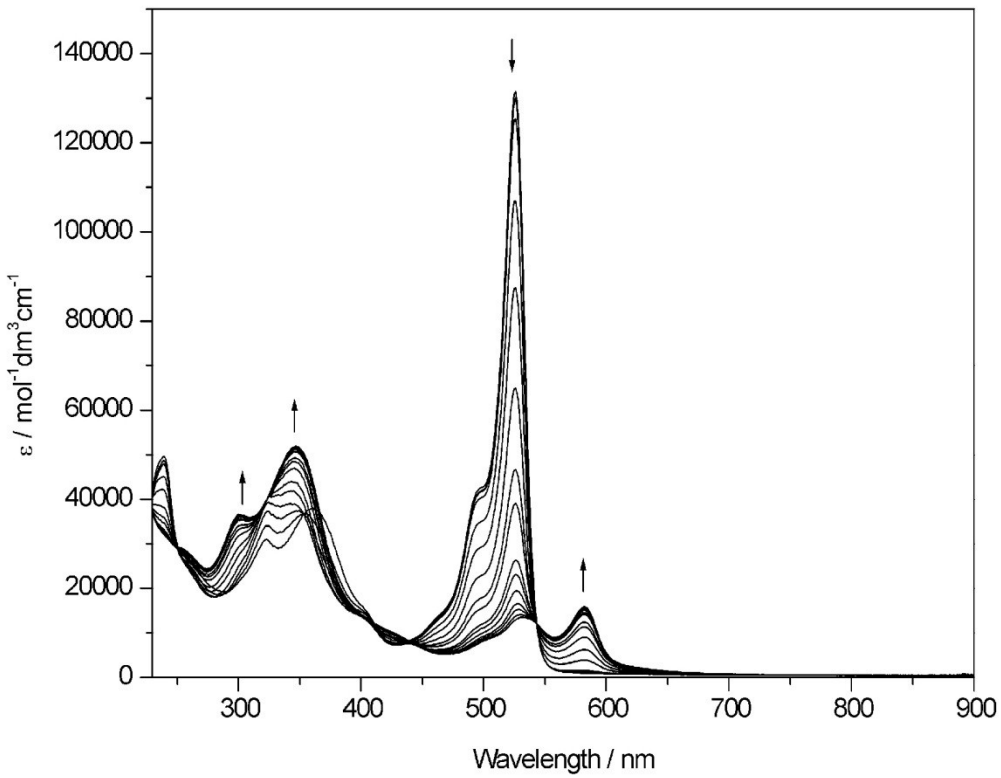

Figure S70 View of UV-visible spectra recorded in CH_2Cl_2 containing $[Bu_4N][ClO_4]$ (0.5 M) using spectroelectrochemical methods for **4** at 248 K showing the inter-conversion of **4** to $\mathbf{4}^{1-}$. Arrows indicate the progress of the reduction.

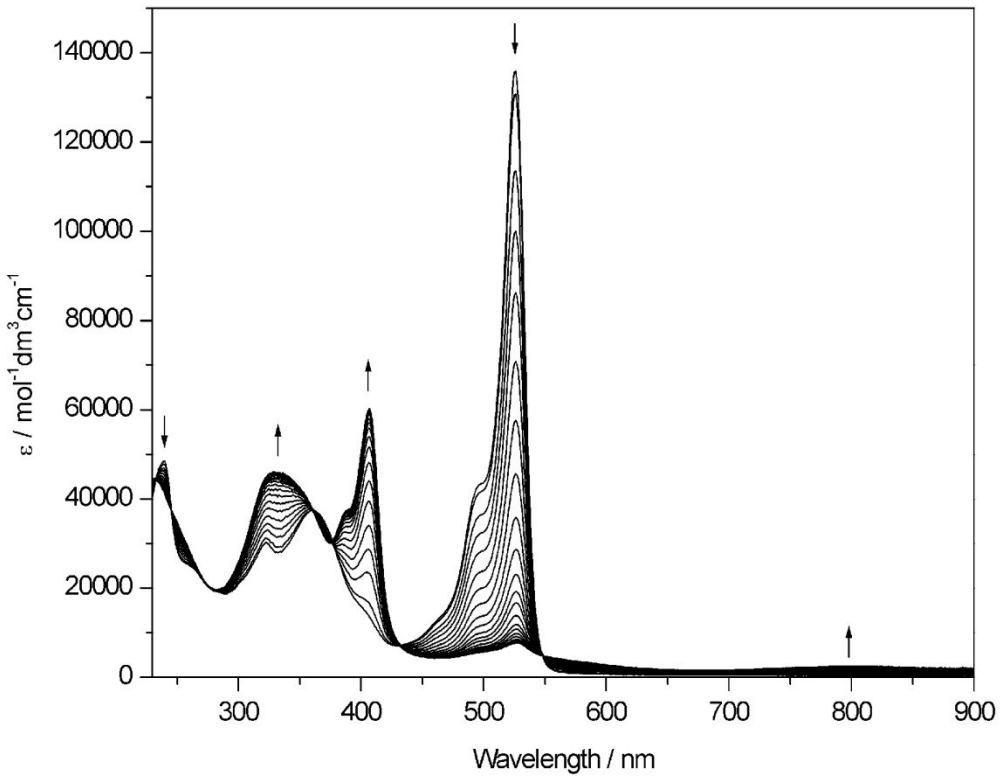

Figure S71 View of UV-visible spectra recorded in CH_2Cl_2 containing $[Bu_4N][ClO_4]$ (0.5 M) using spectroelectrochemical methods for **4** at 248 K showing the inter-conversion of **4** to $\mathbf{4}^{1+}$. Arrows indicate the progress of the oxidation.

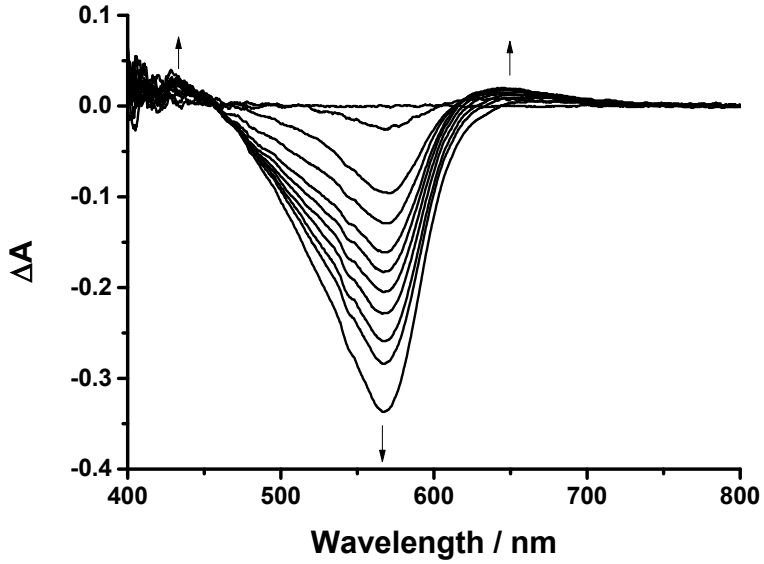

Figure S72 UV-visible absorption difference spectra recorded in CH_2Cl_2 containing $[Bu_4N][ClO_4]$ (0.5 M) for **7** showing the inter-conversion of **7** to $\mathbf{7}^{1-}$ upon electrochemical reduction.

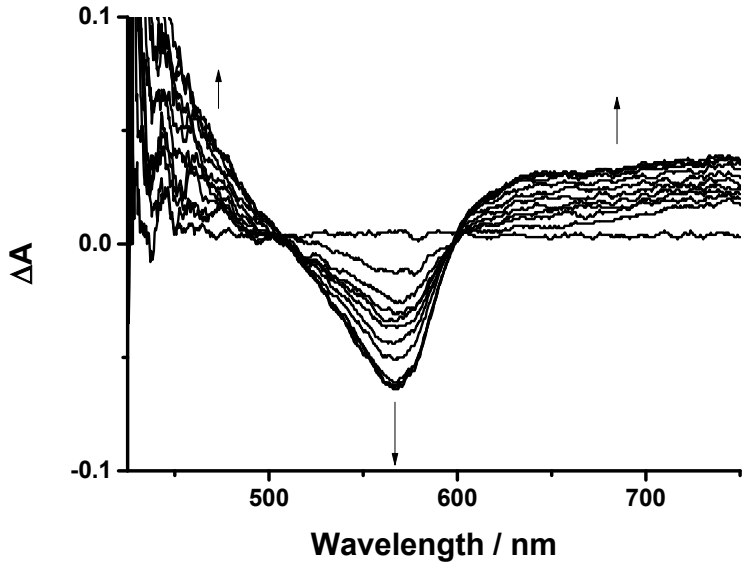

Figure S73 UV-visible absorption difference spectra recorded in CH_2Cl_2 containing $[Bu_4N][ClO_4]$ (0.5 M) for **7** showing the inter-conversion of **7** to $\mathbf{7}^{1+}$ upon electrochemical oxidation.

Table S6. UV-visible data obtain from spectroelectrochemistry measurements.[a]

Compound	λ_{max}/nm (ε x 10^{-4}/$mol^{-1}dm^3cm^{-1}$)
1	235 (1.5), 307 (1.6), 379 (0.4), 525 (4.0)
$\mathbf{1}^{1-}$	301 (2.0), 469 (0.2), 528 (0.4), 582 (0.5)
$\mathbf{2}^{0}$	235 (2.8), 329 (2.4), 357 (3.0), 527 (5.4)
$\mathbf{2}^{1-}$	329 (2.6), 359 (3.5), 432 (0.5), 464 (0.4), 531 (0.5), 582 (0.6)
$\mathbf{2}^{1+}$	230 (2.6), 346 (3.2), 407 (1.7), 488 (0.5), 526 (0.7)
$\mathbf{4}^{1-}$	300 (3.7), 347 (5.2), 531 (1.3), 582 (1.6)
$\mathbf{4}^{1+}$	232 (3.7), 329 (4.6), 390 (3.7), 407 (6.0), 526 (0.8), 802 (0.2)
$\mathbf{5}^{1+}$	615 (1.9)

[a] obtained at a optically transparent electrode cell, in CH_2Cl_2 containing $[^nBu_4N][ClO_4]$ (0.5 M) at 248 K, spectral range: 230 – 900 nm.

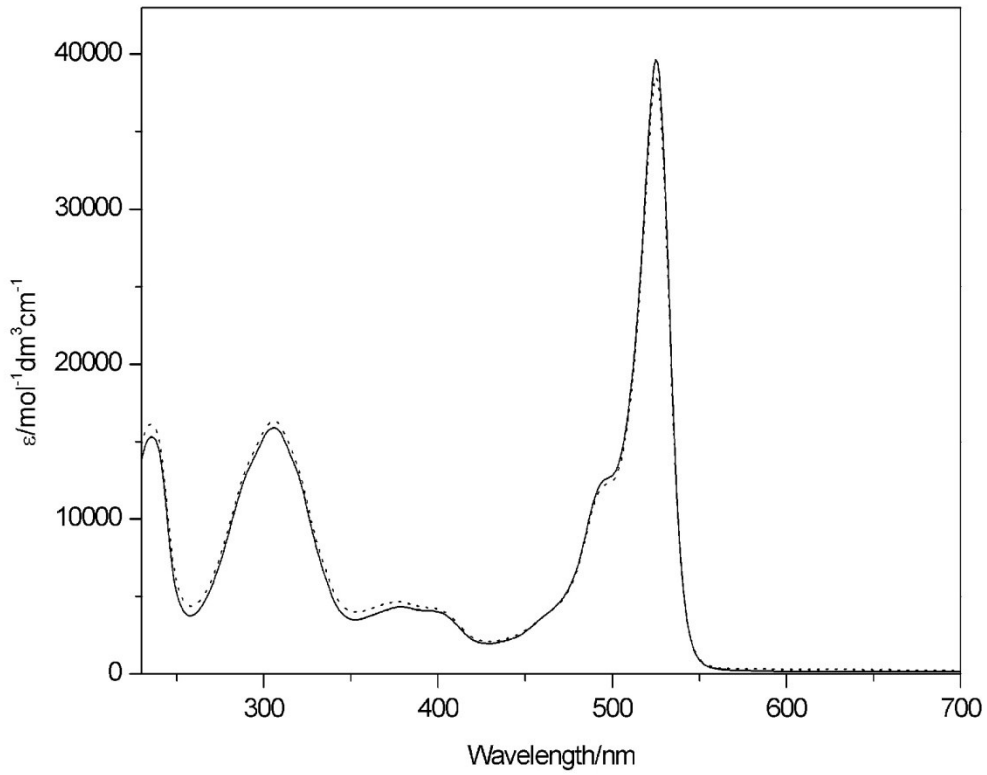

Figure S74 UV-visible spectra recorded in CH_2Cl_2 containing $[Bu_4N][ClO_4]$ (0.5 M) for **1** at 248 K before (solid line) and after (dotted line) reduction to $\mathbf{1}^{1-}$.

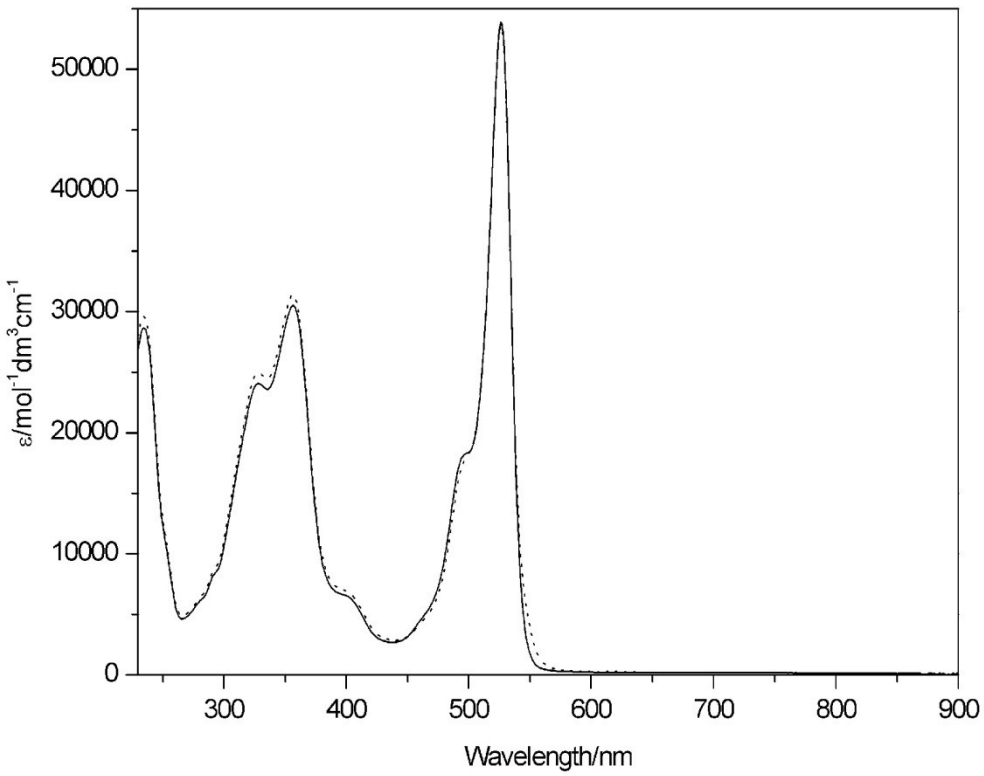

Figure S75 UV-visible spectra recorded in CH_2Cl_2 containing $[Bu_4N][ClO_4]$ (0.5 M) for **2** at 248 K before (solid line) and after (dotted line) reduction to $\mathbf{2}^{1-}$.

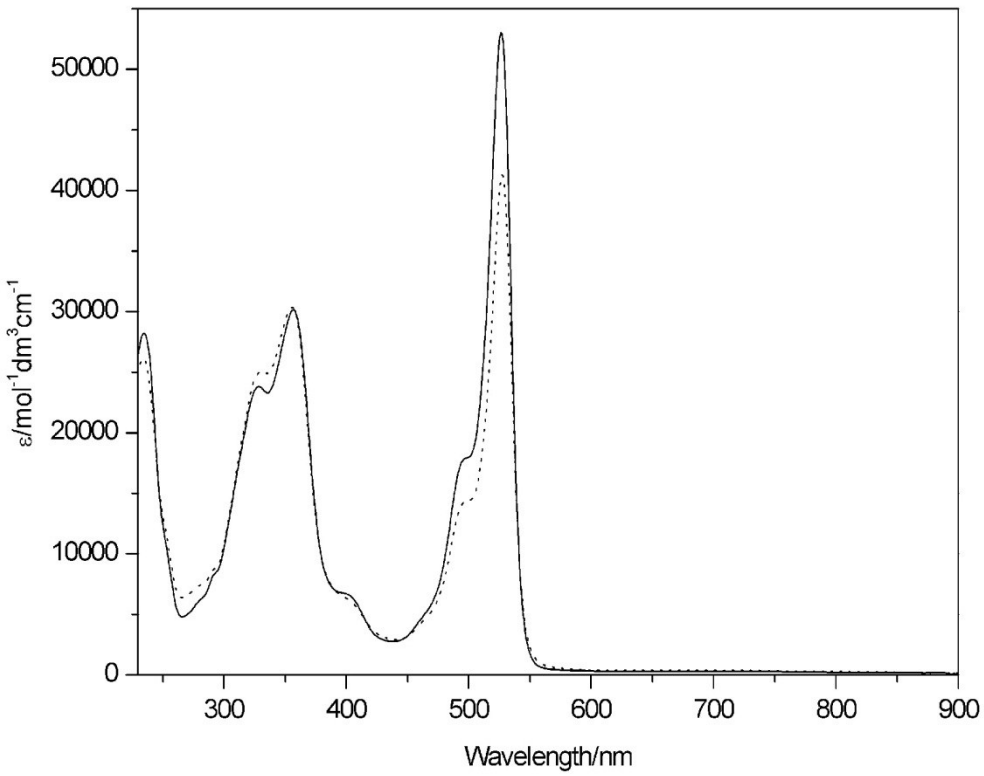

Figure S76 UV-visible spectra recorded in CH_2Cl_2 containing $[Bu_4N][ClO_4]$ (0.5 M) for **2** at 248 K before (solid line) and after (dotted line) oxidation to $\mathbf{2}^{1+}$.

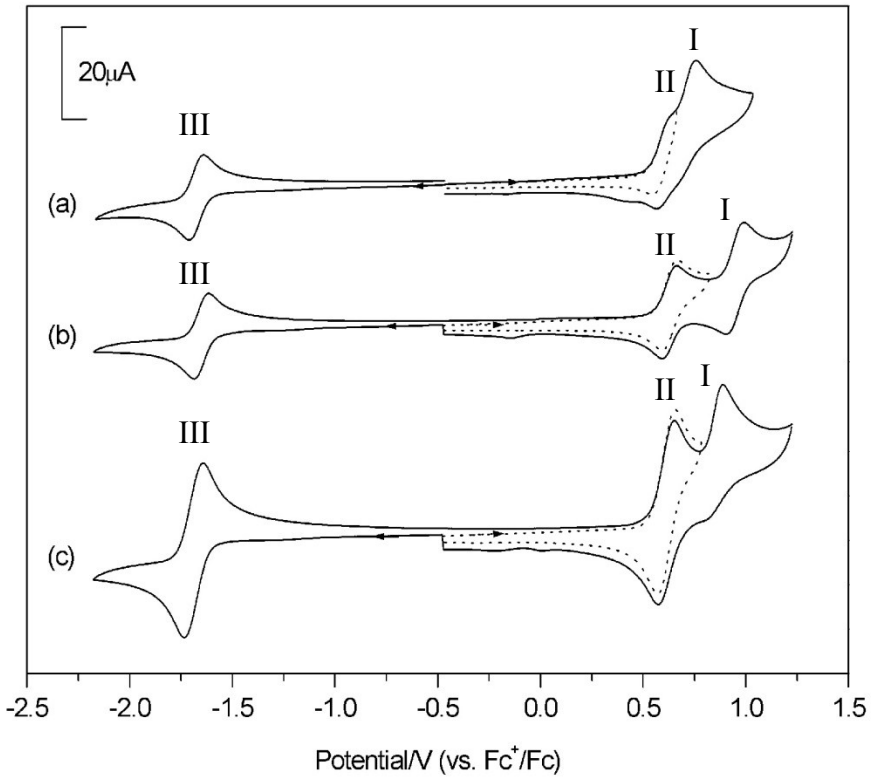

Figure S77 Cyclic voltammograms recorded for (a) **1** (b) **2** and (c) **3** in CH_2Cl_2 containing $[Bu_4N][ClO_4]$ (0.5 M) at 0.1 V s^{-1}.

Time-resolved fluorescence spectroscopy

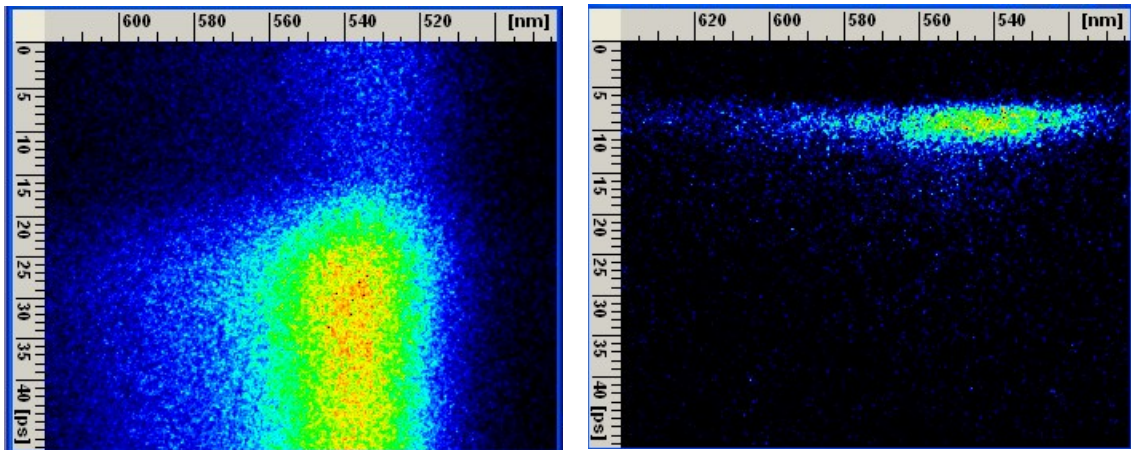

Figure S78 Streak camera image of **4** in dichloromethane (left) and adsorbed on NiO (right). The emission lifetime in solution was longer than 50 ps and on NiO the lifetime was shorter than the instrument response time (<1 ps)

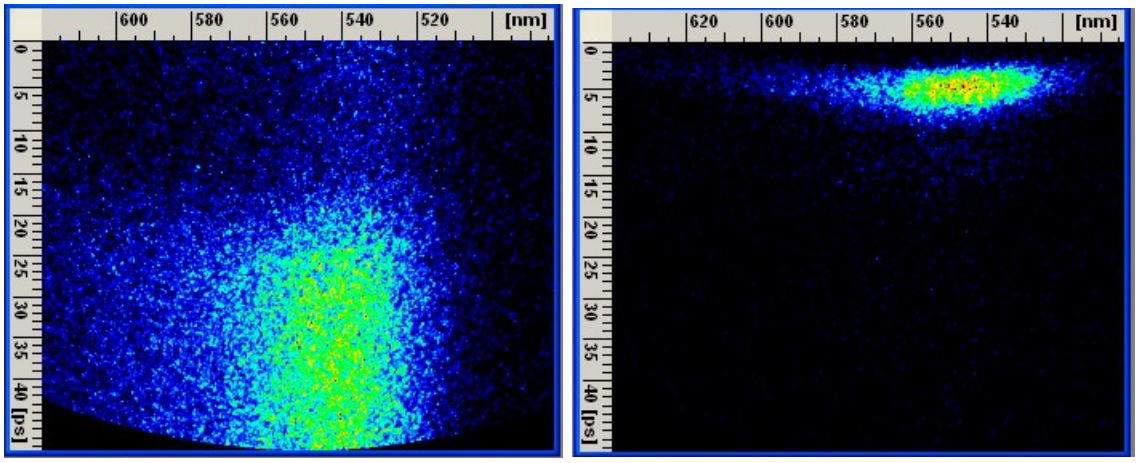

Figure S79 Streak camera image of **Bodipy-CO_2H** in dichloromethane (left) and adsorbed on NiO (right). The emission lifetime in solution was longer than 50 ps and on NiO the lifetime was shorter than the instrument response time (<1 ps)

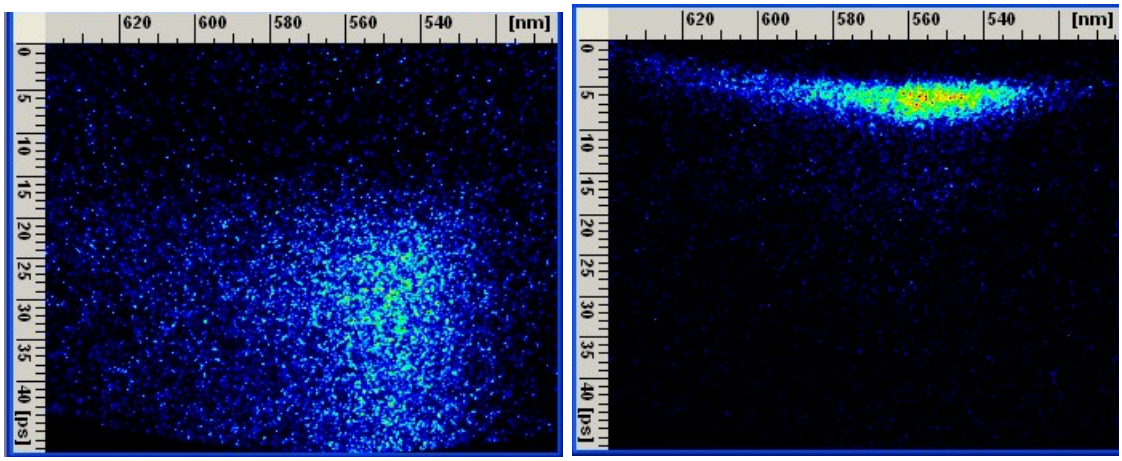

Figure S80 Streak camera image of **6** in dichloromethane (left) and adsorbed on NiO (right). The emission lifetime in solution was longer than 50 ps and on NiO the lifetime was shorter than the instrument response time (<1 ps)

Transient Absorption Spectroscopy

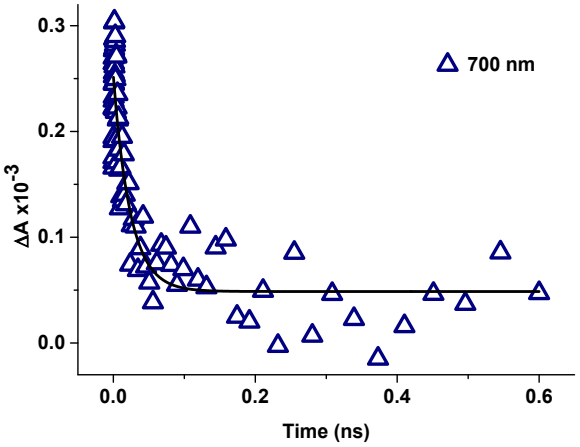

Figure S81 Kinetic trace of **Bodipy-CO_2H** on NiO, corresponding to the decay of the holes formed in NiO, absorbing broadly from 560 nm.

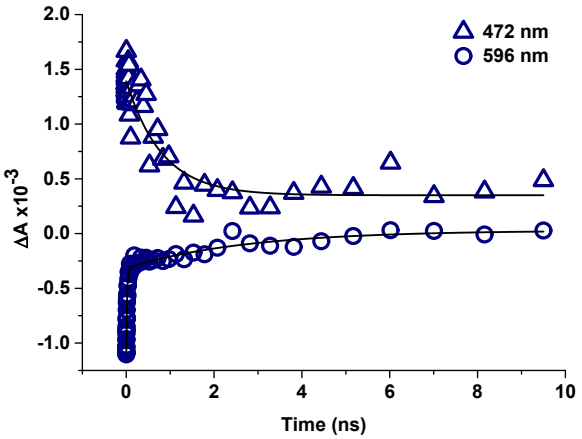

Figure S82 Kinetic traces of **4** in solution, corresponding to the decay of the excited state (472 nm) and stimulated emission and recovery of the ground state (596 nm).

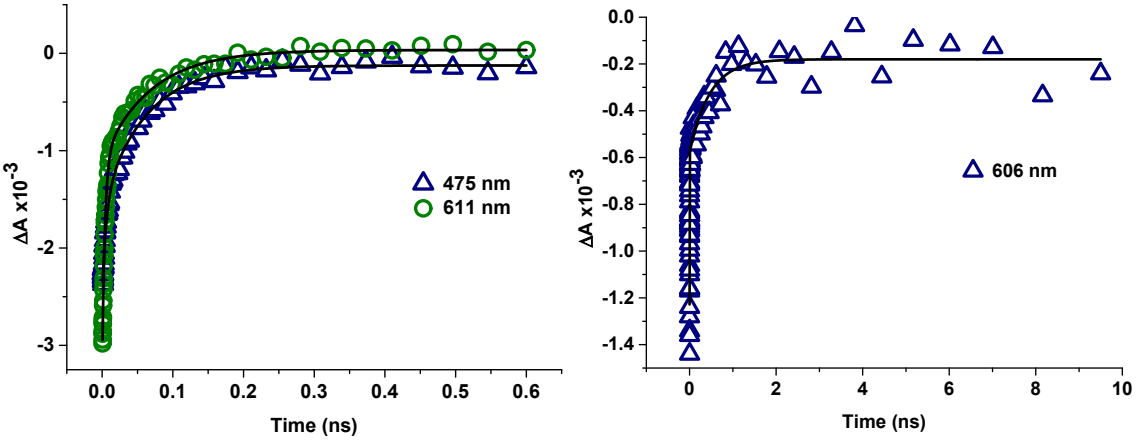

Figure S83 Kinetic traces of **5**, corresponding to the recovery of the bleach at 475 and 611 nm in solution (left) and 606 nm on NiO (right).

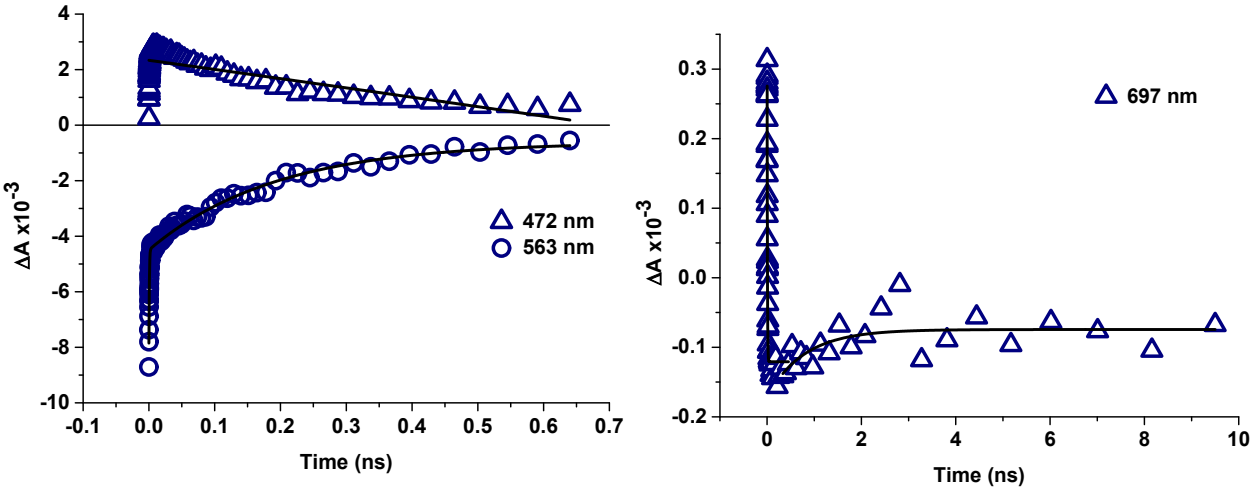

Figure S84 Kinetic traces of excited dye **7**, showing the growth and decay of the excited state (472 nm), and the recovery of the ground state (563 nm) in solution (left) and the decay of the transient observed at 697 nm on NiO (right), which overlaps with the recovery of the bleach.

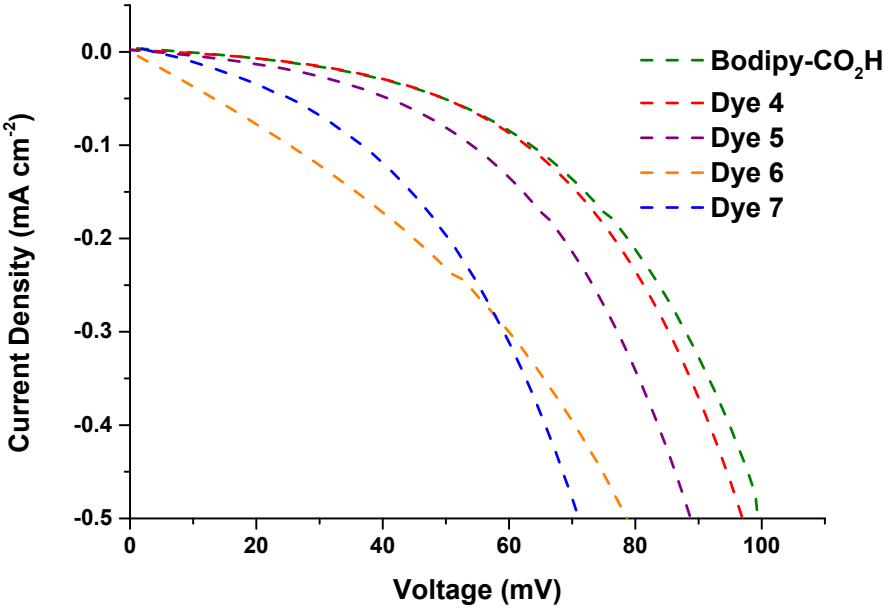

Figure S85 Dark current curves of cells made with 0.1M I_2 electrolyte

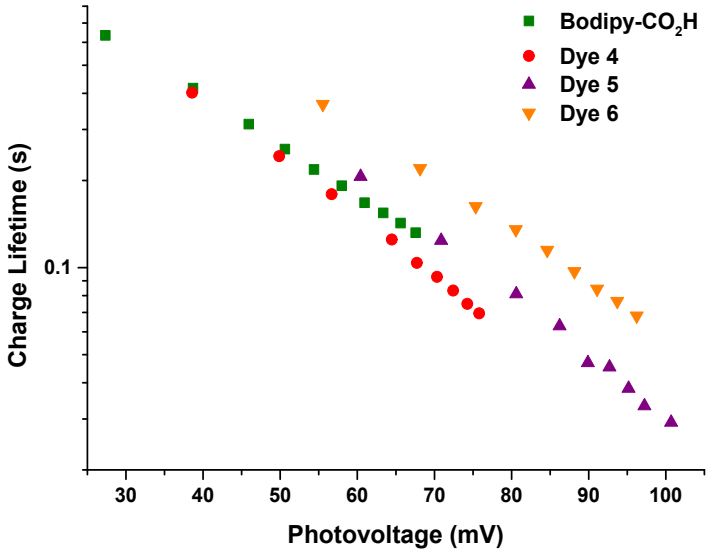

Figure S86 Charge lifetimes of cells with 0.1M I_2 electrolyte.

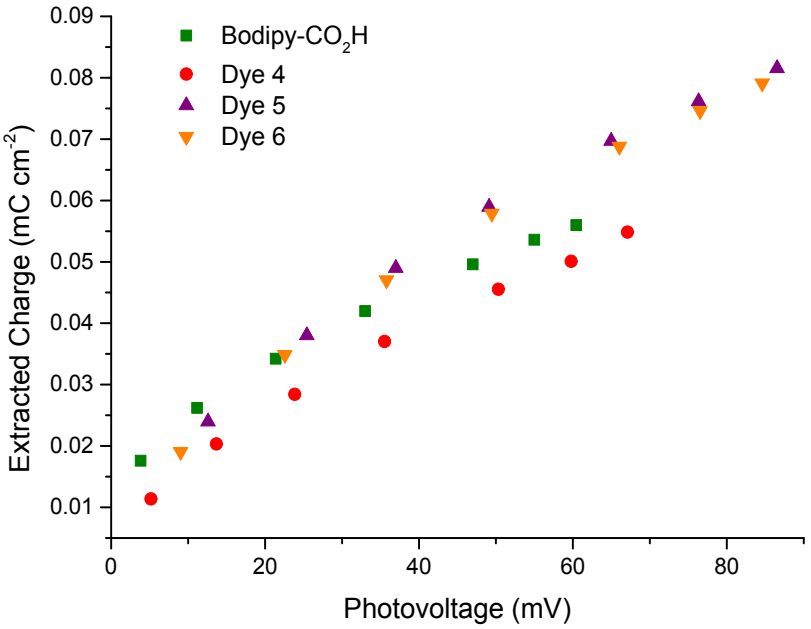

Figure S87 Extracted charge as a function of voltage for cells with 0.1M I_2.

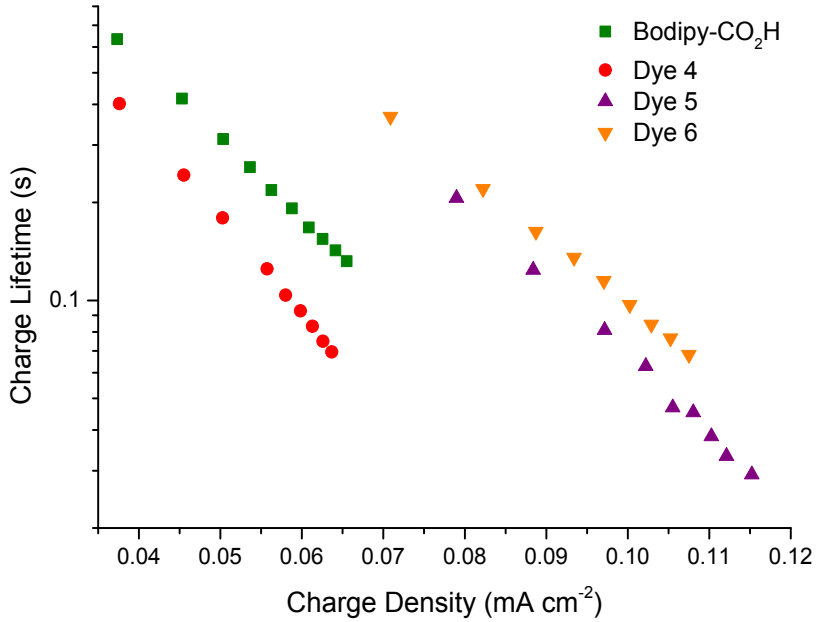

Figure S88 Charge lifetime plot as a function of charge density for cells with 0.1M I_2 electrolyte.

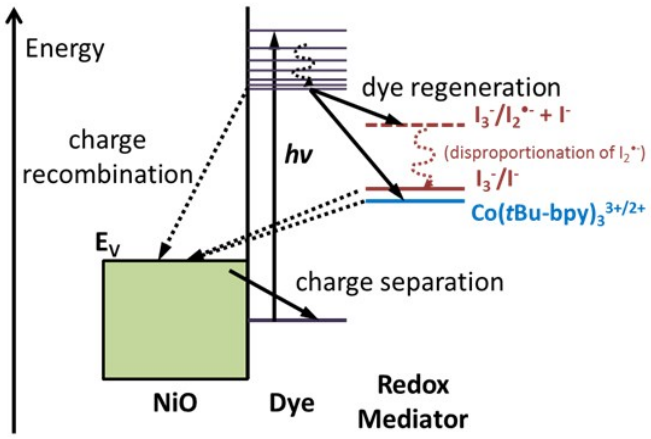

Figure S89 Schematic illustration of the key charge-transfer reactions (arrows depict direction of electron transfer) in a p-type dye-sensitized solar cell highlighting the difference in driving force required for the triiodide/iodide redox couple compared to a simple cobalt complex such as e.g. Co(II/III) tris(4,4'-di*tert*-butyl-2,2'-dipyridyl) perchlorate.

References

[1] Frisch, M. J.; Trucks, G. W.; Schlegel, H. B.; Scuseria, G. E.; Robb, M. A.; Cheeseman, J. R.; Montgomery, J. A. J.; Vreven, T.; Kudin, K. N.; Burant, J. C.; Millam, J. M.; Iyengar, S. S.; Tomasi, J.; Barone, V.; Mennucci, B.; Cossi, M.; Scalmani, G.; Rega, N.; Petersson, G. A.; Nakatsuji, H.; Hada, M.; Ehara, M.; Toyota, K.; Fukuda, R.; Hasegawa, J.; Ishida, M.; Nakajima, T.; Honda, Y.; Kitao, O.; Nakai, H.; Klene, M.; Li, X.; Knox, J. E.; Hratchian, H. P.; Cross, J. B.; Bakken, V.; Adamo, C.; Jaramillo, J.; Gomperts, R.; Stratmann, R. E.; Yazyev, O.; Austin, A. J.; Cammi, R.; Pomelli, C.; Ochterski, J. W.; Ayala, P. Y.; Morokuma, K.; Voth, G. A.; Salvador, P.; Dannenberg, J. J.; Zakrzewski, V. G.; Dapprich, S.; Daniels, A. D.; Strain, M. C.; Farkas, O.; Malick, D. K.; Rabuck, A. D.; Raghavachari, K.; Foresman, J. B.; Ortiz, J. V.; Cui, Q.; Baboul, A. G.; Clifford, S.; Cioslowski, J.; Stefanov, B. B.; Liu, G.; Liashenko, A.; Piskorz, P.; Komaromi, I.; Martin, R. L.; Fox, D. J.; Keith, T.; Al-Laham, M. A.; Peng, C. Y.; Nanayakkara, A.; Challacombe, M.; Gill, P. M. W.; Johnson, B.; Chen, W.; Wong, M. W.; Gonzalez, C.; Pople, J. A. Gaussian, Inc., Wallingford CT, 2004.

[2] M. Bielawski, M. Zhu, B Olofsson, *Adv. Synth. Catal.* **2007**, *349*, 2610

[3] J. Wen, R. Zhang, S. Chen, J. Zhang, X. Yu, *J. Org. Chem.* **2012**, *77*, 76